Materials and Nanostructured Coatings for Soft Tissue Regeneration

POLITECNICO DI TORINO

DEPARTMENT OF MECHANICAL AND AEROSPACE ENGINEERING

DOCTORATE SCHOOL

PhD in Biomedical Engineering – XXV Cycle

PhD Dissertation

Materials and Nanostructured Coatings for Soft Tissue Regeneration

Supervisor
Prof. Gianluca Ciardelli

PhD Candidate
Antonella Silvestri

January 2013

É meglio essere ottimisti ed avere torto piuttosto che pessimisti ed avere ragione.

Albert Einstein

INDEX

ACKNOWLEDGEMENTS

Questi tre anni di dottorato sono stati per me altamente formativi, sia dal punto di vista scientifico sia dal punto di vista umano. Per questo desidero ringraziare il mio tutor, il Prof. Gianluca Ciardelli, per avermi indirizzato su questa strada e per avermi supportato durante questo percorso.

Grazie a questa esperienza mi è stato possibile conoscere molte persone, interagire con altri gruppi di ricerca e lavorare in altri laboratori. Ringrazio pertanto la Prof. Cabrele, con cui ho lavorato per due brevi periodi presso l'Università della Ruhr (Bochum, Germania), sufficienti però per apprezzare lei e il suo lavoro, la Dott.ssa Annette Meeson, la Dott.ssa Rachel Oldershaw e il Dott. Gavin Richardson, dell'Istituto di Medicina Genetica di Newcastle (Regno Unito), per avermi introdotto all'affascinante mondo della coltura cellulare e per avermi assistito con costanza durante la mia esperienza presso i loro laboratori. Rivolgo un grazie sentito anche al Dott. Stefano Milione dell'Università degli Studi di Salerno, relatore della mia tesi di laurea specialistica, che in questi anni ha sempre mostrato nei miei confronti disponibilità e affetto.

Come non ringraziare tutti i colleghi e gli amici dei laboratori di Alessandria e di Torino: Susanna, Valeria, Clara, Marina, Monica, Anna, Ruo, Tian Ran, Fabiana, Jennifer, Cristina, Simone, Piergiorgio, Chiara, Irene, Piero, Andrea, Annalisa, Francesca, Tiziana, VJ, Diana, Diego, Francesco, Giulia e Umberto, perché la loro presenza ha reso viva e indimenticabile questa esperienza. Un ringraziamento speciale va a Clara, Fabiana e Jennifer, con cui ho condiviso i miei viaggi quotidiani da Torino ad Alessandria, "nella gioia e nel dolore", e da cui sono stata iniziata all'uso delle parolacce, che ho trovato a dir poco liberatorio. Ringrazio tanto anche Marina per essere stata in molti casi una saggia "maestra di vita", per avermi fatto conoscere la fantastica pratica dello yoga e per avermi accolto a Newcastle, e Monica, per la sua disponibilità e per aver condiviso con me l'avventura di Bochum.

Un pensiero va naturalmente a mia madre Maria Rosaria e a tutta la mia famiglia (Ferdinando e Giusy, Elena e Roberto, Anna e Dario) che mi incoraggia e mi conforta, facendomi sentire il suo calore e il suo affetto anche a tanti chilometri di distanza. Un abbraccio calorosissimo va ai mie nipotini Matteo, Gabriele e Veronica, perché il pensiero del loro sorriso, delle loro frasi buffe e dei giochi fatti insieme, mi ha sempre riempito in questi anni il cuore di gioia.

Ringrazio tanto anche Anna A., Daniele M., Antonella, Daniele G., Angelo T., Claudia, Gabriella, Dino, Angelo Z., Rita, Carlo, per la loro preziosa amicizia, tanto forte da resistere alla distanza geografica!

Credo di non avere abbastanza parole per ringraziare, infine, Stefano, che in questi anni mi ha sempre supportato e sopportato! e lo ha fatto con tutto l'amore possibile.

SHORT CURRICULUM VITAE

Antonella Silvestri was born in Benevento (Italy) on April 6th 1984. She has a Bachelor Degree cum laude in Chemistry from Università degli Studi di Salerno (March 2006). She has a Master Degree cum laude in Chemistry, obtained in June 2008, with a thesis work dealing with the polymerization of Lactide catalyzed by organo-metallic complexes.

In November 2008 she started working in the Bioengineering research group of Politecnico di Torino, with Prof. Gianluca Ciardelli as supervisor, being involved in the project "Novel Biomaterials for intraoperative and adjustable devices for fine tuning of prostheses shape and performance in surgery" (BIADS), financed by Regione Piemonte, dealing with the synthesis and characterization of polymeric materials for mitral devices.

Since January 2010 she is working as PhD student in Biomedical Engineering with a thesis on the synthesis and characterization of polymeric materials for the preparation of biomimetic scaffolds for myocardial tissue engineering application.

In 2012 she worked for 2 months at the Institute of Human Genetics of Newcastle University (United Kingdom) on human cardiac progenitor cell culture and biological test on the previously developed constructs, in order to evaluate their application for myocardial tissue regeneration.

LIST OF PUBLICATIONS

1. International journal articles

"Ring Opening Polymerization of Lactide Promoted by Alcoholyzed eteroscorpionate Aluminum Complexes"
Antonella Silvestri, Fabia Grisi, Stefano Milione
Journal of Polymer Science Part A: Polymer Chemistry Vol. 48, Issue 16, pages 3632–3639

"Polyurethane based biomaterials for shape adjustable cardiovascular devices"
Antonella Silvestri, Piero Serafini, Susanna Sartori, Patrizia Ferrando, Francesca Boccafoschi, Stefano Milione, Lucia Conzatti, Gianluca Ciardelli
Special Issue of "Journal of Applied Polymer Science" dedicated to the Times of Polymers (TOP) & Composites Conference, Vol. 122, Issue 6, pages 3661-3671

"Synthesis and Structure-property relationship of polyester-urethanes and their evaluation for the regeneration of contractile tissues"
Susanna Sartori, Monica Boffito, Piero Serafini, Andrea Caporale, Antonella Silvestri, Ettore Bernardi, Maria Paola Sassi, Francesca Boccafoschi, Gianluca Ciardelli
Reactive and Functional Polymers (in press)

Submitted:

to Biomedical Materials
"Myocardial Biomimetic Patches Fabricated with Poly(ε-caprolactone) and Polyethylene Glycol Based Polyurethanes"
Antonella Silvestri, Susanna Sartori, Monica Boffito, Clara Mattu, Anna Maria Di Rienzo, Francesca Boccafoschi, Gianluca Ciardelli

to Macromolecular Bioscience (review)
"Biomimetic Materials and Scaffolds for Myocardial Tissue Regeneration"
Antonella Silvestri, Monica Boffito, Susanna Sartori, Gianluca Ciardelli

2. Comunications in National/International conferences

"Polyurethane-based scaffolds for soft tissue engineering"
Susanna Sartori, Antonella Silvestri, Monica Boffito, Ana Marina Ferreira, Anna Maria Di Rienzo, Valeria Chiono, Gianluca Ciardelli
GNB2012, 26-29 giugno 2012, Roma

"Biodegradable polyurethanes for myocardial tissue regeneration"

Antonella Silvestri, Susanna Sartori, Monica Boffito, Piero Serafini, Clara Mattu, Francesca Boccafoschi, Gianluca Ciardelli
World Conference on Regenerative Medicine, 02-04 Novembre 2011, Leipzig, Germany

"Biodegradable polyurethanes for soft tissue regeneration"
Gianluca Ciardelli, Susanna Sartori, Monica Boffito, Piero Serafini, Antonella Silvestri, Francesca Boccafoschi
Congresso Nazionale Biomateriali-SIB 2011-, 23-25 Maggio 2011, Bari, Italy

"ECM-like Polyurethanes for Tissue Engineering Application"
Susanna Sartori, Piero Serafini, Monica Boffito, Andrea Caporale, Michele Zuliani, Chiara Cabrele, Antonella Silvestri, Francesca Boccafoschi, Gianluca Ciardelli
EMRS 2011 San Francisco, USA

"Biomimetic Polyurethanes for Regenerative Medicine"
Gianluca Ciardelli, Susanna Sartori, Piero Serafini, Monica Boffito, Andrea Caporale, Antonella Silvestri, Ettore Bernardi, Francesca Boccafoschi
Nanotech 2011 Vol. 3, Nanotechnology 2011: Bio Sensors, Instruments, Medical, Environment and Energy, Chapter 3: Bio Nano Materials, pages 155-158

"Polysiloxane based Polyurethane Formulations for Cardiovascular Applications"
Antonella Silvestri, Susanna Sartori, Piero Serafini, Patrizia Ferrando , Clara Mattu, Stefano Milione, Gianluca Ciardelli
GNB 2010, 8-10 luglio 2010, Torino

ABSTRACT

Despite several progresses in terms of early diagnosis and prevention, coronary heart disease and heart attack are still the most common causes of death in Western countries. Cardiac Regenerative Medicine appears to be a promising alternative to pharmacologic treatment or organ transplantation although cellular therapies based on progenitor cell injection are still problematic. Myocardial Tissue Engineering (MTE) is a Regenerative Medicine approach, able to integrate cell therapy with the use of polymeric substrates (myocardial scaffolds or heart patches) that can reduce cell loss and potentially prevent remodeling and fibrotic processes. In *in vivo* MTE strategies, scaffolds should be capable to recruit cardiac progenitor and differentiated cells which are present in the adult heart and promote their proliferation/differentiation. Consequently, these substrates have to meet strict requirements in terms of biological, mechanical, surface, biodegradability properties. In particular, they should mimic the natural Extracellular Matrix (ECM), achieving a chemical, morphological and mechanical biomimicry.

In this thesis work, biomimetic polymeric constructs are proposed as heart patches for myocardial functions restoration and cardiac tissue regeneration after a myocardial infarction. These constructs were prepared as dense (films) and porous scaffolds from synthetic biodegradable polyurethanes (PURs), that were selected because of their chemical versatility and elastomeric mechanical behavior**.** In detail, poly(ester urethanes) and poly(ether ester urethanes) were synthesized starting from poly(ε-caprolactone) (PCL) and poly(ethylene glycol) (PEG) as macrodiols, 1,4-diisocyanatobutane (BDI) as diisocyanate, L-Lysine Ethyl Ester and Alanine-Alanine-Lysine (AAK) as chain extenders. PCL was selected to confer biodegradability to the final PUR, while PEG was added in low amounts to tune wettability, mechanical and biological properties of films and scaffolds. BDI was selected since it is an aliphatic diisocyanate and its biodegradation products are non toxic. L-Lysine Ethyl Ester and Alanine-Alanine-Lysine were selected as chain extenders for their biocompatible degradation products and because biodegradability properties can be tuned thanks to the introduction of AAK peptide in the polymer chain, since the Alanine-Alanine sequence is a target for the elastase enzyme. Spectroscopic and chromatographic analysis demonstrated the successful synthesis of the designed PURs. Films, obtained by hot pressing, were thermally and mechanically characterized. They were all characterized by an elastomeric behaviour with elastic moduli ranging from 7 to 14 MPa. Contact Angle measurements revealed slightly hydrophobic film surfaces with contact angle values in the range 78-94°. Based on mechanical testing results, two formulations (KBC1250 and KBC1250-E1500-20) were processed into scaffolds by Thermally Induced Phase Separation (TIPS) with the application of a thermal gradient, that allowed the formation of stretched and unidirectional pores. These microstructures, that were studied trough Scanning Electron Microscopy (SEM) micrographs, mimicked the striated muscle tissue. Tensile tests revealed lower mechanical properties for scaffolds with respect to films (elastic moduli of about 2 MPa, maximum stress in the range 0.3-0.6 MPa and maximum strain in the range 120-160%). Nevertheless, both porous substrates have suitable elastomeric behaviours for contractile tissues regeneration, with elastic

moduli closer to that of myocardial tissue (20 kPa-0.5 MPa) for porous constructs. Viability tests on cardiomyocytes revealed the best cell response for dense film and porous scaffold obtained from the polyurethane KBC1250, with an increasing viability for the porous substrate, which is ascribable to its microstructure features. Hydrolytic and enzymatic degradation tests showed a faster weight loss for the scaffolds in the presence of the enzyme (lipase), probably because the enzymatic degradation mechanism takes place on surface and porous constructs exhibit a larger exposed area. Moreover, elastase degradation tests demonstrated that additional degradation through biological processes can be achieved for these polymers by the simple introduction of specifically designed peptide sequences in the PUR backbone.

Based on biological and mechanical characterization, dense and porous KBC1250 constructs were selected to be surface functionalized by the covalent attachment of Arginine-Glycine-Aspartic Acid (RGD) peptides, in order to promote cell adhesion and proliferation and obtain a "chemical biomimicry". These peptide is the active sequence of laminin and fibronectin proteins, that are responsible for the adhesion of cells to the ECM. This chemical modification was performed on films homogeneously or through a silicone mask, in order to create a linear RGD micropattern. Analogous laminin and fibronectin patterns revealed promising from literature data in promoting mesenchymal stem cell differentiation and cardiomyocyte spatial organization. Spectroscopic analysis, increase in surface wettability and colorimetric assays demonstrated the successful surface modification of PUR films and scaffolds. Functionalized films were characterized by an optimal hydrophylicity (65°) and peptide density (3.2 and 1.7 nmol/mm^2) for cell adhesion promotion. Peptide quantification and cell viability tests demonstrated indirectly the successful use of the siloxane mask in allowing the RGD attachment on the uncovered areas. Cell viability tests and SEM micrographs showed the positive effect of film modification on cardiomyocyte viability and adhesion. Although the same successful peptide attachment was obtained on scaffold surfaces, the biological response on this type of substrate was just slightly higher after the surface modification. This result can be explained considering that the porous surfaces, although an increase in wettability after the functionalization, are still far from the optimal contact angle value promoting cell attachment or that some not covalently bound peptides inside the scaffold microstructure can induce cell detachment and apoptosis.

KBC1250 substrates were also tested with human cardiac Mesenchymal Stem Cells (MSCs) and Cardiosphere Derived Cells (CDCs), which belong to the progenitor cell reservoir present in the adult myocardium. MSCs were detected and extracted for the first time in a human heart by Dr Rachel Oldershaw and Dr Annette Meeson of Newcastle University, while CDCs were extracted from human biopsies through the creation of Cardiospheres (cell clusters containing cardiac stem cells, differentiating progenitors and spontaneously differentiated cardiomyocytes). Subsequent culture of these CDCs and MSCs on KBC1250 films and scaffolds revealed promising results for the application of the porous constructs in MTE. Viability cell test showed that scaffold promoted CDC and MSC growth. Although a decrease in cell health after 14 culture days was observed for MSCs, these preliminary tests on human cardiac progenitor cells showed that KBC1250 porous scaffolds are suitable substrates for both CDC and MSC proliferation.

THESIS OUTLINE

The thesis is divided in 5 chapters, whose content is summarized below.

Chapter 1 gives an overview of the state of the art of the current knowledge cornering myocardial tissue regeneration, focusing on both scientific and technological aspects, crucial for successful approaches in cardiac repair. At the end of the chapter, the goal of the thesis is also described.

Chapter 2 deals with the first experimental step in which polymeric materials such as biodegradable polyurethanes were synthesized and characterized. Two of these formulations were later processed for the preparation of myocardial tissue constructs (both dense and porous ones). The physical-chemical, mechanical and the biological properties of these constructs are also accurately described.

Chapter 3 is focused on the surface chemical modification (functionalization) performed on both the dense and the porous constructs obtained from one of the tested formulations. These constructs were previously selected on the base of their mechanical and biological characteristics. The surface characterization and the biological tests (on cardiomyocytes) of the functionalized substrates are also showed.

Chapter 4 describes additional biological tests performed to further characterize the same previously selected constructs (without surface functionalization) and applied to progenitor cells extracted from human cardiac biopsies. These experiments were carried out in the laboratory of Dr Annette Meeson at Newcastle University (Newcastle, UK).

Chapter 5 contains a general discussion of the obtained results together with the conclusions, referring the goals, the drawbacks and the potential future developments of the presented experimental work.

LIST OF ABBREVIATIONS

A
AA: Alanine-Alanine
AAK: Alanine-Alanine-Lysine
ACE: Angiotensin Converting Enzyme
ADP: Adenosine Diphosphate
Ala: Alanine
Alg-NW: Alginate Nanowires
AM: Antheraea Mylitta
Anova: Single-factor analysis of variance
ARB: Angiotensin Receptor Blocker
ASC: Adipose tissue-derived Stem Cell
ATP: Adenosine Triphosphate
AV: Atrioventricular

B
BDI: 1,4-Diisocyanatobutane or Butyl Diisocyanate
bFGF: basic Fibroblast Growth Factor
BM: Bombyx mori silk fibroin
BMNC: Bone Marrow Mononuclear Cell
BSA: Bovine serum albumin

C
CABG: Coronary Artery Bypass Grafting
CDC: Cardiosphere-derived Cell
CDI: Carbonyl diimidazole
CHD: Coronary Heart Disease
CHF: Congestive Heart Failure
CM: Cardiomyocytes
CNF: Carbon Nanofibers
CNT: Carbon Nanotubes
CPC: Cardiac Progenitor Cell
CS: Chitosan
CSC: Cardiac Stem Cell
CVD: Cardiovascular Diseases
Cx43: Connexin43

D
DC: Direct Current
DCC: Dicyclohexyl-carbodiimide
DCE: 1,2-Dichloethane

DMEM: Dulbecco's modified Eagle's medium
DMF: Dimethylformamide
DNA: Deoxyribonucleic acid
dsDNA: Double-stranded DNA
DSC: Differential Scanning Calorimetry

E
E: Young's modulus (Elastic modulus)
ECM: Extracellular Matrix
EDC: 1-Ethyl-3-(3-dimethylaminopropyl)-carbodiimide
EDTA: Ethylenediaminetetraacetic acid
EGF: Epidermal Growth Factor
ESC: Embryonic Stem Cell and Environmental Stress Cracking

F
FB: Fibroblast
FBS: Fetal Bovine Serum
FDA: Food and Drug Administration
FGF: Fibroblast Growth Factor
FTIR-ATR: Fourier Transform Infrared-Attenuated Total Reflectance Spectroscopy

G
G-CSF: Granulocyte Colony-Stimulating Factor

H
HA: Hyaluronic Acid
HBP: Heparin-binding Peptide
HEMAHex: 2-Hydroxyethylmethacrylate-6-Hydroxyhexanoate
HGF: Hepatocyte Growth Factor
hMSC: human Mesenchymal Stem Cell

I
IABP: Intra-Aortic Balloon Pump
ICD: Implantable Cardiac Defibrillators
IGF: Insulin-like Growth Factor
IMDM: Iscove's Modified Dulbecco's Medium
iPSC: Induced Pluripotent Stem Cell

L
LDI: Lysine Diisocyanate
LMWH: Low-Molecular-Weight Heparin
LV: Left Ventricle
LVAD: left ventricle assist device
Lys: Lysine

M
μCP: Microcontact printing
MDI: 4,4-Methylenediphenyl Diisocyanate
MI: Myocardial Infarction
MGF: Modified Gelfoam® Scaffold
MMP: Membrane Metalloproteinase
MSC: Mesenchymal Stem Cell
MTE: Myocardial Tissue Engineering
MTS: 3-(4,5-dimethylthiazol-2-yl)-5-(3-carboxymethoxyphenyl)-2-(4-sulfophenyl)-2H-tetrazolium
MW: Microwave

N
NHS: N-hydroxysuccinimide
NMVM: Neonatal Murin Ventricular Myocytes
NRVM: Neonatal Rat Ventricular Myocyte
NSTEMI: No Segment Elevation Myocardial Infarction

P
PAA: Poly(acrylic acid)
PAM: Pressure-assisted Microsyringe
PANi: Polyaniline
PBS: Phosphate Buffer Saline
PCI: Percutaneous Coronary Intervention
PCL: Poly(ε-caprolactone)
PCNA: Proliferating Cell Nuclear Antigen
PECUU: Poly(ester carbonate urethane)urea
PECVD: Plasma-enhanced chemical vapor deposition
PED: Poly(ethyleneterephathalate)/dimer fatty acid
PEG: Poly(ethylene glicol)
PEO: Poly(ethylene oxide)
PET: Poly(ethylene therephthalate)
PEUU: Poly(ester urethane urea)
PGA: Poly(glycolic acid)
PGCL: Poly(glycolide-co-caprolactone)
PGS: Poly(Glycerol Sebacate)
PIPAAm: Poly(*N*-isopropylacrylamide)
PLA: Polylactide
PLACL: Poly(L-lactic acid)-*co*-poly(ε-caprolactone)
PLGA: Polylactide-co-glycolide
PLLA: Poly(L-lactide)
PMMA: Poly(methyl methacrylate)
POC: Poly(1,8-octanediol-co-citric acid)

PP: Polypropylene
PPG: blend of PCL, gelatin and PPy
PPy: Polypyrrole
PS: Polystyrene
PUR: Polyurethane
Put: Putrescine

R
RGD: Arginine-Glycine-Aspartic Acid
RGDS: **:** Arginine-Glycine-Aspartic Acid-Serine
RF: Radio Frequency
RP: Rapid Prototyping

S
SA: Sinoatrial
SCM: Smooth Muscle Cell
SCPL: Solvent Casting/Particulate Leaching
SDF: Stromal-cell Derived Factor
SDS: Sodium Dodecyl Sulfate
SDS-PAGE: Sodium Dodecylsulfate Polyacrylamide Gel
SEC: Size Exclusion Chromatography
SEM: Scanning Electron Microscopy
SF: Silk Fibroin
SLS: Selective Laser Sintering
SP: Side Population
ST: Segment Elevation
STEMI: Segment Elevation Myocardial Infarction
SWNT: Single-walled CNT

T
TAH: Total Artificial Heart
TBO: Toluidine Blue O
TDI: Toluene Diisocyanate
TEA: Triethylamine
THF: Tetrahydrofuran
TIPS: Thermally Induced Phase Separation

U
UV-Vis: Ultravioltet-Visible

V
VEGF: Vascular Endothelial Growth Factor
VF: Ventricular Fibrillation
VT: ventricular tachycardia

W
WHO: World Health Organization
WSC: Water Soluble Carbodiimide

X
XPS: X-Ray Photoelectron Spectroscopy

CHAPTER 1
Myocardial regeneration: state of the art and future trends

1.1 Introduction

According to the World Health Organization (WHO), Cardiovascular Diseases (CVD) are the number one cause of deaths in the world (30% of total deaths) and, in particular, Coronary Heart Disease (CHD) represents 42% of all CVD deaths (7.3 million of people). In addition, it has been assessed that by 2030 about 23 millions of people will die mainly from heart disease and stroke, CVD remaining the leading causes of death worldwide [1]. Based on these data, it is evident that the study and the development of resolving and definitive treatments for cardiovascular pathologies has become a demand of prime importance.
Myocardial infarction (MI) is one of the most common CVD. While significant progresses have been made in preventing death from MI, it appears still complex to avoid a common progression to heart failure in the patients who survive the initial acute event [2]. Since adult cardiomyocytes have very limited ability to proliferate [3] and the stem/progenitor population within the adult heart do not provide the adequate replacement needed after a substantial damage [4], myocardial infarction results in the formation of scar tissue with different contractile, mechanical and electrical properties from that of native tissue [5].
As alternatives to pharmacologic treatments or organ transplantation, new approaches belonging to the large field of Regenerative Medicine have been proposed. In particular, Myocardial Tissue Engineering (MTE), which combines different strategies to solve problems of delivery, retention and recruitment of cells, seems to be the most promising means for the treatment of infarcted myocardium.
In this chapter an overview of the characteristics of cardiac tissue, myocardial infarction, materials and devices used in tissue engineering approaches, and the goal of this thesis work will be described and discussed.

1.2 The heart

The heart is the muscular organ of the circulatory system that constantly pumps blood throughout the body. It has approximately the size of a clenched fist and it is composed of cardiac muscle tissue that is able to contract and relax rhythmically throughout a person's lifetime [6].
The heart is located between the lungs in the middle of the chest, behind and slightly to the left of the sternum. A double-layered membrane called the pericardium surrounds the heart like a sac. The outer layer of the pericardium surrounds the roots of the heart's major blood vessels and is attached by ligaments to the spinal column, diaphragm, and other parts of the body. The inner layer of the pericardium is attached to the heart muscle. A coating of fluid separates the two layers of the membrane, letting the heart move as it beats.

The heart is characterized by four separate compartments or chambers. The upper chambers are called the left and right atria, which receive and collect the blood coming to the heart, and the lower chambers are called the left and right ventricles, which pumps blood away from the heart through powerful, rhythmic contractions. A wall of muscle called the septum separates the left and right atria and the left and right ventricles (see figure 1.1).
Four types of valves regulate blood flow through the heart:

- the tricuspid valve, which regulates blood flow between the right atrium and right ventricle;
- the pulmonary valve, which controls blood flow from the right ventricle into the pulmonary arteries that carry blood to your lungs to pick up oxygen;
- the mitral valve, which lets oxygen-rich blood from the lungs pass from the left atrium into the left ventricle;
- the aortic valve, which opens the way for oxygen-rich blood to pass from the left ventricle into the aorta, body's largest artery, where it is delivered to the rest of the body [7].

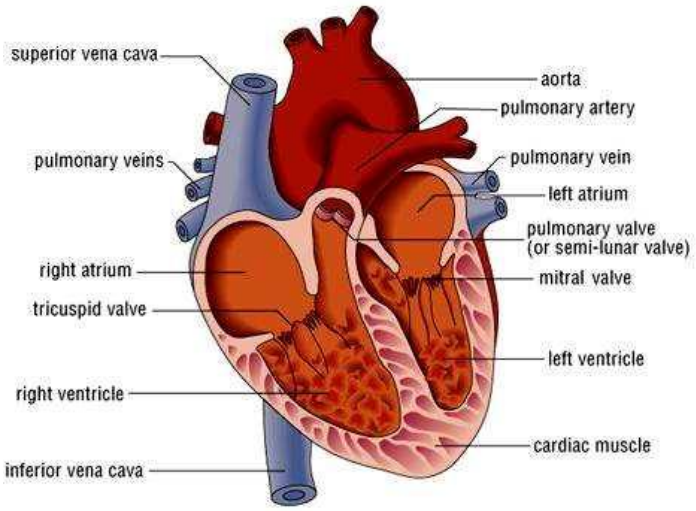

Fig. 1.1 Anatomy of the heart [8].

The human heart can be considered two pumps in one. The right side receives oxygen-poor blood from the various regions of the body and delivers it to the lungs. Here blood absorbs oxygen and get the left side of the heart. This oxygen-rich blood coming from the lungs is delivered to the rest of the body [6].
The contraction of the cardiac muscle tissue in the ventricles is called systole. When the ventricles contract, they force the blood from their chambers into the arteries. The left ventricle empties into the aorta and the right ventricle into the pulmonary artery. The increased pressure due to the contraction of the ventricles is called systolic pressure. The relaxation of the cardiac muscle tissue in the ventricles is called diastole. When the ventricles relax, they make possible to accept the blood from the atria. The decreased pressure due to the relaxation of the ventricles is called diastolic pressure [6].

A network of nerve fibers coordinates the contraction and relaxation of the cardiac muscle tissue to obtain an efficient, wave-like pumping action of the heart. The Sinoatrial Node (or SA node) serves as the natural pacemaker for the heart. Nestled in the upper area of the right atrium, it sends the electrical impulse that triggers each heartbeat. The impulse spreads through the atria, prompting the cardiac muscle tissue to contract in a coordinated wave-like manner. The impulse that originates from the sinoatrial node strikes the Atrioventricular node (or AV node) which is situated in the lower portion of the right atrium. The atrioventricular node in turn sends an impulse through the nerve network to the ventricles, initiating the same wave-like contraction of the ventricles. The electrical network serving the ventricles leaves the atrioventricular node through the Right and Left Bundle Branches. These nerve fibers send impulses that cause the contraction of cardiac muscle tissue [6].

1.2.1 Cardiac muscle

The heart is composed mainly of muscle tissue. The muscular walls of the heart consist of three major "layers". The myocardium constitutes the bulk of the walls and it is enclosed on the outside by the epicardium and on the inside by the endocardium. As described in the previous paragraph, the heart is also covered completely by a protective sac called the pericardium.

The myocardium is responsible for the contraction and relaxation of the ventricles and atria and it is composed almost completely of cardiomyocytes (CM) [9]. These cells, also called myocardiocyteal muscle cells, contain one, two, or very rarely three or four cell nuclei [10], are narrower and much shorter than skeletal muscle cells, being about 0.02 mm wide and 0.1 mm long, and are more rectangular than smooth muscle cells, which are normally spindle-shaped. They are often branched, and contain a high number of mitochondria, which provide the energy required for contraction. Only 20–40% of the cells in the heart are CMs, but they occupy 80–90% of the heart volume [11].

Fibroblasts (FBs) and smooth muscle cells (SCMs) are other two cellular components of the myocardial tissue and collectively range in size 3–15 μm. Cardiac FBs, that constitute most of the non-myocytes in the myocardium, secrete the components of the ECM and transmit mechanical force by the receptor mediated connections to the ECM [12]. Endothelial cells (ECs) line the blood vessels of the myocardial vasculature and engage in cross-talk with CM through several secreted factors [13]. It was also reported that the heart contains small numbers of resident cardiac progenitor cells (~1 in 10^7 cells) [14, 15], as it will be discussed in chapter 4.

Like the skeletal muscle, the cardiac muscle is striated with narrow dark and light bands, due to the parallel arrangement of actin and myosin filaments that extend from end to end of each myocyte (see figure 1.2).

A prominent and unique feature of cardiac muscle is the presence of irregularly-spaced dark bands between myocytes. These are known as intercalated discs, and are due to areas where the membranes of adjacent myocytes come very close together. From a mechanical point of view, intercalated discs are the “glue” that enables contractile force to be transmitted from one cardiomyocyte to another [17]. They are complex adhering structures which connect single

cardiac myocytes to an electrochemical syncytium (in contrast to the skeletal muscle, which becomes a multicellular syncytium during mammalian embryonic development) and are mainly responsible for force transmission during muscle contraction. Intercalated discs also support the rapid spread of action potentials and the synchronized contraction of the myocardium [18]. Cardiac-muscle contraction is actin-regulated and, in contrast to skeletal muscle, requires extracellular calcium ions. They bind to an enzyme complex on myosin, called calmodulin-myosin light chain kinase. The enzyme complex breaks up ATP (adenosine triphosphate) into ADP (adenosine diphosphate) and transfers the phosphate directly to myosin. This phosphate transfer activates myosin, that forms crossbridges with actin (as occurs in skeletal muscle). When calcium is pumped out of the cell, the phosphate gets removed from myosin by another enzyme. The myosin becomes inactive, and the muscle relaxes [19].

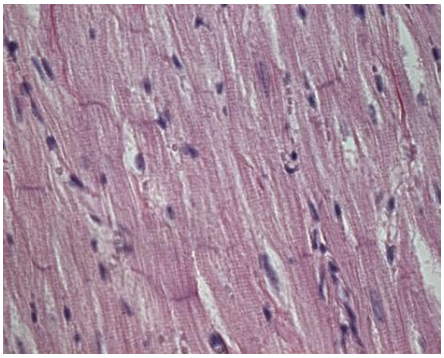

Fig. 1.2 Cardiac muscle tissue [16].

1.3 Myocardial infarction

The general term infarction refers to tissue death or necrosis due to an obstruction of the tissue's blood supply, leading to a local lack of oxygen. The resulting lesion is defined as an infarct [20].

A myocardial infarction (MI), also known as a heart attack, is the death of heart cells from the sudden blockage of a coronary artery by a blood clot. Blockage of a coronary artery deprives the heart muscle of blood and oxygen, causing injury to the heart muscle. Injury to the heart muscle causes chest pain and chest pressure sensation. If blood flow is not restored to the heart muscle within 20-40 minutes, irreversible death of the heart muscle will begin to occur. Muscle continues to die for six to eight hours at which time the heart attack is usually "complete."

A very common cause of a heart attack is atherosclerosis that consists is a gradual process by which plaques of cholesterol are deposited in the walls of arteries. Cholesterol plaques cause hardening of the arterial walls and narrowing of the inner channel (lumen) of the artery. Plaques can become unstable, rupture, and additionally promote a thrombus (blood clot) that occludes the artery, resulting in a heart attack (see figure 1.3). The cause that leads to the formation of a clot is still unknown, but contributing factors may include cigarette smoking or other nicotine exposure, elevated low-density lipoprotein cholesterol, elevated levels of blood

catecholamines (adrenaline), high blood pressure, and other mechanical and biochemical stimuli.

Typical symptoms of acute myocardial infarction include sudden chest pain (typically radiating to the left arm or left side of the neck), shortness of breath, nausea, vomiting, palpitations, sweating, and anxiety (often described as a sense of impending doom) [21]. Women may experience fewer typical symptoms than men, most commonly shortness of breath, weakness, a feeling of indigestion, and fatigue [22]. A sizeable proportion of myocardial infarctions (22–64%) are "silent", that is without chest pain or other symptoms [23].

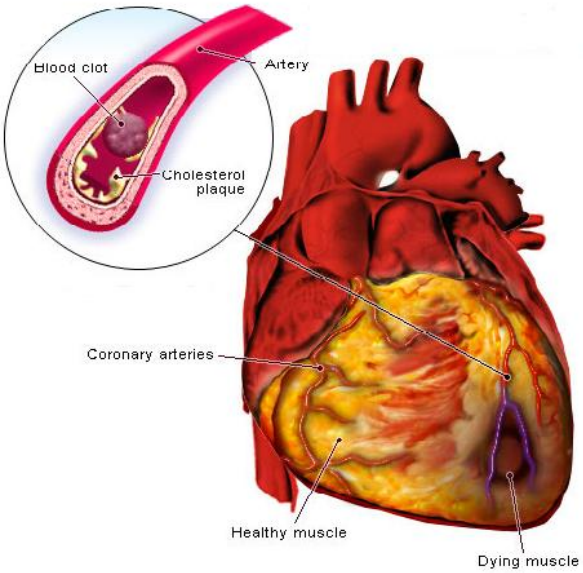

Fig. 1.3 Myocardial infarction [24].

Myocardial infarction can be categorized on the basis of anatomic, morphologic, and diagnostic clinical information. From an anatomic or morphologic point of view, we can distinguish transmural and nontransmural MI. A transmural MI is characterized by ischemic necrosis of the full thickness of the affected muscle segment, extending from the endocardium through the myocardium to the epicardium. A nontransmural MI reefers to an area of ischemic necrosis that does not extend through the full thickness of myocardial wall segment. In a nontransmural MI, the area of ischemic necrosis is limited to the endocardium or to the endocardium and myocardium. It is the endocardial and subendocardial zones of the myocardial wall segment that are the least perfused regions of the heart and the most vulnerable to conditions of ischemia.

MI may be classified by the clinical scenario into various types. Type 1 is a spontaneous MI related to ischemia from a primary coronary event (e.g., plaque rupture, thrombotic occlusion). Type 2 is secondary to ischemia from a supply-and-demand mismatch. Type 3 is an MI resulting in sudden cardiac death. Type 4a is an MI associated with percutaneous coronary intervention, and 4b is associated with in-stent thrombosis. Type 5 is an MI associated with coronary artery bypass surgery.

A more common clinical diagnostic classification is also based on electrocardiographic findings as a means of distinguishing between two types of MI: STEMI (Segment Elevation

Myocardial Infarction), with ST elevation in the electrocardiograph, and NSTEMI, without ST elevation. ST-segment elevation is associated with higher early mortality and morbidity [25].

1.3.1 Inflammatory and healing response

Cardiac wound healing in mammals is hampered by the fact that regeneration of heart muscle is virtually absent and damaged myocardium is replaced by scar tissue, in the process called ischemic cascade.

After cardiomyocyte death, an inflammatory reaction starts within the first day after MI. Inflammatory cells invade the infarct, followed by myofibroblasts. Alterations of connective tissue are present as early as 40 min after an experimental coronary occlusion and degradation of collagen is significant at 24 h in the rat. The normal collagen structure disappears during the first week after the infarct. The extent of collagen damage depends by the degree of infarct expansion. Collagenases and other neutral proteinases increase their activities rapidly degrading extracellular matrix collagen in MI. Inflammatory cells release proteases and contribute to removal of died tissue, while myofibroblasts reconstruct a new collagen network. The actions of myofibroblasts are constant and essential for the organization of scar formation under the difficult condition of the rhythmic contraction of the heart. After several weeks, a solid scar has been formed with a stable collagen structure, with some myofibroblasts that remain in the scar tissue [26, 27].

The collagen scar can lead to potentially life threatening arrhythmias. Injured heart tissue conducts electrical impulses more slowly than normal heart tissue. The difference in conduction velocity between injured and uninjured tissue can trigger re-entry or a feedback loop that is the probable cause of many lethal arrhythmias, such as ventricular fibrillation (*V-Fib*/VF), an extremely fast and chaotic heart rhythm that is the leading cause of sudden cardiac death. Another life-threatening arrhythmia is ventricular tachycardia (*V-Tach*/VT), which may or may not cause sudden cardiac death [28].

Ventricular remodeling is a process closely connected with the post-infarction healing response and the balance between these two processes constitutes the most important parameter that determines long-term outcome. It consists of alterations in the architecture of both the infarcted and non-infarcted regions of the left ventricle. It is characterized by an inflammatory response, initiated during the first hours after coronary occlusion, and it is mediated by the migration of macrophages, monocytes, and neutrophils into the infarct area. Degradation of the extracellular matrix by metalloproteinases results in cardiomyocyte slippage, which lead to the infarct area thinning and elongation (infarct expansion). Additionally, wall stress in the infarct area increases and the resultant distending forces contribute to infarct expansion. As it will be described ahead, after the initial inflammatory phase, collagen deposition increases and resists deformation and rupture. Infarct expansion increases wall stress in the remaining myocardium, resulting in dilatation of the left ventricle and distortion of its shape, as it is schematically illustrated in figure 1.4. These processes may evolve up to several months, eventually leading to impaired left ventricular function and cardiac failure [29].

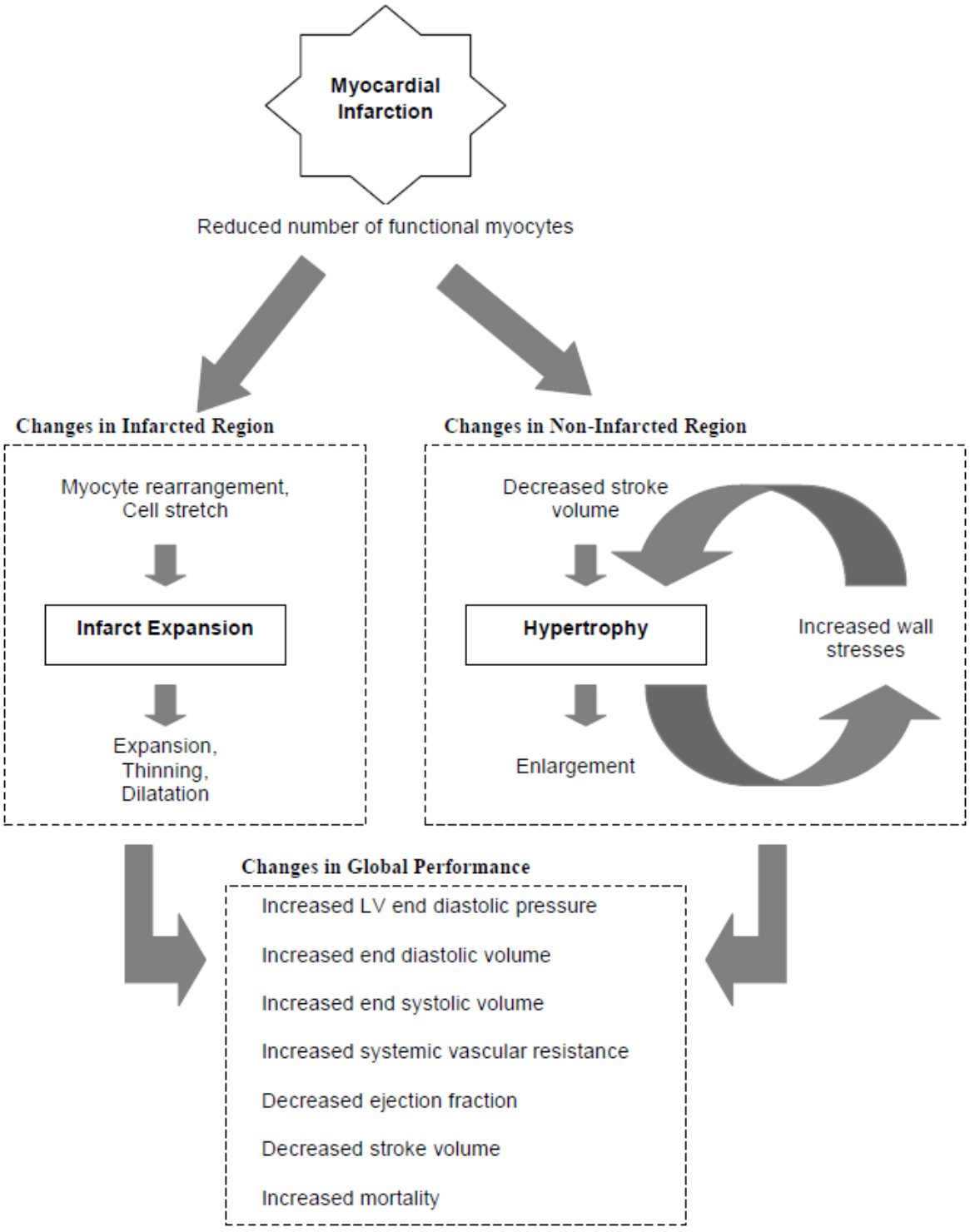

Fig. 1.4 Overview of LV remodeling [30].

1.3.1.1 Phases of healing process

The complex healing process after myocardial infarction can be divided in three phases, characterized by different structural and mechanical properties of the damaged tissue.

The necrotic phase

The necrotic phase generally begins within a few hours, when the infarcted tissue begins to stiffen, and ends when the number of fibroblasts and amount of new collagen begin to increase rapidly in the healing infarct (approximately 7 days after infarction in the human and 5 days after infarction in the rat). Infarct rupture is most common during this period [27].
During this phase, within hours after infarction, several structural changes of the injured tissue take place. The infarcted muscle loses its striations and changes its staining properties. Within 24 h, 94% of human infarcts have wavy fibers and 90% have clear necrosis characterized by altered staining properties. By the fourth or fifth day, removal of dead tissue is observed. Collagenase and gelatinase activity of metalloproteinase MMP-1, MMP-2, and MMP-9 is high and disruption of the collagen network continues. As the necrotic phase concludes, deposition of new ECM components begins. Fibronectin, laminin, and collagen type IV all appear at 3–4 days in the healing rat infarct.
In the necrotic infarct two changes mainly take place from a mechanical point of view: an increase of circumferential and longitudinal stiffness under multiaxial loading, and an increase of unstressed segment length, at least in the circumferential direction. By contrast, uniaxial tests of strips of healing infarct tissue have indicated that infarcted tissue properties do not change during the necrotic phase of healing.
Titin and collagen are the two primary structural proteins degraded in passive myocardium during the necrotic phase. If these proteins normally bear some tension in the stress-free state, their degradation could produce the increase in unstressed segment length reported in necrotic infarcts, but would not explain the reported increase in infarct stiffness [27].

The fibrotic phase

This phase is characterized by new collagen deposition, that is determinant for structural and mechanical changes. It starts when the number of fibroblasts and amount of new collagen begin to increase rapidly and ends when collagen production slows and mechanical properties become independent from collagen content. This occurs at approximately 3 weeks in large animal models, presumably earlier in the rat and later in humans [27]. Proliferating fibroblasts acquire specialized contractile features differentiating into contractile cells, termed myofibroblasts. These phenotypically modulated fibroblasts secrete large amounts of extracellular matrix proteins in the infarct [31]. The healing infarcted tissue generally contains a mixture of collagen types I, III, and other minor subtypes. In detail, an initial mesh of type III collagen forms the scaffold for subsequent deposition of large, highly aligned type I collagen fibers.
During this phase infarct stiffness achieves the higher value and the healing infarct acquires a distinctive anisotropy. Since infarct stiffness and collagen amount increase in parallel, it can be deduced that collagen content mainly determines the mechanical properties of the healing infarct during this phase. The primary determinant of infarct mechanical properties in the fibrotic phase is the presence of a highly aligned large collagen fiber structure, oriented in the circumferential direction, where the scar is stiffer.

The remodeling phase

During this phase, although collagen content may continue to rise for several weeks, mechanical properties of the infarct become independent from collagen amount and a remodeling process takes place, at the macroscopic and microscopic level. At the macroscopic level, the shrinkage of the scar occurs, occupying a reduced percentage of the left ventricular (LV) wall. A changes in size, shape, and function of the left ventricle occurs. At the microscopic level, even if rise in collagen content slows, the process of fiber cross-linking continues to increase and mechanical properties seem to be dependent by the degree of collagen cross-linking. In addition, most fibroblasts and vascular cells undergo apoptosis [27]. Several studies have noted an initial improvement in ventricular function during this phase, but with further expansion, function declines. Over time, as the heart undergoes ongoing remodeling, it becomes less elliptical and more spherical. Spheralization has been shown to be associated with higher end-systolic wall stress and an abnormal distribution of fiber shortening. More spherical ventricles are characterized by severely depressed contractility at rest and have been correlated with reduced survival.

1.4 Treatments of myocardial infarction [25, 32]

1.4.1 Pharmaceutical and surgical treatments

The modern treatment of acute myocardial infarction consist mainly in reperfusion therapy, which is aimed to open the blocked artery and restore blood flow to the damaged area of the heart. Reperfusion can be obtained through a pharmaceutical or surgical approach. In both cases, this therapy is also aimed at preventing further damage and the possibility of other heart attacks in the future. The most common therapeutic approaches used are listed and described below.

Anti-platelet medicines

Anti-platelet medicines, such as aspirin, reduce the tendency of platelets to clump and clot. Within minutes, aspirin prevents additional platelet activation and interferes with platelet adhesion and cohesion. This effect benefits all patients with acute coronary syndromes, including those with amyocardial infarction. Aspirin alone has one of the greatest impacts on the reduction of MI mortality. Its beneficial effect is observed early in therapy and persists for years with continued use.

Nitrates

Nitrates, such as Nitroglycerin, have a vasodilator effect. They are metabolized to nitric oxide in the vascular endothelium. Nitric oxide widens the blood vessel by relaxing the muscular wall of the blood vessel. Clinical trial data have supported the initial use of nitroglycerin for up to 48 hours in MI. There is little evidence that nitroglycerin provides significant benefit as

long-term post-MI therapy, except when severe pump dysfunction or residual ischemia is present.

ACE (angiotensin converting enzyme) inhibitors

ACE inhibitors, another type of vasodilator, improve the heart muscle healing process, by blocking the production of a hormone called angiotensin II. Contraindications to ACE inhibitor use include hypotension and declining renal function. For patients intolerant of ACE inhibitors, angiotensin receptor blocker (ARB) therapy may be considered.

Beta-blocking agents

Beta-blocking agents interfere with the nerves controlling the heart by blocking the action of noradrenaline, that they release. They also block the adrenaline hormone, carried in the blood. This makes decrease the rate and force of myocardial contraction and decreases overall myocardial oxygen demand, helping to prevent serious arrhythmias and reinfarction. The use of a beta blockers have some recognized adverse effects. The most serious are heart failure, bradycardia, and bronchospasm. Beta blocker therapy is recommended within 12 hours of MI symptoms and is continued indefinitely. During the acute phase of a MI, beta blocker therapy may be initiated intravenously; later, patients can switch to oral therapy for long-term treatment. In some patients who are considered high risk due to age or hemodynamic instability, intravenous therapy can be avoided.

Unfractionated Heparin

Unfractionated Heparin is beneficial until the inciting thrombotic cause (ruptured plaque) has completely resolved or healed. This drug has been shown to be effective when administered intravenously or subcutaneously according to specific guidelines. The minimum duration of heparin therapy after MI is generally 48 hours, but it may be longer, depending on the individual clinical situation. Heparin has the added benefit of preventing thrombus through a different mechanism than aspirin.

Low-Molecular-Weight Heparin (LMWH)

LMWH can be administered to MI patients who are not treated with fibrinolytic therapy and who have no contraindications to heparin. The LMWH drugs includes a large number of agents that have distinctly different anticoagulant effects. LMWHs are proved to be effective for treating acute coronary syndromes characterized by unstable angina and NSTEMI. Their fixed doses are easy to administer, and laboratory testing to measure their therapeutic effect is usually not necessary.

Warfarin

Warfarin is not routinely used after MI, but it has a role in selected clinical settings. The use of this drug is recommended for at least 3 months in patients with left ventricular aneurysm or thrombus, a left ventricular ejection fraction less than 30%, or chronic atrial fibrillation.

Fibrinolytics

Fibrinolytics are indicated for patients who present with a STEMI (which is the most severe type of heart attack and is characterized by the completely blocked off coronary artery). In within 12 hours of symptom onset without a contraindication. Absolute contraindications to fibrinolytic therapy include history of intracranial hemorrhage, ischemic stroke or closed head injury within the past 3 months, presence of an intracranial malignancy, signs of an aortic dissection, or active bleeding. An example of this type of drug are plasminogen activators, which have been shown to restore normal coronary blood flow in 50% to 60% of STEMI patients.

Glycoprotein IIb/IIIa Antagonists

Glycoprotein IIb/IIIa receptors on platelets bind to fibrinogen in the final step of platelet aggregation. Antagonists to glycoprotein IIb/IIIa receptors are potent inhibitors of platelet aggregation. The use of these inhibitors during percutaneous coronary intervention (PCI) and in patients with MI and acute coronary syndromes has been shown to reduce the risk of death, reinfarction, and the need to revascularize the target lesion at follow-up.

Supplemental Oxygen

Oxygen should be administered to patients with symptoms or signs of pulmonary edema or with pulse oximetry less than 90% saturation. Because MI impairs the circulatory function of the heart, oxygen extraction by the heart and by other tissues may be diminished. Supplemental oxygen guarantees that erythrocytes will be saturated to maximum carrying capacity. The recommended duration of supplemental oxygen administration in a MI is 2-6 hours, longer if congestive heart failure occurs or arterial oxygen saturation is less than 90%. However, there are no published studies demonstrating that oxygen therapy reduces the mortality or morbidity of an MI.

Concerning the surgical approach for restoring blood flow in a MI, several solutions are applied, depending on the severity of the damage and the specific clinical pre-status of the single patient. A set of the most common interventions is listed below.

Percutaneous Coronary Intervention

PCI consists of diagnostic angiography combined with angioplasty and, usually, stenting. It is well established that emergency PCI is more effective than fibrinolytic therapy in centers in which PCI can be performed by experienced personnel in a timely fashion. Centers that are

unable to provide such support should consider administering fibrinolytic therapy as their primary MI treatment.
PCI can successfully restore coronary blood flow in 90% to 95% of MI patients. Several studies have shown that PCI has an advantage over fibrinolysis with respect to short-term mortality, bleeding rates, and reinfarction rates. However, the short-term mortality advantage is not durable, and PCI and fibrinolysis appear to yield similar survival rates over the long term. PCI provides a definite survival advantage over fibrinolysis for MI patients who are in cardiogenic shock. The use of stents with PCI for MI is superior to the use of PCI without stents, primarily because stenting reduces the need for subsequent target vessel revascularization.

Surgical Revascularization

Urgent coronary artery bypass grafting (CABG) is necessary in case of failed PCI in patients with hemodynamic instability and coronary anatomy amenable to surgical grafting. Surgical revascularization is also indicated in the setting of mechanical complications of MI, such as ventricular septal defect, free wall rupture, or acute mitral regurgitation. Restoration of coronary blood flow with CABG can limit myocardial injury and cell death if performed within 2 or 3 hours of symptom onset.

Implantable Cardiac Defibrillators

It has been observed a 31% relative risk reduction in all-cause mortality with the prophylactic use of an Implantable Cardiac Defibrillators (ICD) in post-MI patients. Nevertheless, the current guidelines recommend waiting 40 days after an MI to evaluate the need for ICD implantation.

Heart transplantation [33]

Heart transplantation is the procedure by which the failing heart is replaced with another heart from a donor. It is appropriate for patients with end-stage congestive heart failure (CHF) and a life expectancy of less than one year without the transplant or that have not been helped by conventional medical therapy or that have been excluded from other surgical options because of the poor condition of the heart.
Temporary therapies, including the described oral pharmaceutical agents or mechanical support with the intra-aortic balloon pump (IABP) or implantable assist devices (left ventricular assist devices), can be for some patients as a bridge to transplantation. However, mechanical support does not improve waiting list survival in adult patients with congenital heart disease.
The annual frequency of heart transplantation is about 1% of the general population with heart failure. Improved medical management of CHF has decreased the candidate population; however, organ availability remains an issue [33].

1.4.2 Regenerative Medicine and Myocardial Tissue Engineering

Despite optimal medical therapy, thousands of patients per year worldwide, who survive an extensive myocardial infarction, develop advanced heart failure [34]. Heart transplant remains the best solution to patients with this pathology but problems such as the decrease of donor supply, that increase the gap between supply and demand for heart replacement therapies, are still present. Left ventricular assist devices may provide a temporary therapeutic solution for patients with heart failure, but they serve as only a bridge to transplantation and do not provide a definitive therapy [35]. As a result, there has been great interest in alternative therapeutic strategies to treat this common and deadly disease [36].
Cardiac regeneration is an exciting novel therapeutic approach for the treatment of heart diseases, in particular of infarcted myocardium. The revolutionary base-concept introduced by Regenerative Medicine consists in growing heart muscle and vascular tissue through cellular therapies. Cardiac repair strategies mainly include the direct transplantation of cells into damaged environments and Tissue Engineering (TE) techniques for the development of replacement tissue.

1.4.2.1 Cell injection therapy

Transplantation or injection of cells has been researched since the early 1990's and focuses on repopulation of the injured myocardium by the use of healthy cells. Although the mechanism of myocardial tissue regeneration has not been completely cleared, many researchers have demonstrated that transplanted cells secrete several cytokines which promote neovascularization, prohibit fibrosis, and recruit stem cells, leading to heart function improvement [37]. Several cell types have been considered, such as fetal cardiomyocytes, skeletal myoblasts, and bone marrow stem cells. Nevertheless, they have all shown to be not efficient in restoring damaged heart tissue and its function, since they failed to produce new myocardial tissue, causing cell loss and cell death after engraftment [36].
According to cell sourcing, different routes are used for cell administration. Systematic intravenous infusion is performed through a central or peripheral vein. This method is simple and less invasive, although widespread distribution cause low ratio of cell engraftment. The most common approach is intracoronary cell infusion via a balloon-catheter. Injected cells are reached directly in the target myocardial region but cells have to transmigrate across the endothelium wall. Intracardiac injection is performed via pericardium during open heart surgery and via endocardium by a catheter with a 3-D electromechanical mapping system (NOGA mapping system). These methods realize relatively targeted delivery, but problems such as myocardial damage and arrhythmia induction may arise.
Future clarification will be needed to understand which is the best approach for cell injection [37].

Skeletal myoblasts

Skeletal myoblasts were the first cell source to be used in clinical applications for cardiac repair.

They lie in a quiescent state on the basal membrane of myofibers and can proliferate and differentiate into skeletal muscle in response to muscle damage. They can be isolated autologously and be expanded from a single biopsy. In addition, they are relatively resistant to ischemia. Menasche and colleagues first applied skeletal myoblast injection via epicardium for patients undergoing coronary artery bypass grafting (CABG) [38]. Although the phase I clinical study have shown the feasibility of the implantation of this type of cells, it increased risk of ventricular arrhythmias after the operation [39]. On the other hand, the trial indicated the possibility that high dose cell injection might recover left ventricular dilatation. Therefore, this cell source should not be excluded for heart tissue repair [37].

Bone marrow-derived cells

Bone marrow-derived cells are the most used cells in clinical trials for myocardial tissue repair [40]. Bone marrow cells contain different stem and progenitor cells which can differentiate into various types of cells including endothelial cells, smooth muscle cells and cardiomyocytes. Bone marrow mononuclear cells (BMNCs) can be isolated simply by gradient sedimentation after bone marrow aspiration without culture expansion. BMNCs include heterogeneous cell population of monocytes, hematopoietic stem cells and endothelial progenitor cells (EPCs). As another cell population, mesenchymal stem cells (MSCs) have been deeply researched and clinically used. MSCs represent between 0.01 and 0.001% of all nucleated cells in bone marrow but they can be readily expanded in culture. These cells have the potential to differentiate into various types of cells and seem to differentiate into myocardial cells when injected in heart. Recent studies have revealed that MSCs rarely differentiate into cardiomyocytes and that recover of heart function is due to their cytokine secretion and partial differentiation into vascular cells. As a unique feature, MSCs have the potential to escape from immune detection due to the direct inflammatory inhibition and the lack of cell-surface molecules. This property allowed allogenic mesenchymal stem cell transplantation to be applied in the clinics, with consequent high impact on the cell therapy research field [37].

Adipose-derived stem cells

Adipose tissue-derived stem cells (ASCs) are stem cells isolated from the stroma of adipose tissues. They have features similar to that of bone marrow-derived MSCs with additional angiogenic potential. Some studies have also revealed cardiomyocyte differentiation from ASCs. It has not been clarified which mesenchymal stem cells are superior to other cell types, however, relatively easy isolation of adipose tissue may push the clinical application of ASCs [37].

Cardiac stem cells

Another possible cell source for myocardial tissue regeneration is given by cardiac stem cells (CSCs), discovered by two research groups in 2003 [14, 41]. Until then, it was common knowledge that heart was a post mitotic organ, but those reports pushed the researches to identify surface marker of CSCs and culture them. Islet-1, Sca-1 and c-kit have been known as

CSC markers. Recently, it has been also confirmed that heart has renewal ability at normal state and the annual rate of turning over is 1% at the age of 25 [42]. Although the ability of CSCs may increase after heart injury, newly formed cardyomyocytes are not sufficient for replacing damaged muscle tissues. Therefore isolation and expansion of CSCs have been extensively examined. Some groups have used the approach of cardiospheres from biopsied myocardium, which lead to efficient CSC expansion [37, 43]. This type of study will be discussed in chapter 4.

Embryonic stem cells

Although many studies have demonstrated that MSCs, ASCs and CSCs have the potential of cardiomyocyte differentiation for their gene and protein expression, there are no studies clearly showing beating cardiomyocytes differentiated from those stem cells. On the other hand, several researchers have showed that embryonic stem cells (ESCs) can differentiate into beating cardiomyocytes *in vitro* and that implantation of ESC-derived cardiomyocytes improves damaged heart function. Fibloblast growth factor (FGF), retinoic acid, ascorbic acid and cyclosporine A seem to enhance cardiac differentiation from ESCs. An important issue is also the purification of cardiomyocytes from heterogeneous cell mixture, because the presence of immature cells leads to teratoma formation [44]. Immune response of the host is another critical issue. Nuclear transfer or cell banking is a possible approach to avoid immune-reaction. Electrical communication and simultaneous beating of implanted ESC-derived cardiomyocytes should be also requested for improving damaged heart function without arrhythmia. *In vivo* electrophisiological analyses and the transplantation technology for synchronization will be essential for clinical application of these cells [37].

Induced pluripotent stem cells

Induced pluripotent stem cells (iPSCs) also seemed to be promising for myocardial tissue engineering [5]. Terminally differentiated cells can be reprogrammed to have the same potential as ESCs by introducing 3 or 4 transcriptional factor genes. The advantageous aspect of iPSCs to ESC is that these cells are autologous and therefore do not cause immune response. Cardiac differentiation of human iPSCs has been reported as for ESCs. Several critical issues must be clarified for clinical use, but ESCs/iPSCs-derived cardiomyocytes should give a very significant contribution to myocardial tissue engineering especially for their pulsatile function [37].

1.4.2.2 Problems of cell injection therapy

Cell injection therapies for heart failure are now world-widely performed. Nevertheless, although moderate success of direct cell injection has been observed, none of the cell types studied seemed to trigger the restoration of the damaged heart tissue and its function, since they failed to produce new myocardial tissue, causing cell loss and cell death after engraftment

[36]. Optimization of cell source, cell preparation process, injection route, injection timing and patient population are needed to increase the effectiveness of this therapy.
One of the essential issues is the procedure adopted for cell delivery, since cell injection therapy has significant difficulties about cell retention in the target tissue. The shape, size, and position of the grafted cells are often uncontrollable and large amount of the cells are washed-out. In addition, most of retaining cells die due to necrosis and apoptosis. In the clinical trial using bone marrow-derived cells, it has been also demonstrated that only 1-3% of the cells infused via coronary arteries could be detected by 3D positron emission tomography imaging of the patient heart. In this study, a large percentage of cells were found in the liver and spleen immediately after the operation [45].
To solve the problem of cell loss, hydrogel-cell mixture injection has been considered. Fibrin, collagen and alginate hydrogels are now used as carriers. They are injected with cells as a liquid phase through syringe or catheter and fixed in the target tissues [46]. In hydrogel-cell mixture injection therapy, local tissue damage due to space occupation of hydrogel itself and inflammatory reaction due to hydrogel biodegradation products can turn out problematic. In conclusion, more advanced cell delivery systems are required to spread cell therapy as a reliable treatment for myocardial infarction [37].

1.4.2.3 Myocardial Tissue Engineering

Tissue engineering adopts the principles of engineering and of life sciences in order to understand the structure-function relationships in normal and pathological tissues and to develop engineered substitutes that can restore, maintain or improve native tissue and organ function.
The approach of myocardial TE is based on the transplantation of a tissue-engineered construct ("myocardial patch") covering the damaged heart surface instead of simple cell injection into myocardium. Grafted cells within myocardial patches can survive more and secrete more cytokines, resulting in increased heart function improvement [37].
As illustrated in figure 1.5, scaffold-, hydrogel- and cell sheet-based TE are three different strategies for *in vitro* myocardial patch fabrication. The most popular strategy consists in seeding cells into 3-D pre-fabricated biodegradable scaffolds which are made from synthetic polymer or biological material [37]. As showed in detail in figure 1.6, specific cells are isolated through a biopsy from a patient (a) and expanded (b), to grow them on a three-dimensional (3D) biomimetic scaffold under precisely controlled culture conditions (c, d), to implant the construct to the desired site in the patient's body (e), and to direct new tissue formation into the scaffold that can be degraded over time. As it will be discussed in the following section, scaffold modification can control its biodegradation and tissue formation while the presence of biomolecules, such as growth factors, leads to acceleration of tissue formation.

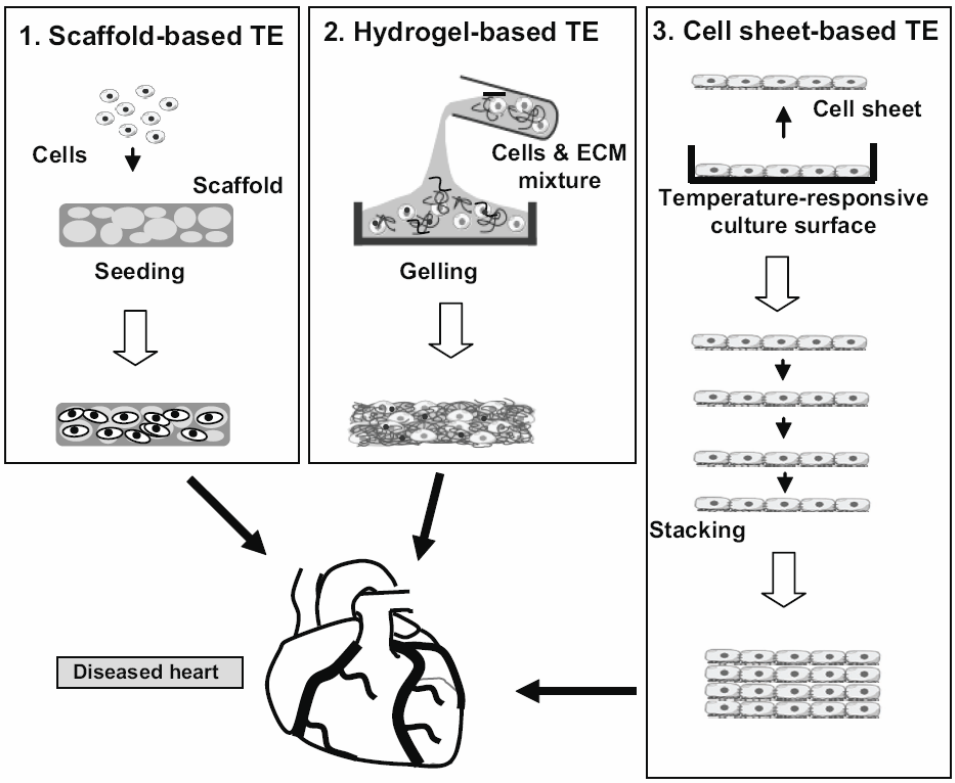

Fig. 1.5 Tissue engineering in vitro strategies for myocardial repair.

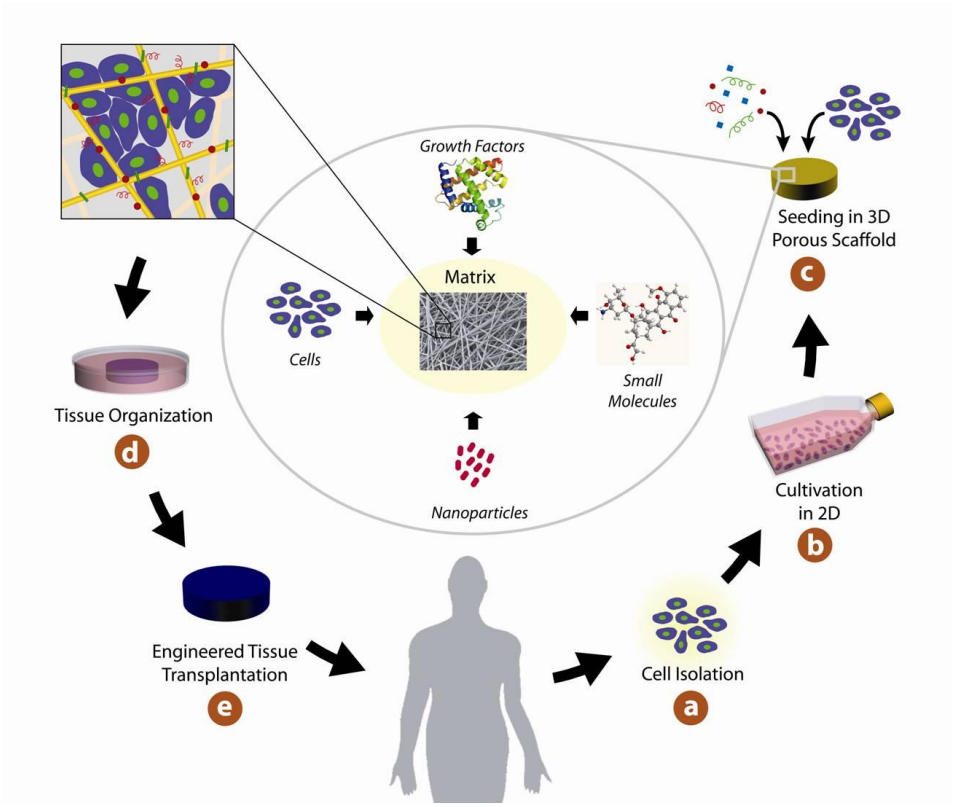

Fig. 1.6 Classic scaffold- based TE in vitro strategy [47].

The second approach is to form 3-D tissues by gelling of cardiac cells and matrix solution mixture. Generally collagen gel is used to suspend cells. The mixture is poured into a mold and after gelling, constructs are stretched with a mechanical devise [48].
In contrast to scaffold- and hydrogel-based tissue engineering, another approach has been developed, involving 2-D cell sheet stacking to fabricate 3-D tissues without scaffold [49]. Cell sheets are harvested from smart "temperature-responsive culture surface", which are covalently grafted with temperature-responsive poly(*N*-isopropylacrylamide) (PIPAAm) [50]. The surfaces are slightly hydrophobic and cell-adhesive at 37°C, while they change into hydrophilic and not cell adhesive below 32°C. Confluent cultured cells on the surface can detach as a whole cell sheet simply by reducing temperature. Cell sheet-based TE has been employed for several regenerative medicine applications, including corneal epithelial replacement, heart tissue and liver repair.
Concerning the optimal cell for *in vitro* myocardial TE, it should be easy to harvest, proliferative, nonimmunogenic, and has the ability to differentiate into mature and functional cardiomyocytes. As for injection cell therapy, several cell types have been proposed for myocardial tissue engineering, including donor (allogenic) and autologus cells. Allogenic cells are relatively easy to obtain but can provoke immune suppression. Autologous cells, on the other hand, are more difficult to obtain and to expand but cause no immunological reaction. Cardiomyocytes appear to be the ideal donor cell type due to their natural electrophysiological, structural, and contractile properties. However, cardiomyocytes are difficult to obtain, to expand, are sensitive to ischemic insults, and are allogenic, evoking an immune response in the host tissue. The use of autologous adult stem cells is particularly restricted by their low recovery from the bone marrow, adipose tissue, or circulation, and therefore, the difficulty in obtaining reasonable numbers of cells [51].
Furthermore, as previously discussed, safety issues have been raised regarding the use of various cells for myocardial repair: arrhythmias with skeletal myoblasts [39], cardiac calcifications with bone-marrow mononuclear cells [52], myocardial scarring with mesenchymal stem cells [49], and teratoma with human embryonic stem cells [44]. However, the search for an efficient and reproducible method to control and direct cell proliferation and differentiation, in myocardial tissue engineering continues.
In addition to in vitro TE strategies, *in vivo* TE methods has been investigated. While i*n vitro* TE envisages the use of a culture dish or a bioreactor to produce an engineered cardiac graft from a scaffold or gel seeded with cells, *in vivo* TE uses an unseeded scaffold recruiting endogenous cells after implant [36]. Injection of thermo-responsive polymeric solutions (hydrogel forming at body temperature) are also included in this type of approach. A wide range of hydrogels from purely biological materials such as fibrin, collagen and alginate to the fully synthetic ones such as polyethylene glycol (PEG) and thermoresponsive poly-N-isopropyl acrylamide hydrogels have been shown to provide potentially therapeutic outcomes after delivery. Decreased infarct size, increased wall/scar thickness, reduction of LV remodeling and improvement of functional parameters have been demonstrated [53].
Both in the case of seeded and unseeded scaffolds, crucial issues, that are objective of TE researchers, are the appropriate scaffold 3D-structures and their chemical, biological and mechanical properties, as discussed in the following sections.

1.4.2.3.1 Scaffold and biomaterials requirements for MTE

TE approach is particularly appropriate for the regeneration of tissues that require a mechanical support to the reparative process, such as the cardiac one [36]. As already discussed, one of the most fatal consequences of MI is LV remodeling, which consists in changes in size, shape, and function of the ventricle and is due to the cascade of biochemical intracellular signals that regulate the reparative processes, such as dilatation, hypertrophy, and the formation of a collagen scar [54]. As a consequence, a critical requirement for a MTE scaffold (also called *heart patch*) is to mechanically support the infarcted left ventricle. In order to restore its right shape and functionality, a heart patch should show suitable strength and an elastomeric mechanical behavior, able to temporarily support the regeneration of the contractile tissue. However, a 3D scaffold may offer other several advantageous functions: (i) to temporarily replace the injured tissue, providing a transitional support to cell colonization, migration and proliferation and degrading with times compatible with native tissue regeneration; (ii) to allow the control over graft dimensions, shape, mechanical properties and composition; (iii) to avoid cell loss, a process that generally takes place with cell injection, where about 90% of the injected cells is lost to the blood circulation and 90% of the successfully injected ones dies within a week; (iv) to control their distribution in the infracted area (generally 1.3-17.8% of the injected cells reaches the infracted area [123]) [122, 124-126].
In order to fulfill the described functions, MTE scaffolds have to meet restrictive requirements that concern both the biomaterial and the structure of the substrate.
The first and most important requirement is ECM biomimicry: the scaffold should replicate cardiac ECM properties in terms of chemical and biological characteristics (to interact with the surrounding cells), structure, morphology and mechanical behavior [55]. Therefore, the scaffold has to be able to promote specific cellular responses during the regeneration process [56].
The biological and chemical biomimicry can be mainly obtained selecting an appropriate biomaterial. It should show not only cell- and tissue compatibility with a minimal inflammatory response after implantation, but especially the capability to support cell attachment, differentiation, and proliferation. In order to achieve specific interaction with cells, biomaterials are often enriched with bioactive molecules, such as growth factors. In MTE, a crucial role is assigned to the vascular endothelial growth factor (VEGF), whose concentration in the micro-environment around the implanted matrix seems to be very important for the development of vascular networks. It has also observed that an excessive amount of VEGF can cause an abnormal growth of blood-vessels [57]. So far, significant therapeutic effects of VEGF have not been reported, probably due to its short half life after direct injection in bolus. The tuning of VEGF release kinetics over time through the use of scaffolds loaded with micro- or nano-particles could offer a solution [58].
Biomimetic materials may be obtained also by the incorporation of proteins or peptides able to specifically interact with receptors on the cellular surface. Whole proteins, such as Fibronectin and Laminin (cell adhesion proteins of the ECM), are characterized by low stability and availability and high costs. As alternatives, cheaper and more stable short peptides, containing the amino acid sequences that are responsible for the bioactivity of these proteins, can be synthesized [59, 60] and linked to the polymer chains (bulk modification) or to the

biomaterial surface (surface modification). In the case of surface modification, both the chemical nature of the ligand and the spatial distribution on the material's surface have to be considered to have a successful biomaterial-cells interaction [59]. Bulk modifications may be achieved through a copolymerization reaction or by attachment of functional groups to the polymer chains, followed by reaction with the desired biomolecule. Since these reactions can alter polymer mechanical properties and its processability, surface functionalization is generally preferred to bulk modification. Surface functionalization is often carried out introducing functional groups, such as amino and carboxylic groups, by irradiation (e.g. plasma), layer-by-layer coatings, or chemical methods (e.g. aminolysis). These groups can successively react with proteins or peptides forming amide bonds [61].

Another key requirement for MTE scaffolds is (bio)degradability: scaffolds should degrade *in vivo* at rates compatible with cardiac tissue regeneration, after myocardial functions have been restored, without the release of toxic products. This property and its kinetics strongly depends from the chemical characteristics of the biomaterial and, in case of enzymatic degradation, from the porosity grade of the scaffold. Since enzymatic degradation processes generally take place on the scaffold surface, the rate of the degradation process can depend on the amount of exposed surface.

Porosity is also fundamental for the promotion of cell penetration, tissue growth and vascularization and nutrient delivery [62]. In detail, a MTE scaffold should have an interconnected porous structure, with appropriate pore dimensions. It is known that large pores favour cell colonization and migration and nutrients supply, while small pores (tens μm) can promote vascularization [55, 63, 64]. A pore diameter of about 40 μm seems to be the right compromise to favor cellular homing and migration, vascularization and nutrients, metabolites and oxygen diffusion [55, 64].

Since myocardial infarction can damage up to 50 g of tissue [65], scaffold micro-architecture should be characterized by high cellular density, capillary density in the range of 2400-3300 capillaries/mm^2 and intercapillary distance of about 20 μm [57, 62, 66].

It has also observed that the presence of oriented and well-defined pores has positive influence on the mechanical and biological performance of scaffolds for tissues with anisotropic mechanical and structural properties, such as muscles, since they are able to guide tissue regeneration and mechanical transduction along preferred directions [63, 67, 68]. In particular, *in vitro* cell tests showed a higher cell viability and a greater amount of ECM on scaffolds with an oriented internal structure, probably because a more efficient cell seeding and nutrients and oxygen diffusion are promoted [67, 68]. Based on these results, MTE researchers have recently given an higher attention on scaffold topography and internal architecture, besides to bioactive functionalization of biomaterials.

Concerning matrix thickness, some restrictions exist for non-porous membranes since the maximum distance that nutrients and oxygen are able to cover by diffusion is 200 μm. A possible solution to this restriction can be the promotion of angiogenesis [65, 69].

For both dense and porous matrices, mechanical features are particularly important since the heart patch should restore the heart geometry and provide a mechanical support to the damaged left ventricle, accommodating to the rhythmic movements of the heart without plastic deformation or failure [70]. This goals can be achieved if scaffolds have mechanical

properties mimicking those of the native tissue, where the most abundant ECM protein is elastomeric collagen.

The myocardium collagen matrix mainly consists of types I and III collagens, characterized by different physical and mechanical properties. Type I collagen mainly provides rigidity, while type III collagen contributes to elasticity. The two types of collagens jointly support myocytes to maintain their alignment, whereas their tensile strength and resilience resist the deformation, maintain the shape and thickness, prevent the rupture and contribute to the passive and active stiffness of myocardium [71]. The content of different collagen types is very important for the resulting mechanical performance of the heart. It is well known that tissues with predominance of type I collagen (such as tendon) are characterized by relatively higher strength and stiffness, whereas tissues containing large amount of type III collagen (such as skin) are characterized by greater flexibility (compliance) [71]. After myocardial infarction, the fibrotic phase of cardiac reparative process is characterized by collagen deposition that induce structural and mechanical changes. In detail, an increase of collagen type I takes place and this process can explain the observed increase in tissue stiffness.

A more direct reference for the mechanical requirements is given by the mechanical properties of heart muscle. Figure 1.5 shows that the passive strains of the heart muscle could reach values up to 15–22% at the end of diastole. Therefore the heart muscle mainly works within the nonlinear elastic region. The stiffness (Young Modulus) of the heart muscle about 10–20 kPa at the early stage of diastole (strain <10%), and rises up to 50 kPa (healthy heart) or 200–300 kPa (congestive heart failure) at the end of diastole. Stress and strain at break should be respectively in the ranges of 3-15 KPa and 22-90% [72, 73].

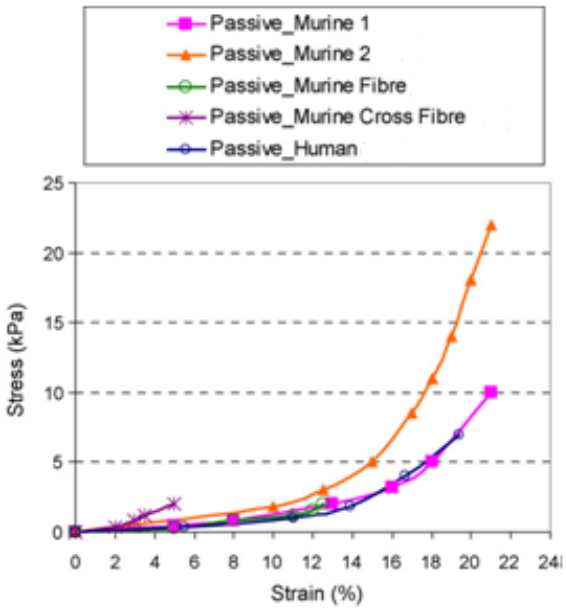

Fig 1.6. Passive stress-strain curves of heart muscles of different murine and human [74].

Consequently, an ideal heart patch should be characterized by Young Moduli encompassing from tens of kPa to 1MPa [62] and by an elastomeric behaviour, able to withstand the contractile and expansive forces originated during the cardiac cycle [74].
Based on the described requirements for MTE scaffolds, both several biomaterials and scaffold fabrication techniques have been deeply explored in search of a suitable chemical formulation and scaffold architecture able to promote cardiac tissue regeneration.
In the next sections, an overview of the main polymeric materials (natural and synthetic) studied and used in myocardial tissue engineering (see Table 1 for a list) and of the different conventional and unconventional technique for scaffold preparation are discussed.

Table 1. Natural and synthetic polymeric materials for myocardial tissue engineering.

Natural materials	**Synthetic Materials**
Collagen	Polylactide (PLA)
Gelatin	Polyglycolide (PGA)
Matrigel	Polylactide-co-glycolide (PLGA)
Fibrin	Poly-ε-caprolactone (PCL)
Alginate	Poly(glycolide-co-caprolactone) (PGCL)
Cellulose	Polyurethanes (PUR)
	Poly(Glycerol Sebacate) (PGS)
	Poly(1,8-octanediol-co-citric acid) (POC)
Chitosan	Poly(L-lactic acid)-*co*-poly(ε-caprolactone) (PLACL)
Hyaluronic Acid	Poly(N-isopropyl acrylamide) (PNIPPAm)
Silk Fibroin	Polyaniline (PANi)

1.4.2.3.1.1 Natural polymers

Natural polymers are generally highly biocompatible, leading to a weak *in vivo* inflammatory response and providing a natural substrate for cell attachment, proliferation, and differentiation in their native state [75]. They particularly favour cell attachment and proliferation, due to their adhesion properties [76, 77]. Despite these positive features, natural polymers are often characterized by poor mechanical properties, poor workability and rapid degradation kinetics, which limit their clinical applications [76-78]. In addition, depending on their source, proteins can provoke immune rejection or pathologies and the transmission of disease [79].
These types of natural polymers are generally ECM components [78, 80]. It is well known that ECM has a fundamental role for tissue life, since it provides support to cells, regulates the intercellular communication and is a storage of growth factors [81]. Recent studies suggest that it is also deeply involved in the regulatory and electromechanical aspect of myocardium functions [79, 82, 83]. To sum up, ECM has proven to be essential for cell survival, differentiation, proliferation, metabolism, and integrative function, both under *in vivo* and *in vitro* conditions [79].
These results induce research efforts of cardiac tissue regeneration towards the design of materials as similar as possible to the ECM. Among natural polymers, collagen, gelatine, fibrin and alginate have been mainly investigated.

Collagen, Matrigel and Gelatin

Collagen is the major constituent of ECM [81, 84]. Myocardium collagen matrix mainly consists of type I and III collagens, which are synthesised by the same type of cells, cardiac fibroblasts, but are characterized by different physical and mechanical properties, providing rigidity and elasticity, respectively [85].
For a long time, collagen, mainly of type I, has been used in biomedical applications as haemostatic agent for tissue injuries [86]. After its regenerative properties were discovered, it found applications in 3D cell culture for TE [79]. Research groups in Germany (Eschenhagen, Zimmermann [87], Kofidis [88, 89]) and Canada (Akhyari [88, 89]) are currently working with collagen for myocardial tissue regeneration. Kofidis and Akhyari have developed a novel tissue engineered myocardial construct using a clinically approved collagen-based matrix (Tissue Fleece®, bovine collagen type I) [88, 89], while Eschenhagen and Zimmermann have studied a mixture of liquid collagen type I, Matrigel® [87]. This material is a basal membrane extract from a sarcoma cell line and is characterized by the presence of collagen, other several ECM proteins and bioactive substances such as growth factors. This liquid natural mixture offers some advantages such as versatility, since it can be combined with other ECM components, and the possibility to be casted in the desired shape. Nevertheless, its growth factors content and the regulatory approval for use in humans of some of its components have been questioned [79].
Several researchers have achieved good results in heart tissue regeneration by the use of gelatin, denaturated collagen, obtained from connective tissue of bones, ligaments, tendons and cartilage [76], although it can induce an unspecific inflammatory response that can affect the survival and function of the inoculated cells inside the implanted matrix [79]. In 1999 Li and co-workers used a gelatin-mesh to seed foetal rat ventricular muscle *in vitro* [90]. The commercial product of this kind of gelatin is a foam, known as Gelfoam, made from purified pork skin and supplied by Upjohn, Ontario, Canada [75]. Both Akhyari and Zimmermann used Gelfoam to seed heart cells [87, 91, 92]. Zimmermann described the improvement of the proliferation of seeded human heart cells as a consequence of applying cyclical mechanical stress to the material [91].

Fibrin

Fibrin, a natural polymer which has gained FDA approval for human use [93] is obtained from fibrinogen by a thrombin-mediated reaction. When fibrinogen is converted into fibrin, a provisional matrix is produced. Then, a degradation process by Membrane Metalloproteases (MMPs) starts and the fibrin matrix is replaced by an ECM, rich in collagen, hyaluronic acid and fibronectin [84, 94].
This process is used by myocardial engineering through *in situ* matrix formation. By varying the concentration of fibrinogen it is possible to modulate density and mechanical strength [95], while variation of the amount of thrombin or the addition of acetone can affect not only the mechanical properties but also the conformation of the matrix [96]. Unlike other xenogenic natural polymers, such as gelatin and collagen, fibrin can avoid the inflammatory response, since it can be extracted from the patient's own blood [97]. Biological interaction

with the enclosed cells can be improved by the use of additives in the mixture before polymerization. An advantage derived from the addition of thrombin to the reaction mixture is the possibility to postpone polymerization after injection in the infarcted area [96]. Moreover, this approach permits an alignment of the fibrin-cell mixture within the myocardial fibers, that results in an increase of cell survival, a reduction of the infarct scar size and microvessel formation [98, 99].
There are several studies of the beneficial effects of the use of fibrin in infarcted myocardium, especially on neovascularization [100] [101]. Nevertheless, myocardium repair through the use of fibrin remains limited. Although the mechanical properties of this natural polymer can be tuned, they remain low compared with the properties of native tissue, and cardiac remodeling cannot be prevented [102] [103].

Silk Fibroin

Among natural polymers for TE, silkworm silk protein fibroin shows the highest mechanical performance. Scaffolds (10mm in diameter and 10mm in height) obtained by Antheraea mylitta silk protein fibroin are characterized by 84 kPa of compressive strength [104], while collagen and chitosan scaffolds have a mechanical strength of 15 kPa and 45 kPa, respectively [105]. In particular, this non-mulberry silk fibroin has shown to be mechanically superior to mulberry silk (Bombyx mori silk fibroin) [104] and highly biocompatible, with low level of inflammatory response [106] [107].
Recently, Patra and co-workers have thoroughly studied fibroin from Antheraea mylitta (AM), containing RGD sequences, as potential biomaterial for 3D cardiac tissue engineering scaffolds, comparing it with Bombyx mori silk fibroin (BM), gelatin and fibronectin [108]. 2D matrices have been used to investigate cellular metabolic activity, cell to-cell communication, cell cycle activity and contractility, with very promising results. Adhesion test on cardiomyocytes have revealed that only after 6 hours, significantly more cells attached on AM, with respect to BM and gelatin, with no differences with fibronectin, the positive control. MTT assays showed a similar trend: cardiomyocytes on AM and fibronectin exhibited similar metabolic activity at all investigated time points, and it was always higher than the activity of cardiomyocytes on BM. Finally, immunofluorescence analysis showed that cells on AM and fibronectin contained aligned sarcomeres, crucial for a high contractility, and expressed high amounts of connexin 43, an important protein which regulates electrical signal propagation, in correspondence of cellular junctions.

Alginate, Cellulose, Chitosan and Hyaluronic acid

Alginate, cellulose and hyaluronic acid belong to the class of polysaccharides, but only hyaluronic acid derives from the native ECM [109, 110].
Alginate is made up of mannuronic acid and guluronic acid units, which can form different sequences affecting the 3D structure [110]. It is mainly produced by a brown seaweed, but also by certain types of bacteria [76]. It is known for its capacity to form hydrogels in the presence of calcium ions [110]. These calcium-alginate hydrogels have been used to encapsulate different type of cells [111-113]. Leor et al. investigated cardiac cell proliferation in alginate

porous scaffolds with very promising results. Cells showed viability not only during the culture *in vitro* but also during the successive implantation, after which the scaffold was completely absorbed in 9 weeks [114].
Cellulose has found several applications in the biomedical field but it has only recently been investigated as myocardial tissue engineering material [115]. It is the most important structural components of plants and made of glucose based units linked by 1,4-beta-glucosidic bonds [110]. It is known for being poorly water soluble and not digestible for mammals [110, 115]. Entcheva et al. tested cellulose acetate and regenerated cellulose as substrates for the growth of cardiac cells *in vitro*. Both materials proved to be easily casted in molds with micro and sub-micro grooves and their scaffolds showed their potential for promoting cardiac cell proliferation and improving cell connectivity and electromechanical functionality. They also revealed *in vitro* resistance to biodegradation [115]. From the studies of Martson's group, cellulose showed to be slowly degradable also *in vivo* [116].
Chitosan is a polysaccharide derived from the partial de-acetylation of chitin, found in crustacean shells, and made of β(1-4) linked D-glucosamine units [117]. For a long time it has been studied and used for bone and dermal tissue regeneration but recently it has been investigated for cardiac tissue repair, mostly as injectable hydrogel [118-120]. However, several properties of this naturally occurring polymer have induced Nicole et al. to study and use it as a scaffolding material for myocardial regeneration [121] as will be described in detail below. The pH dependence of solubility of chitosan allows polymer processing under mild conditions and the fabrication of porous scaffolds and membranes [122]. The structural similarity with glycosaminoglycans and the hydrophilic surface [123] can allow specific interactions with ECM-biomolecules, such as growth factors and receptors. In addition, degradation kinetics of chitosan are well known [124]: chitosan membranes can be degraded *in vivo* by macrophages in 12 weeks. Finally, chitosan is not only biocompatible but also non thrombogenic [125-127].
Hyaluronic acid acts in the ECM as space filler and significantly contributes to the mechanical properties of a tissue, by linking proteoglycans and maintaining hydration [109]. Its fragments are very important from a biological point of view, since they have a bioactive role in several regulatory processes, such as angiogenesis, inflammation, wound healing, tissue regeneration and tumor growth [128, 129]. Although positive results on cell differentiation in cardiomyocites have been reported for hyaluronic acid based substrates [130], this biopolymer often needs to be mixed with other ECM components, both natural and synthetic, in order to improve the mechanical and biological performance of the scaffold [131, 132].

1.4.2.3.1.2 Synthetic polymers

Synthetic materials are widely used in myocardial tissue regeneration, due to some excellent characteristics. First of all, they generally show superior mechanical properties than natural polymers that make them suitable for mechanical support and resistance to cyclic stress of force-generating contractile tissue [75, 78]. In addition, these properties, together with hydrophilicity and degradability, can be controlled in a reproducible manner. Their drawbacks regard their often poor interaction with cells and the biological environment [78]. Although synthetic polymers are designed as biodegradable and biocompatible in order to be used for

TE applications, they inevitably induce a higher inflammatory reaction with respect to natural ones [55]. Nevertheless, they can be replaced *in vivo* by native ECM created by the cells seeded inside the scaffolding material, after a period depending on the degradation/erosion properties of the polymer [75, 78] and their use eliminates pathogen transmission risks, which can be caused by some biological materials [79].

Polyesters

The most popular synthetic polymers employed in cardiac tissue regeneration are degradable polyesters, mainly synthesized from lactide, glycolide and ε-caprolactone. Although their biocompatibility has been proved and several reports on their successful applications in regenerative medicine exist, synthetic polymers have not yet considered optimal scaffolding materials. They are basically hydrophobic, preventing a good cell adhesion, and tend to crumble rather than slowly degrade. In addition, their acid biodegradation products can induce high inflammatory responses, and a drop in local pH, upon degradation process, can affect the viability of the surrounding cells [78].
Depending on the monomer, mechanical, physical and degradation properties of these polyesters can greatly change. For example, polylactide (PLA) is characterized by a higher hydrophobicity with respect to polyglycolide (PGA) and, as a consequence, by a higher resistance to hydrolytic degradation. From a mechanical point of view, the higher stiffness and plasticity allow it to support the structural integrity of 3D cell cultures [79]. Several research groups investigated PGA and PLA matrices for myocardial regeneration. Bursac's group explored the *in vitro* engineering of PGA scaffolds with neonatal rat ventricle myocytes cultured in a bioreactor. After one week, they observed differentiated cardiac myocytes, organized in multiple layers [133]. Ke et al. studied embryonic stem cells (ESCs)-seeded PGA patches after implantation on infarcted hearts in mice and observed that after 8 weeks the biodegradable matrix guarantees the survival of the engrafted cells [134]. From the combination of lactide and glycolide, copolymers (PLGA) with new properties have been obtained. Like PLA and PGA, PLGA has a long history in clinical applications, as suture (Vycryl) and TE material [135, 136].
Another frequently employed monomer is ε-caprolactone. Its homopolymer poly-ε-caprolactone (PCL) is known to be biocompatible and to have a long-term degradability, if compared to PLA, PGA and PLGA. PCL has also been used as suture material (Monocryl), but it has found few applications in TE with respect to other polyesters [79]. Nevertheless, the successful use of PCL based scaffold for cardiac tissue regeneration has been reported recently: both Shin and Ishii showed the formation of contractile cardiac grafts *in vitro* using PCL meshes as substrates for cardiomyocytes culture [137, 138]. A copolymer based on glycolide and ε-caprolactone (PGCL) has been evaluated by Piao et al. They demonstrated that a PGCL based scaffold attenuated *in vivo* left ventricular remodeling and systolic dysfunction [139].
In order to encourage cardiomyocytes adhesion or induce cell differentiation in myocardial phenotype, polyester films have been functionalized with adhesion proteins (Fibronectin, Laminin) or RGD based peptides. Brown et al. have investigated the effect of plasma modification followed by fibronectin adsorption on PLGA substrates on neonatal rat

ventricular myocyte (NRVM) function. They observed that NRVMs showed a better spreading and myofibril development on the modified films respect to the unmodified ones and that protein absorption affected gene expression of adherent cells [140]. The differentiation process can be strongly influenced by the particular protein or peptide surface micropattern. The work of Chor Yong Tay has shown that derived human mesenchymal stem cells (hMSCs) cultured on PLGA film with adhesive fibronectin strips were highly elongated, and markers, associated to myogenesis, were up-regulated [141].
Poly (Glycerol Sebacate) (PGS), a synthetic polyester obtained from the polycondensation reaction of glycerol and sebacic acid [142] has been explored by Qi-Zhi Chen et al., as potential material for the production of heart patches. Mechanical characterization of PGS films, synthesized at three different temperatures, demonstrated elastomeric properties very close to those of the heart muscle, with Elastic Moduli in the range between tens kPa and 1MPa. Degradation tests, carried out in PBS (Phosphate Buffered Saline) and DMEM (Dulbecco's Modification of Eagle Medium), showed varying kinetics for the three different PGSs and the consequent possibility to tune this property according to specific clinical requirements [143].
In a recent work by Daniel J. Stuckey and co-workers, PGS films revealed able to reduce hypertrophy in a rat model of myocardial infarction, limiting post-infarct remodeling. In addition, PGS seemed to be more suitable for the delivery of cardiac stem and progenitor cells with respect to other materials, such as poly(ethyleneterephathalate)/dimer fatty acid (PED), and TiO2-reinforced PED (PED-TiO_2). Moreover, its degradation kinetics are compatible with the process of cell assimilation by the heart [144].
Poly(1,8-octanediol-co-citric acid) (POC), obtained by the reaction of 1,8-octanediol and citric acid, has recently been investigated as elastic scaffolding material by Yang et al. Its degradation rates and cytocompatibility can be tuned modifying the conditions for the synthesis and molecular ratios of the reagents [145]. Based on Yang's results, Hidalgo-Bastida and his co-workers have considered this material for cardiac tissue engineering applications. In their work they reported HL-1 cardiomyocyte attachment and survival on POC films coated with fibronectin, collagen or laminin. HL-1 cells adhered to both coated and uncoated films after 18h of incubation. POC uncoated film showed a monolayer of cells covering less than 10% of the total area, while fibronectin coated films showed a higher and quicker cell adhesion and proliferation with respect to collagen- and laminin-coated samples. Moreover, cells seeded on the latter samples did not assume the characteristic elliptical shape of cardiomyocytes. The best biological results obtained with fibronectin coatings can be explained considering that fibronectin is overexpressed during cell migration and proliferation at the embryonic stage of heart development, while collagen and laminin levels increase during heart growth [146].

Polyurethanes

Polyurethanes (PURs) are a large group of polymers widely used in the biomedical and industrial field. Due to the possibility of selecting several different starting reagents (polydiols, diisocyanates and chain extenders), materials with varying chemical, mechanical, biological and degradation properties can be achieved [84, 147, 148]. In cardiac TE, degradable PURs, based on polyester polyols, have been studied for a long time, because of their biocompatibility [76,

77] and elastomeric properties (and, as a consequence, their capability to resist to cyclic stress without plastic deformation or failure) that fit the requirement of materials for cardiovascular applications [149].
Rechichi et al. investigated the tuning of the properties of this kind of polymers by synthesizing and characterizing PCL and PCL-PEG-PCL based polyurethanes with different aliphatic and aminoacid-based chain extenders. Cellular tests with fibroblasts and thermal-mechanical characterizations have showed that all these materials are non toxic and suitable for tissue engineering applications. However, their particular biological and mechanical behavior strongly depends on their chemical composition [150].
Recently, ECM-like PURs have been synthesized, incorporating peptides and bioactive molecules [151, 152]. Amino-acid sequences have been introduced in PUR chains to control the enzymatic degradation process of the resulting scaffolds for myocardial TE. Guan and co-workers, that successfully developed PCL and putrescine based polyurethanes in 2004 [153], more recently prepared an elastase sensitive PUR containing the enzyme-target Alanine-Alanine (AA) sequence as chain extender [68]. The degradation study showed a more pronounced weight loss for the peptide based formulations with respect to putrescine-based PURs in the presence of elastase [68, 153]. As it will be discussed below, Fujimoto and colleagues also successfully explored a biodegradable putrescine based PUR for the preparation of porous scaffolds for cardiac repair [154, 155]. Ciardelli et al. investigated the introduction of an Alanine-Alanine-Putrescine (Ala-Ala-Put) chain extender in a PCL based PUR and compared mechanical, thermal and biological properties of the final polymer with those of other biodegradable formulations, containing aliphatic and Lysine based chain extenders. Although the peptide showed the capacity to be enzymatically degraded to the polymer, tensile tests demonstrated that the Lysine based PUR has the mechanical properties closest to those required for contractile tissue regeneration (low Elastic Modulus and high Strain at Break) [156]. This formulation has also shown the best results in cellular adhesion tests, carried out on myoblasts: on this sample a significant cell spreading was observable already after 3 hours of incubation. This cell response could be linked to the mechanical properties of the polymer, since some cell types appear to be sensitive to substrate stiffness [157].
In order to impart adhesion properties to polyurethanes, laminin coated PURs were realized by McDevitt et al. to pattern cardiomyocyte cultures. They printed laminin lanes 5–50 μm wide on polymer surface to guide cardiomyocyte alignment and observed highly organized arrays [158]. Siepe et al. subsequently investigated the use of myoblasts in similar patterns and have observed that cells survived *in vitro* for several weeks, maintaining the initial spatial distribution. Even if no differentiation in cardiomyocytes was obtained, the investigated substrates seemed to be promising for myocardial tissue engineering [159].

1.4.2.3.1.3 Polymer Blends

A very interesting strategy to produce suitable materials for myocardial engineering is to blend two different polymers, generally a natural and a synthetic one. The purpose is to obtain a material that combines the biocompatibility and the biological ECM properties of the natural

component and the superior mechanical characteristics of the synthetic one, the latter acting as a physical support and degrading then with the desired pattern [76]. In literature, blends where the natural component is either collagen or gelatin have been mainly investigated. Mukherjee's group evaluated the biocompatibility of poly(L-lactic acid)-*co*-poly(ε-caprolactone)/collagen (PLACL/collagen) composite, fabricating nanofibers in order to mimic the native myocardial environment for freshly isolated cardiomyocytes. The study demonstrated that cell proliferation is significantly higher on PLACL/collagen nanofibers with respect to the synthetic co-polymer alone [160]. "Bioartificial systems" based on poly(N-isopropyl acrylamide) (PNIPPAm) with collagen, gelatin and alginate, respectively were also investigated, including a blend of PNIPAAm/alginate/gelatin, and their biological behavior was compared with that of a tri-block poly(ester-ether-ester) co-polymer and a PCL based PUR [161, 162]. Biological analyses were performed on C2C12 cell line of skeletal myoblasts, as a model of a possible cell source for myocardial regeneration. Proliferation and adhesion tests highlighted the best results for collagen and gelatin blends, the three components blend and the two single synthetic polymers, even if a general decrease of cell number at three or five days after seeding, followed by a new increase, is observed. Differentiation tests, evaluated as the elongation of actin filaments, showed to be the most suitable evaluation parameter for the bioartificial systems [162].

Another important subset of polymer blends includes formulations based on conductive polymers that can allow control of tissue contraction and electrical signals transmission [163]. The use of these materials as cell culture substrates shows that some cell functions, such as adhesion, migration, proliferation and differentiation, can be promoted and influenced by electrical cues [164]. In detail, previous studies have highlighted the possibility to induce cell orientation, angiogenesis, muscle tissue regeneration, cardiomyogenesis and mature cardiac phenotype taking advantage of electrical stimulations [165-167].

Polyaniline (PANi) is one of the conducting polymers explored for myocardial regeneration, since it has revealed to be biocompatible for a certain number of cell lines, including cardiac myoblasts [168]. Mengyan Li has examined a novel type of blend, composed of gelatin and polyaniline. Conductivity measurements and biological tests evidenced an increase of conductivity by increasing PANi percentage, with the more promising results obtained for rat cardiac myoblast cells proliferation for the hybrid substrates [169]. In order to enhance PANi biocompatibility and provide the resulting scaffold with swelling and adhesive properties to promote cardiac cells attachment, infiltration, proliferation and differentiation, Fernandes at al. functionalized it by grafting a peptide sequence (hyperbranched poly-L-Lysine dendrimes) prior to scaffold fabrication [170]. D. A. Stout's group considered the addition of carbon nanofibers (CNF) to Poly(lactic-co-glycolic acid) to obtain a conductive scaffold. They examined different PLGA/CNF ratios on cardiomyocytes cultures and observed that conductivity and cell functions were enhanced by increasing the CNF content. It was assumed that the CNF nanoscale geometry mimics the ECM, determining an improved cytocompatibility [171]. Ming-Chia Yang and colleagues used polysaccharides and silk fibroin (SF) to produce SF/chitosan (CS) or SF/CS–hyaluronic acid (SF/CS–HA) microparticles, that were mechanically pressed and cross-linked with genipin to obtain cardiac scaffolds. Biological tests performed with rat mesenchimal stem cells on hybrid patches and on fibroin control,

showed higher cell growth rates and cardiomyogenic differentiation for the blended substrates [172].

1.4.2.3.2 Scaffold preparation techniques

Among conventional scaffold fabrication techniques, solvent casting/particulate leaching, freeze drying, electrospinning, thermally induced phase separation (TIPS), particles pressing and photolithography have been extensively studied for the production of scaffolds for cardiac regeneration.

Solvent casting/particulate leaching technique

In solvent casting and particulate leaching (SCPL), a polymer is dissolved in an organic solvent and particles, generally salts, are then added to the solution. The mixture is shaped into its final geometry, onto a glass plate or in a three dimensional mold. After the solvent has evaporated, the resulting composite material is placed in a bath which dissolves the particles, leaving behind a porous structure [173]. This technique is one of the most popular scaffold fabrication procedure since it allows an easy and quick production of porous structures [174].
Hidalgo-Bastida et al. used salt leaching to produce elastomeric, flexible, porous patches starting from POC. These scaffolds showed suitable properties for application in myocardial repair since scaffolds stiffness and elongation at break varied in the range of 0.2-3.3 kPa and 60-95%, respectively [146]. Lee at al. prepared PGCL-based scaffolds showing a rubber-like behavior with and ability to sustain cyclic tensile loading [175]. These scaffolds were used by Piao used thes scaffolds to develop cardiac patches cellularized with rat bone marrow-derived mononuclear cells and cell-free scaffolds, both implanted on the epicardial infarcted surface of a rat model. Four weeks after implantation, connective tissue covered both the scaffolds, some cells underwent differentiation into cardiomyocytes and newly blood vessels formed with a higher blood vessel density in the cell-seeded scaffolds compared to the non-cell-seeded ones [139].
Radisic and coworkers prepared bioresorbable, elastomeric macroporous PGS-based scaffolds containing micropores through a modified salt leaching technique [176, 177]. They demonstrated that a pretreatment with cardiac fibroblasts prior to cardiomyocytes seeding can create a suitable environment for cardiac myocytes adhesion, migration, proliferation and contraction [176, 178, 179]. Preliminary *in vivo* tests carried out in a rat model with cell-free scaffolds, showed that these matrices could be easily sutured, did not induce any infection and completely integrated in the host tissue within two weeks [176].
A mixed technique based on gas foaming (described ahead) and particulate leaching has been used by Park and colleagues to produce composite scaffold based on poly(DL-lactide-co-ε-caprolactone), PLGA and type I collagen. These scaffolds showed the highest cell density and metabolic activity when compared with their controls (collagen or PLGA sponges) probably due to their higher elasticity and mechanical stability. In addition, cells seeded on their surface responded to electrical cues with a synchronous contraction and expressed troponin I (TnI) and connexin-43 (Cx43) [180].

Pressing of particles

A simple and fast technique based on the pressing of particles to produce porous scaffolds has been employed by Yang and colleagues [172]. They first spray-dried microparticles of silk fibroin (SF) or its blend with chitosan (SF/CS) or chitosan-hyaluronic acid (SF/CS-HA), then they pressed the produced particles using a mechanical pressing machine at room temperature and finally crosslinked with genipin. SF/CS and SF/CS-HA scaffolds showed promising cellular response when cultured with rat mesenchymal stem cells (rMSCs). Cell proliferation on SF and SF-hybrid scaffolds significantly exceeded that of the control (cell culture plates) on day 7 post seeding. In addition, SF-hybrid scaffolds showed a higher proliferation rates compared to SF substrates, demonstrating that the incorporation of polysaccharides significantly contribute to mimic ECM microenvironment. Concerning differentiation, SF-hybrid scaffolds induced rMSCs to upregulate cardiac markers, such as NKx2.5, Gata4, Tnnt2 and Actc1, and express some cardiac proteins, such as cardiotin and connexin 43 [172]. More recently, Chi et al. studied the effects on LV remodeling and cardiac repair induced by the implantation of cellularized (bone marrow mesenchymal stem cells -BMSCs-) and non-cellularized SF/HA porous patches, obtained by this fabrication technique, in rat hearts [181]. Eight weeks after implantation weak signs of immunological response were observed in rats treated with non-cellularized and cellularized patches, respectively, while two months after implantation, SF/HA-treated rats showed improvement in cardiac function compared to the non-treated animals. This effect is ascribable to the mechanical and biochemical properties of the developed scaffolds. Moreover, cellularized scaffolds prevented cardiomyocytes apoptosis, induced the restoration of contractile proteins and promoted the release of vascular endothelial growth factor (VEGF), basic fibroblast growth factor (bFGF) and hepatocyte growth factor (HGF) [181].

Freeze drying

Freeze-drying, also known as lyophilisation, is a dehydration process that works by freezing the material and then reducing the surrounding pressure to allow the frozen water in the material to sublimate directly from the solid phase to the gas phase [182].
These technique has been mainly used for the fabrication of porous scaffolds obtained from natural polymers. Cohen's group produced cellularized alginate-based scaffolds that were completely integrated in the host tissue and totally coated with vascularized connective tissue, with myofibrils showing the typical striations and gap junctions of cardiac muscle, after two months after implantation [114, 183-187]. A reduction in cardiac remodeling was also observed [114, 184]. The same research group successively studied the implantation of analogue uncellularized scaffolds demonstrating that, even in these conditions, scaffolds promoted new blood vessels formation and stem cells recruitment in the infarcted area, providing a mechanical support to angiogenesis probably because alginate has a chemical structure similar to heparin sulfate, an ECM component regulating a wide variety of biological activities, including angiogenesis [184].
Perets and coworkers incorporated PLGA microspheres loading bFGF into the previously described scaffolds. They demonstrated that bFGF-loaded scaffolds induced cardiac fibroblast

proliferation and enhanced vascularization with respect to unloaded ones [186]. Dvir and colleagues proposed a pre-vascularization process to be performed before scaffold implantation [188]. They seeded the previously described alginate scaffolds with neonatal cardiac cells and loaded them with pro-survival and pro-angiogenic factors (insulin-like growth factor-1 -IGF-1-, stromal-cell derived factor1 -SDF-1- and VEGF) to promote cell survival and vascularizatio and induce maturation of the newly formed tissue. After 48 hours of cell culture, the pre-vascularization process started with scaffold implantation onto the omentum, a membrane rich in blood vessels. On day 28 post implantation, the vascularized scaffold showed integration in the host tissue from the structural and electrical points of view.

These alginate-based scaffolds were bulk functionalized by Sapir et al. prior to scaffold fabrication with two peptides: an amino acid sequence containing the adhesion triplet RGD and a heparin-binding peptide (HBP). After 14 days of cell culture with cardiac cells, RGD/HBP-functionalized samples showed a newly formed contractile tissue, while single-attached scaffolds (RGD- and HBP-attached scaffolds) exhibited a less organized tissue. These results suggested that HBP contributes in promoting cardiac tissue development, probably retarding the spreading process that appears only after the reorganization of cells into a cardiac-like arrangement [185].

Blan and Birla used freeze-drying to prepare chitosan-based scaffolds, characterized by the addiction of fibrin gel to favor cell retention. The in vitro formation of contractile tissue compared to the direct cell injection was observed [121]. Shi and co-workers covalently functionalized freeze-dried collagen-based sponges with the anti-Sca-1 antibody that is able to recruit and capture Sca-1 expressing hematopoietic, cardiac and skeletal muscle stem cells, demonstrating that the functionalized collagen scaffolds had the capacity for inducing an enhancement in cardiomyocytes regeneration when used to treat myocardial defects in mice [189].

At the beginning of the XXI century, the gelatin sponge Gelfoam® turned out to be an attractive substrate for myocardial TE, able to promote cell infiltration and engraftment [90, 190]. Since Gelfoam® scaffolds lack in suitable mechanical properties and show a thickness that makes oxygen and nutrients supply difficult, Miyagi et al. proposed a modified Gelfoam® scaffold (MGF) [191, 192], spray-coated on one surface with PCL to improve its mechanical behavior. To induce neoangiogenesis, the implanted MGF and the infarct border zone were injected with a biodegradable, thermo-sensitive hydrogel based on a triblock copolymer of poly δ-valerolactone-*b*-poly ethylene glycol-*b*-poly δ-valerolactone loaded with pro-angiogenic cytokines and/or bone marrow mesenchymal stem cells (BMSCs). Animals treated with the MGF scaffold showed an improvement in cardiac function compared to non-treated rats and animals treated with un-modified Gelfoam® [191]. More recently, Grover and colleagues used this technique to prepare porous scaffolds based on a blend of type I collagen and gelatin or elastin [193]. The addiction of gelatin or elastin to collagen allows to reduce its stiffness and, in the case of elastin, to increase strain at break. The replacement of collagen with gelatin in the blends with elastin seems not to be promising for cardiac TE since it induces a reduction in mechanical performances.

Patra et al. used freeze-drying to produce 3D scaffolds starting from non-mulberry silk fibroin extracted from Antheraea Mylitta (AM) [194]. AM seemed to be a good substrate for cardiomyocytes adhesion and spreading. In details, cell tests on AM showed better results than

those carried out on silk fibroin extracted from Bombyx mori (BM) probably due to the presence of RGD sequences inside the polymer chains. AM exhibits higher elasticity and tensile strength compared to BM, resulting a more suitable substrate for cardiac TE constructs. Cardiomyocytes seeded on freeze-dried AM scaffolds appeared to be uniformly distributed on pores' wall, expressed connexin 43, beat spontaneously and synchronously for at least 20 days and exhibited aligned sarcomers [194].
Collagen scaffolds with an internal honeycomb structure, characterized by parallel pores whose diameter ranged between 100 and 1000 μm, can be produced by freeze-drying a neutralized atelopeptide Type I collagen solution (1%, pH 3.0) [195]. The formation of the honeycomb structure is induced by neutralization of an acidic collagen solution with ammonia gas that cause insoluble collagen fibrils separation and rearrangement in multiple cores that grow from the surface to the bottom of the solution. Pore size can be varied depending on concentration of the collagen solution or that of ammonia gas. To improve mechanical properties of the scaffold, heat crosslinking was performed. In 2012, Guo and colleagues investigated rat cardiac cell behavior on this type of scaffolds [196]. After 16 days of culture, the seeded cells successfully adhered to scaffolds' walls and by the first day of cell culture, cells started to beat with a frequency rate higher that that observed on cell culture plates [196].

Thermally Induced Phase Separation (TIPS)

According to TIPS, polymer is dissolved at high temperature in a solvent with high freezing point (typically dimethyl sulfoxide or dioxane) and subsequently the solution is quenched, in order to decrease polymer solubility and induce its separation. Then the frozen solvent is washed away, leaving a porous structure.
Guan et al. used this technique to obtain scaffolds with random and oriented pores, using the previously described polyurethane based on PCL-diol, 1,4-diisocyanatebutane and the peptide sequence Ala-Ala-Lys. Subcutaneous implantation in rats demonstrated the absence of postoperative infections and the progressive cell infiltration inside the scaffold [68]. Fujimoto et al. explored a similar polyurethane containing putrescine as chain extender to produce porous interconnected scaffolds for cardiac TE [153-155]. *In vitro* cell tests showed promotion of cell adhesion, migration and proliferation, while *in vivo* tests carried out by implantation of acellular patches on rat model infracted area showed that the patch surface was completely integrated in the host muscle, eight weeks after implantation [153-155, 197]. In the case of scaffold-treated animals, it was observed that the infarcted area was rich in proteins connected to cardiac functionality, such as caldesmon and calponin and a there was a high capillary density and the re-establishment of the ventricular wall thickness [155].

Electrospinning

It is a highly versatile technique used to produce continuous fibers from submicron to nanometer diameters. Generally, a polymeric solution is fed through a spinneret and a high voltage is applied to the tip. The buildup of electrostatic repulsion within the charged solution, causes it to eject a thin fibrous stream. A collector plate or rod with an opposite charge draws in the continuous fibers, which will form a highly porous network. A typical electrospinning

set-up requires a high voltage power supply (up to 30 kV), a syringe, a flat tip needle and a conducting collector. By modifying parameters such as the distance to the collector, magnitude of applied voltage and solution flow rate, it is possible to change the scaffold architecture and, as a consequence, its physical and mechanical properties [198].

This technique was used by Kai and colleagues to produce scaffolds with both random or oriented morphology, showing that fiber alignment promoted cardiomyocytes adhesion and orientation [199]. Zong and coworkers also demonstrated that cardiomyocytes seeded on oriented PLLA-scaffolds tended to assume an elongated morphology compared to randomly oriented ones [136]. Similar results on cell behavior and morphology were obtained by Rockwood et al. that studied electrospun structures fabricated using a biodegradable polyurethane based on PCL-diol, 2,6-diisocyanate methylcaproate and 1-phenylalanine as chain extender [200].

The same polyurethane was used by Fromstein and coworkers to produce collagen IV coated structures by electrospinning and TIPS and study the effect of scaffold architecture on cell response. The different thickness of the two scaffolds (1000 μm for TIPS scaffolds vs 70 μm for electrospun ones) affected oxygen and nutrients supply and, as a consequence, embryonic stem cell-derived cardiomyocytes morphology and viability. In details, cells seeded on TIPS scaffolds exhibited a rounded shape and preferably localized themselves on the surface, while the same cells cultured on electrospun constructs spread and colonized all the thickness. Despite these differences in cell morphology, cells on both scaffolds expressed sarcomeric myosin and Cx43 and exhibited spontaneous contractility [201].

More recently, Prabhakaran et al. reported for the first time the electrospinning of the elastomeric POC blended with poly(L-lactic acid)-co-poly(ε-caprolactone) (PLCL) [202]. POC/PLCL scaffolds resulted characterized by a lower fiber diameter with respect to pure PLCL fibers. In addition, blended scaffolds showed Young Modulus (0.5-1 MPa) and elongation at break (150-280%) suitable for application in cardiac TE. Cell tests carried out with H9C2 cardiac myoblasts showed increased cell proliferation, organization, alignment, migration and spreading in the composite scaffolds compared to PLCL fibrous substrates.

Stankus and colleagues developed a new technique for the preparation of *in vitro* cellularized graft [203] based on smooth muscle cells electrospray combined with electrospinning of a biodegradable, cytocompatible and elastomeric poly(ester urethane)urea synthesized from PCL-diol, 1,4-diisocyanatobutane and putrescine [153, 203]. A fiber orientation able to promote cell alignment in a preferred direction was achieved, allowing a better mimesis of the anisotropic properties of the cardiac tissue [203]. More recently, Guan and colleagues employed this technique to integrate mesenchymal stem cells (MSCs) with an elastic poly(ester carbonate urethane)urea (PECUU) [204]. An anisotropic cellularized scaffold with MSCs uniformly distributed along its thickness was produced. It exhibited a non-linear anisotropic mechanical behavior that matched that of porcine cardiac tissue. However, since MSCs didn't align themselves to PECUU fibers and maintained a round shape, the cellularized constructs were cultured under stretching in order to induce cell alignment. Both in the presence and absence of a mechanical strength, the cellularized construct upregulated MEF2C, Nkx2.5 and GATA4. In the case of strengthen of scaffolds, this upregulation was strongly increased. These results suggest that a cardiac-like structural and mechanical environment can promote MSCs differentiation toward the cardiac lineage, without biochemicals or co-culture with other

cells, but simply mimicking structure, mechanical properties and cell organization of the native tissue [204].
The research group of Vacanti used PCL-based porous and randomly oriented electrospun scaffolds to develop cardiac grafts by overlapping several cell sheets. Cells cultured on the different sheets started to show a synchronized contraction with increasing strength with time [137, 138]. Moreover, the sheets connected each other created an homogeneous tissue showing cardiac-like structures. However, this approach is limited by the absence of a vasculature network able to supply nutrients and oxygen in the deeper regions of the graft [137, 138]. Kenar et al. overcame this limit developing a cellularized myocardial patch with a tubing system for nutrients supply [205].
Nanofibrous electrospun matrices can be easily functionalised to biochemically promote tissue regeneration and improve cell adhesion and proliferation [206-209]. Heydarkhan-Hagvall and colleagues prepared electrospun scaffolds from a blend of PCL with a natural polymer (collagen/elastin or gelatin type B) [210]. Spadaccio and colleagues functionalized PLLA electrospun scaffolds incorporating the granulocyte colony-stimulating factor (G-CSF), which stimulate angiogenesis, Cx43 expression and the hemodynamic cardiac function after MI [208, 211-213]. G-CSF has also an antiapoptotic activity, inhibits LV remodeling and protects the heart from arrhythmias [208, 211-213]. Myoblasts C2C12 seeded on these scaffolds adopted an elongated muscle-like morphology and expressed TnI and Cx43 [208, 213].
Ravichandran and colleagues experimented coaxial electrospinning to produce core/shell fibers containing the elastomeric synthetic PGS as core and a natural polymer as shell. PGS was used to obtain mechanical properties matching those of the native cardiac tissue while the natural polymer was used to promote cell adhesion and proliferation [214, 215]. Fibrous scaffolds produced with gelatin as shell resulted biocompatible and had promising mechanical properties for cardiac TE application [214]. Then, they replaced xenogenic gelatin with fibrinogen because it can be extracted from patient's own blood avoiding risk of foreign body reaction [215] and obtained scaffolds with Young Modulus of about 3 MPa, matching that of the myocardial tissue. showed normal expression of cardiac markers (α-actinin, Troponin, ß-myosin and connexin 43) and formed gap junctions to each other. The biological response of neonatal cardomyocytes cultured on these substrates was more promising, with higher expression of cardiac marker proteins, formation of gap junctions and functionality, with respect to fibrinogen control and tissue culture plates. Probably higher elasticity of PGS/fibrinogen core/shell fibrous structures allows cardiomyocytes to maintain their contractility and electrical activity [215].

Photolithography

Photolithography is a technique in which microscale features are fabricated based on selective exposure of a material to light. It allows to fabricate scaffolds with well-defined and geometrically precise topographies [216]. In 2003, Motlagh et al. demonstrated that topographical properties significantly affect cardiomyocytes morphology, gene expression and protein distribution. Cardiomyocytes seeded on textured substrates tended to adhere to the vertical surface of pegs or grooves and exhibited a decrease in cell area and an increase in the thickness of the myofibrillar layer due to changes in cell shape [217]. As previously discussed,

bioartificial systems based on PNIPAm and natural polymers have been studied for their application in cardiac TE [162]. More recently, the same research group assembled microfabricated substrates of a blend of poly(NIPAAm-co-HEMAHex), alginate and gelatin, having a rectangular geometry, in order to reproduce the architecture and anisotropic mechanical properties of the cardiac ECM [161, 218]. The micropatterned geometry was characterized by rectangular cavities (500 x 100 μm) able to lodge 2-3 cardiomyocytes and thick lines of 30 and 70 nm that reproduced the regions of connective tissue present in the native tissue [219]. Preliminary cell tests carried out with myoblasts showed scaffold ability to promote cells proliferation and orientation in a preferred direction [161].
In 2012, Srinivasan and Sehgal, that previously proposed a microbial treatment to extract collagen fibers from Achilles tendons of bovine origin maintaining collagen fibers' properties unchanged [220], wove collagen fibers to produce 3D fleece with good mechanical strength and handiness to be a suitable substrate for application as a cardiac patch [221]. Neonatal ventricular rat cardiomyocytes (NVRCMs) cultured on these scaffolds remained viable and metabolically active, and showed pulsation up to 18 days of culture, probably due to the suitable mechanical properties and elasticity of the developed substrates [221].

Rapid prototyping techniques (RP)

Rapid prototyping techniques (RP) are considered non conventional techniques and have been recently introduced to overcome the limitations of conventional scaffold fabrication methods, since they allow the fabrication of scaffolds with controlled resolution [222-228]. They include: selective laser sintering (SLS), pressure-assisted microsyringe (PAM) and laser microablation [222, 227].
Yeong et al. recently used SLS to produce porous PCL-based scaffolds with a well-defined porosity, geometry and mechanical properties [229]. The selected repetitive unit (square pyramid-shaped) allowed the production of an omogeneus interconnected porosity that favors nutrients and catabolites exchange and promotes cell homing and migration [229, 230]. This scaffold fabrication technique allows to obtain both micro- and macro-porosity as a result of the low particle-particle compaction force and the chosen repetitive cell, respectively. C2C12 myoblasts seeded on these scaffolds were found to proliferate up to 4 days; after 7 days a decrease in cell population was observed probably due to the beginning of differentiation phenomena that led myoblasts to fuse and create multinucleated cells [229].
Laser-based techniques have been largely employed in recent years due to the possibility to modify a wide family of materials at micro- and submicro-scale in a short time and in a computer-controlled manner [231]. Patz et al. studied the possibility to modulate C2C12 myoblasts adhesion, alignment, proliferation and differentiation acting on surface structure, particularly on the diameter of the channels produced on agar surface by excimer laser ablation. C2C12 seemed to have a better alignment, proliferation and differentiation on surfaces exposing channels with diameter of 60-150 μm [231, 232]. Moreover, this technique can be easily combined with others, such as photolithography and electrospinning [209, 233, 234]. Guillemette and colleagues demonstrated the possibility to successfully combine photolithography and laser ablation to produce PGS-based scaffolds with anisotropic and elastomeric mechanical properties that met the force-generating demands of myocardial tissue.

Cell tests carried out with C2C12 myoblasts showed that the topographical features created by photolithography and the pores produced by laser ablation induced a preferential cell alignment in a parallel direction to the linear pattern and the pore sides [233]. Park at al. used the same polymer and combined technique to produce multi-layered elastomeric scaffolds with an accordion-like honeycomb structure, mimicking the ondulated shape of perimysial collagen fibers [235-237]. Heart cell culture studies showed poor apoptosis and Cx43 expression [236].
A well-defined geometry at both micro- and macro-scale can also be achived by PAM [238, 239]. A comparative study carried out by Mattioli-Belmonte et al. between PAM and salt-leached scaffolds showed that, under application of a load, the former underwent a reorganization of its structure with fiber alignment in the direction of the applied force compared to the latter [238, 240]. In addition, only PAM-fabricated scaffolds assured homogeneous cell-substrate interactions, uniform distribution of cells inside the scaffold and good perfusion [238].
On the basis of the promising results reported by Lionetti et al. [241] and the success in skin, cartilage, vessels and nerves repair [242], several researchers have investigated the possibility to employ the commercial hyaluronan-based biomaterial HYAFF® for application in myocardial TE [243, 244]. Gallina and colleagues studied the interaction between a knitted HYAFF® mesh (HYALONECT®) and neonatal murin ventricular myocytes (NMVMs) [243]. Adhesion tests after 24h of cell culture revealed an adhesion of about 5% of the seeded cells that can be ascribed to the HYALONECT® structure, characterized by large empty spaces between its knittings. It was also observed a progressive change in cell morphology, from rounded-shaped with low degree of organization on day 1 to spindle- and spreaded-shaped and aligned organization in the fiber direction on day 7 post seeding, and a spontaneous contractile activity up to 48h. This feature is almost completely lost on day 7 post seeding due to the progressive cell differentiation toward an adult phenotype, characterized by absence of spontaneous contractile activity [243].

1.4.2.3.3 Conductive scaffolds

Scaffold conductivity is an important property that may allow the control on tissue contraction and electrical signals transmission within the graft. As previously described, several conductive polymers have been studied for cardiac TE applications.
Kai and colleagues developed electrospun scaffolds starting from a blend of PCL, gelatin and PPy (PPG). Cells cultured on PPG scaffolds showed a higher expression of Cx43 compared to PCL/gelatin constructs, due to the improvement in electrical and chemical signals transmission, resulting from the presence of PPy [245]. Similar conductive electrospun scaffolds were produced by Li and colleagues starting from a blend of gelatin and PANi. These scaffolds were cultured with cardiac myoblasts H9C2 and revealed able to promote cell adhesion and proliferation. In detail, scaffolds with smaller fiber diameter showed better results in term of cell spreading and muscle-like morphology, probably because they provided a more faithful reproduction of the ECM structure [169].

Carbon nanotubes (CNTs) are now being largely used as conductive components of scaffolds for cardiac TE. Mooney and colleagues studied the effects of single-walled CNTs (SWNTs) on human mesenchymal stem cells (hMSCs) demonstrating that at low concentrations SWNTs did not have negative effects on cell viability, proliferation and differentiation [246]. Based on these results, Mackle et al. produced electroactive randomly oriented electrospun fibrous scaffolds from a composite of SWNTs (2 wt%) dispersed in a poly-L-lactide acid (PLA) matrix. Degradation tests, demonstrated that the addiction of SWNTs increases scaffold structural stability and induces only slight alteration in PLA mechanical properties [247]. hMSCs seeded on these substrates and subjected to electrical stimulation adopted an elongated morphology and rearranged perpendicularly to the direction of the applied stimulus [248]. Moreover, hMSCs upregulated several cardiac markers, suggesting that electroactive stimuli can guide hMSCs differentiation to the cardiac phenotype [248].
Dvir, Timko and colleagues developed 3D freeze-dried scaffolds based on alginate and gold nanowires (Alg-NW) [249]. Gold nanowires have been adequately designed to minimize toxicity and have suitable size to be longer than pore wall thickness (approx. 500 nm) to promote signal transmission and cell-cell interaction through the scaffold. Cell tests carried out with cardiomyocytes and fibroblasts extracted from neonatal rats' left ventricles showed that the introduction of gold nanowires promotes the formation of more aligned and thicker tissues with respect to those observed in case of culture on pure alginate scaffolds. Moreover, cells seeded on composites scaffolds showed spontaneous and synchronous contraction when electrically stimulated and expressed higher level of proteins involved in contractility (Troponin I and connexin 43). Interestingly, gold nanowires seem to have positive effects on the physiology even in absence of an applied electrical stimuli, inducing cells to produce higher levels of connexin 43 on Alg-NW scaffolds compared to virgin alginate scaffold [249].

1.5 Thesis goal

The main purpose of this work is the fabrication of biomimetic bioartificial constructs (heart patches), able to restore myocardial functions and promote cardiac tissue regeneration after a myocardial infarction. These scaffolds are based on synthetic biodegradable polyurethanes and are prepared as dense (bidimensional) and porous (tridimensional) constructs.

Since biomimicry is a key requirement for applications of biomaterials in tissue engineering, they are prepared as biomimetic devices, from a mechanical, morphological and biochemical point of view.
Mechanical biomimicry is achieved by using elastomeric polymeric materials. In this work, the selected materials belong to the large family of polyurethanes, that will be widely described in the next chapter. As discussed above, the most employed synthetic polymers in myocardial TE are degradable polyesters, thanks to their biodegradability and biocompatibility. However, they are generally characterized by high stiffness, unsuitable for soft and contractile tissue regeneration [78]. A fine tuning of chemical, mechanical and degradation properties is required in the fabrication of heart patches and a restrict number of polymers, such as PGS [142] [143]

[144], POC [145] [146] and PURs [84, 147, 148], assure such requirements. Among these, polyurethanes seem to be the most versatile, since they can be prepared starting from a large number of building blocks (macrodiols, diisocyanates and chain extenders), opening the way to the introduction of peptide-sequences and several types of biomolecules in the polymeric chain. In cardiac TE, degradable PURs have been studied for a long time, thanks to their biocompatibility and elastomeric behavior that makes them capable to withstand cyclic stresses without incurring in plastic deformation or failure [76, 77].

In this thesis work, biodegradable poly(ester urethanes) and poly(ether ester urethanes) based on poly(ε-caprolactone) (PCL) and poly(ethylene glycol) (PEG) as macrodiols, 1,4-diisocyanatobutane (BDI) as diisocyanate, L-Lysine Ethyl Ester and Alanine-Alanine-Lysine (AAK) as chain extenders, are proposed as starting materials for the fabrication of heart patches. PCL is introduced in the polymer backbone to confer biodegradability to the final PUR. PEG is added in low amounts to tune wettability, mechanical and biological properties of films and scaffolds. BDI is an aliphatic diisocyanate, which is selected because its biodegradation products are non toxic [150]. Amino acids-based chain extenders are also chosen for their biocompatible degradation products.

Alanine-Alanine-Lysine peptide can be introduced also to tune biodegradability properties, since the Alanine-Alanine sequence is a target for the elastase enzyme. This enzyme is a member of the chymotrypsin family of proteases and it is involved in ECM degradation. Elastases can cleave elastin as well as having a broad substrate portfolio including collagen, fibronectin and other ECM proteins [250].

In this work, morphologically biomimetic scaffolds are obtained processing the synthesized PURs into tridimensional porous structures by Thermally Induced Phase Separation, with the application of a thermal gradient. In this way, the formation of oriented stretched pores is pursued, with a resulting anisotropic structure that confers to the substrates a remarkable similarity to the streaked muscle tissue. Similar scaffolds fabricated by Guan at co-workers gave promising results in terms of muscle-derived stem cell growth with respect to random orientated scaffolds [68].

In order to increase biocompatibility and surface wettability, and promote cell adhesion, proliferation and differentiation, the produced dense and porous constructs are surface functionalized by covalently linking RGD (Arginine-Glycine-Aspartic Acid) adhesion peptides. The process involves the activation of the top nanometer surface of the biomaterial by a plasma treatment to initiate graft copolymerisation of acrylic monomers. The formed carboxyl groups are used to covalently bind the bioactive molecule.

As it will be discussed in Chapter 3, ECM proteins containing this amino acid sequence, such as laminin and fibronectin (which are responsible for cell attachment to the ECM) have been successfully and widely employed in myocardial tissue engineering [158] [159] [251]. The use of their active sequences has been less investigated, but it seems to be a cheaper and promising strategy to promote myocardial regeneration [252]. Several authors have also studied the importance of density and distribution of adhesion proteins and RGD peptides on biomaterial surfaces, obtaining interesting results. For example, Rowley and co-workers created a range of surface density (1-100 fmol/cm^2) on alginate substrates and observed that myoblast proliferation and differentiation can be regulated by varying RGD density and the alginate monomeric ratio [253]. Moreover, the effect of fibronectin and lamin linear micro-

patterns on new tissue growth (cardiomyocytes organization and proliferation) [158] and mesenchymal stem cells differentiation into myogenic lineage [159] has been successfully studied.

Based on these observations, surface functionalization with the RGD peptide is performed in this work on both dense and porous substrates. In details, surface modification on films is carried out homogenously and with linear micro-patterned RGD domains, by using a silicone stencil after the plasma treatment, that allows for a regular distribution of biomimetic cues on the polymer surface.

Dense and porous scaffolds are biologically characterized by viability tests with cardiomyocytes. The most promising formulations are selected to be surface modified and tested with progenitor cells (Human Cardiac Mesenchymal Stem Cells and Cardiosphere-derived Stem Cells) in order to investigate the effect of the anisotropic structure on stem cells proliferation and differentiation.

References

1. *Global Atlas on cardiovascular disease prevention and control*, P.P. S. Mendis, B. Norrving, Editor 2011, World Health Organization in collaboration with the World Heart Federation and the World Stroke Organization: Geneva.
2. Boccaccini, A.R., S.E. Harding, and SpringerLink (Online service), *Myocardial Tissue Engineering*, in *Studies in Mechanobiology, Tissue Engineering and Biomaterials,*2011, Springer-Verlag Berlin Heidelberg,: Berlin, Heidelberg. p. 1 online resource.
3. Anversa, P., et al., *Myocyte growth and cardiac repair.* J Mol Cell Cardiol, 2002. **34**(2): p. 91-105.
4. Dimmeler, S., A.M. Zeiher, and M.D. Schneider, *Unchain my heart: the scientific foundations of cardiac repair.* J Clin Invest, 2005. **115**(3): p. 572-83.
5. Vunjak-Novakovic, G., et al., *Challenges in cardiac tissue engineering.* Tissue Eng Part B Rev, 2010. **16**(2): p. 169-87.
6. *Physiology*. Available from: http://www.cardioconsult.com/Physiology/.
7. *Anatomy of the Human Heart with Flash Illustration*. Available from: http://www.texasheartinstitute.org/HIC/Anatomy/Anatomy.cfm.
8. *Heart Pictures* Available from: http://pictures-heart.blogspot.it/2012/07/importance-of-human-heart.html.
9. *Walls of the Heart*. Available from: http://library.thinkquest.org/C003758/Structure/walls.htm.
10. Pollard, T.D.a.E., William. C., , *Cell Biology*2008, Philadelphia: Saunders.
11. Nagano, Y., P. Wong, and A.D. Roses, *Altered erythrocyte spectrin extractability in Duchenne muscular dystrophy.* Clin Chim Acta, 1980. **108**(3): p. 469-74.
12. Sussman, M.A., A. McCulloch, and T.K. Borg, *Dance band on the Titanic: biomechanical signaling in cardiac hypertrophy.* Circ Res, 2002. **91**(10): p. 888-98.
13. Parratt, J.R., et al., *Bradykinin and endothelial-cardiac myocyte interactions in ischemic preconditioning.* Am J Cardiol, 1997. **80**(3A): p. 124A-131A.
14. Beltrami, A.P., et al., *Adult cardiac stem cells are multipotent and support myocardial regeneration.* Cell, 2003. **114**(6): p. 763-76.
15. Laugwitz, K.L., et al., *Postnatal isl1+ cardioblasts enter fully differentiated cardiomyocyte lineages.* Nature, 2005. **433**(7026): p. 647-53.
16. *Tissues*. Available from: http://washington.uwc.edu/about/wayne.schaefer/TissuesPage.htm.
17. *The Cardio Research Web Project*. Available from: http://www.cardio-research.com/cardiomyocytes.
18. *Cradiac Muscle*. Available from: http://en.wikipedia.org/wiki/Cardiac_muscle.
19. *Cardiac and Smooth Muscle.*
20. *Infarction*. Available from: http://en.wikipedia.org/wiki/Infarction.

21. *Myocardial Infarction.*
22. Kosuge, M., et al., *Differences between men and women in terms of clinical features of ST-segment elevation acute myocardial infarction.* Circ J, 2006. **70**(3): p. 222-6.
23. Valensi, P., L. Lorgis, and Y. Cottin, *Prevalence, incidence, predictive factors and prognosis of silent myocardial infarction: a review of the literature.* Arch Cardiovasc Dis, 2011. **104**(3): p. 178-88.
24. *Heart Attack.* Available from: http://www.medicinenet.com/heart_attack/page2.htm.
25. *Acute Myocardial Infarction.* Available from: http://www.clevelandclinicmeded.com/medicalpubs/diseasemanagement/cardiology/acute-myocardial-infarction/.
26. Ertl, G. and S. Frantz, *Healing after myocardial infarction.* Cardiovasc Res, 2005. **66**(1): p. 22-32.
27. Holmes, J.W., T.K. Borg, and J.W. Covell, *Structure and mechanics of healing myocardial infarcts.* Annu Rev Biomed Eng, 2005. **7**: p. 223-53.
28. *Myocardial Infarction.* Available from: http://en.wikipedia.org/wiki/Myocardial_infarction.
29. Kolettis, T.M., et al., *Tissue engineering for post-myocardial infarction ventricular remodeling.* Mini Rev Med Chem, 2011. **11**(3): p. 263-70.
30. Lau, A., *Design of a new Left Ventricular Restraint Device for the Treatment of Heart Failure*, Worcester Polytechnic Institute.
31. Dobaczewski M., G.-Q.C., Frangogiannis N. G., *The extracellular matrix as a modulator of the inflammatory and reparative response following myocardial infarction.* Journal of Molecular and Cellular Cardiology 2010. **48**: p. 504–511.
32. *Heart Attack.* Available from: http://www.patienthealthinternational.com/heart-attack/]
33. *Heart Transplantation.* Available from: http://emedicine.medscape.com/article/429816-overview.
34. Jessup, M. and S. Brozena, *Heart failure.* N Engl J Med, 2003. **348**(20): p. 2007-18.
35. Copeland, J.G., et al., *Cardiac replacement with a total artificial heart as a bridge to transplantation.* N Engl J Med, 2004. **351**(9): p. 859-67.
36. Leor, J., Y. Amsalem, and S. Cohen, *Cells, scaffolds, and molecules for myocardial tissue engineering.* Pharmacol Ther, 2005. **105**(2): p. 151-63.
37. *Tissue Engineering for Tissue and Organ Regeneration*, D. Eberli, Editor 2011, InTech: Janeza Trdine, Croatia.
38. Menasche, P., et al., *Myoblast transplantation for heart failure.* Lancet, 2001. **357**(9252): p. 279-80.
39. Smits, A.M., et al., *Human cardiomyocyte progenitor cells differentiate into functional mature cardiomyocytes: an in vitro model for studying human cardiac physiology and pathophysiology.* Nat Protoc, 2009. **4**(2): p. 232-43.
40. Wollert, K.C., *Cell therapy for acute myocardial infarction.* Curr Opin Pharmacol, 2008. **8**(2): p. 202-10.
41. Oh, H., et al., *Cardiac progenitor cells from adult myocardium: homing, differentiation, and fusion after infarction.* Proc Natl Acad Sci U S A, 2003. **100**(21): p. 12313-8.
42. Bergmann, O., et al., *Evidence for cardiomyocyte renewal in humans.* Science, 2009. **324**(5923): p. 98-102.
43. Lee, S.T., et al., *Intramyocardial injection of autologous cardiospheres or cardiosphere-derived cells preserves function and minimizes adverse ventricular remodeling in pigs with heart failure post-myocardial infarction.* J Am Coll Cardiol, 2011. **57**(4): p. 455-65.
44. Thomson, J.A., et al., *Embryonic stem cell lines derived from human blastocysts.* Science, 1998. **282**(5391): p. 1145-7.
45. Hofmann, M., et al., *Monitoring of bone marrow cell homing into the infarcted human myocardium.* Circulation, 2005. **111**(17): p. 2198-202.
46. Kofidis, T., et al., *Injectable bioartificial myocardial tissue for large-scale intramural cell transfer and functional recovery of injured heart muscle.* J Thorac Cardiovasc Surg, 2004. **128**(4): p. 571-8.
47. *Molecular Microbiology and Biotechnology*. Available from: http://www.tau.ac.il/lifesci/departments/biotech/members/dvir/dvir.html.
48. Zimmermann, W.H. and R. Cesnjevar, *Cardiac tissue engineering: implications for pediatric heart surgery.* Pediatr Cardiol, 2009. **30**(5): p. 716-23.
49. Vulliet, P.R., et al., *Intra-coronary arterial injection of mesenchymal stromal cells and microinfarction in dogs.* Lancet, 2004. **363**(9411): p. 783-4.

50. Okano, T., et al., *A novel recovery system for cultured cells using plasma-treated polystyrene dishes grafted with poly(N-isopropylacrylamide).* J Biomed Mater Res, 1993. **27**(10): p. 1243-51.
51. Scheubel, R.J., et al., *Age-dependent depression in circulating endothelial progenitor cells in patients undergoing coronary artery bypass grafting.* J Am Coll Cardiol, 2003. **42**(12): p. 2073-80.
52. Yoon, Y.S., et al., *Unexpected severe calcification after transplantation of bone marrow cells in acute myocardial infarction.* Circulation, 2004. **109**(25): p. 3154-7.
53. Kadner, K., et al., *The beneficial effects of deferred delivery on the efficiency of hydrogel therapy post myocardial infarction.* Biomaterials, 2012. **33**(7): p. 2060-6.
54. Sutton, M.G. and N. Sharpe, *Left ventricular remodeling after myocardial infarction: pathophysiology and therapy.* Circulation, 2000. **101**(25): p. 2981-8.
55. Causa, F., P.A. Netti, and L. Ambrosio, *A multi-functional scaffold for tissue regeneration: The need to engineer a tissue analogue.* Biomaterials, 2007. **28**(34): p. 5093-5099.
56. Patel H., B.M., Srinivasan G., *Biodegradable Polymer Scaffold for Tissue Engineering.* Trends Biomater. Artif. Organs, 2011. **25**(1): p. 20-29.
57. Davis, M.E., et al., *Custom design of the cardiac microenvironment with biomaterials.* Circ Res, 2005. **97**(1): p. 8-15.
58. Simon-Yarza T., e.a., *Vascular endothelial growth factor-delivery system for cardiac repair: an overview.* Theranostic, 2012. **2**: p. 541-52.
59. Lutolf, M.P. and J.A. Hubbell, *Synthetic biomaterials as instructive extracellular microenvironments for morphogenesis in tissue engineering.* Nature Biotechnology, 2005. **23**(1): p. 47-55.
60. Saha, K., et al., *Designing synthetic materials to control stem cell phenotype.* Current Opinion in Chemical Biology, 2007. **11**(4): p. 381-387.
61. Ma, P.X., *Biomimetic materials for tissue engineering.* Adv Drug Deliv Rev, 2008. **60**(2): p. 184-98.
62. Chen, Q.Z., et al., *Biomaterials in cardiac tissue engineering: Ten years of research survey.* Materials Science & Engineering R-Reports, 2008. **59**(1-6): p. 1-37.
63. Guan, J.J., et al., *Preparation and characterization of highly porous, biodegradable polyurethane scaffolds for soft tissue applications.* Biomaterials, 2005. **26**(18): p. 3961-3971.
64. Cohen, S. and J. Leor, *Rebuilding broken hearts. Biologists and engineers working together in the fledgling field of tissue engineering are within reach of one of their greatest goals: constructing a living human heart patch.* Sci Am, 2004. **291**(5): p. 44-51.
65. Curtis, M.W. and B. Russell, *Cardiac tissue engineering.* J Cardiovasc Nurs, 2009. **24**(2): p. 87-92.
66. Yeong, W.Y., et al., *Porous polycaprolactone scaffold for cardiac tissue engineering fabricated by selective laser sintering.* Acta Biomater, 2010. **6**(6): p. 2028-34.
67. de Mulder, E.L.W., P. Buma, and G. Hannink, *Anisotropic Porous Biodegradable Scaffolds for Musculoskeletal Tissue Engineering.* Materials, 2009. **2**(4): p. 1674-1696.
68. Guan, J., K.L. Fujimoto, and W.R. Wagner, *Elastase-sensitive elastomeric scaffolds with variable anisotropy for soft tissue engineering.* Pharmaceutical Research, 2008. **25**(10): p. 2400-2412.
69. Eschenhagen, T. and W.H. Zimmermann, *Engineering myocardial tissue.* Circ Res, 2005. **97**(12): p. 1220-31.
70. Christman, K.L. and R.J. Lee, *Biomaterials for the treatment of myocardial infarction.* J Am Coll Cardiol, 2006. **48**(5): p. 907-13.
71. Marijianowski, M.M.H., et al., *Dilated Cardiomyopathy Is Associated with an Increase in the Type-I/Type-Iii Collagen Ratio - a Quantitative Assessment.* J Am Coll Cardiol, 1995. **25**(6): p. 1263-1272.
72. Hidalgo-Bastida, L.A., et al., *Cell adhesion and mechanical properties of a flexible scaffold for cardiac tissue engineering.* Acta Biomater, 2007. **3**(4): p. 457-462.
73. Aygen, M.M. and E. Braunwald, *Studies on Starling's law of the heart. VIII. Mechanical properties of human myocardium studied in vivo.* Circulation, 1962. **26**: p. 516-24.
74. Jawad, H., et al., *Myocardial tissue engineering.* Br Med Bull, 2008. **87**: p. 31-47.
75. Chen, Q.-Z., et al., *Biomaterials in cardiac tissue engineering: Ten years of research survey.* Materials Science and Engineering Reports, 2008. **59**(1–6): p. 1-37.
76. Jawad, H., et al., *Myocardial tissue engineering.* British Medical Bulletin, 2008. **87**(1): p. 31-47.
77. Jawad, H., et al., *Myocardial tissue engineering: a review.* J Tissue Eng Regen Med, 2007. **1**(5): p. 327-42.
78. Sui, R., et al., *The current status of engineering myocardial tissue.* Stem Cell Rev, 2011. **7**(1): p. 172-80.

79. Akhyari, P., et al., *Myocardial tissue engineering: the extracellular matrix.* Eur J Cardiothorac Surg, 2008. **34**(2): p. 229-41.
80. Zammaretti, P. and M. Jaconi, *Cardiac tissue engineering: regeneration of the wounded heart.* Curr Opin Biotechnol, 2004. **15**(5): p. 430-4.
81. Corda, S., J.-L. Samuel, and L. Rappaport, *Extracellular matrix and growth factors during heart growth.* Heart Failure Reviews, 2000. **5**(2): p. 119-130.
82. Coghlan, H.C., et al., *The structure and function of the helical heart and its buttress wrapping. III. The electric spiral of the heart: The hypothesis of the anisotropic conducting matrix.* Semin Thorac Cardiovasc Surg, 2001. **13**(4): p. 333-41.
83. Lunkenheimer, P.P., et al., *The myocardium and its fibrous matrix working in concert as a spatially netted mesh: a critical review of the purported tertiary structure of the ventricular mass.* Eur J Cardiothorac Surg, 2006. **29 Suppl 1**: p. S41-S49.
84. Chen, Q., S. Liang, and G.A. Thouas, *Elastomeric biomaterials for tissue engineering.* Progress in Polymer Science, (0).
85. Marijianowski, M.M., et al., *Dilated cardiomyopathy is associated with an increase in the type I/type III collagen ratio: a quantitative assessment.* J Am Coll Cardiol, 1995. **25**(6): p. 1263-72.
86. Silverstein, M.E., et al., *Collagen fibers as a fleece hemostatic agent.* J Trauma, 1980. **20**(8): p. 688-94.
87. Zimmermann, W.-H., I. Melnychenko, and T. Eschenhagen, *Engineered heart tissue for regeneration of diseased hearts.* Biomaterials, 2004. **25**(9): p. 1639-1647.
88. Kofidis, T., et al., *Bioartificial grafts for transmural myocardial restoration: a new cardiovascular tissue culture concept.* European Journal of Cardio-Thoracic Surgery, 2003. **24**(6): p. 906-911.
89. Kofidis, T., et al., *A novel bioartificial myocardial tissue and its prospective use in cardiac surgery.* European Journal of Cardio-Thoracic Surgery, 2002. **22**(2): p. 238-243.
90. Li, R.-K., et al., *Survival and function of bioengineered cardiac grafts.* Circulation, 1999. **100**(suppl 2): p. II-63-II-69.
91. Akhyari, P., et al., *Mechanical stretch regimen enhances the formation of bioengineered autologous cardiac muscle grafts.* Circulation, 2002. **106**(12 Suppl 1): p. I137-42.
92. Eschenhagen, T., et al., *Cardiac tissue engineering.* Transpl Immunol, 2002. **9**(2-4): p. 315-21.
93. Ravichandran, R., et al., *Expression of cardiac proteins in neonatal cardiomyocytes on PGS/fibrinogen core/shell substrate for Cardiac tissue engineering.* Int J Cardiol, 2012.
94. Rohr, S., et al., *Quantitative image analysis of angiogenesis in rats implanted with a fibrin gel chamber.* Nouv Rev Fr Hematol, 1992. **34**(4): p. 287-94.
95. Linnes, M.P., B.D. Ratner, and C.M. Giachelli, *A fibrinogen-based precision microporous scaffold for tissue engineering.* Biomaterials, 2007. **28**(35): p. 5298-306.
96. Rowe, S.L., S. Lee, and J.P. Stegemann, *Influence of thrombin concentration on the mechanical and morphological properties of cell-seeded fibrin hydrogels.* Acta Biomater, 2007. **3**(1): p. 59-67.
97. Ye, Q., et al., *Fibrin gel as a three dimensional matrix in cardiovascular tissue engineering.* Eur J Cardiothorac Surg, 2000. **17**(5): p. 587-91.
98. Christman, K.L., et al., *Fibrin glue alone and skeletal myoblasts in a fibrin scaffold preserve cardiac function after myocardial infarction.* Tissue Eng, 2004. **10**(3-4): p. 403-9.
99. Christman, K.L., et al., *Injectable fibrin scaffold improves cell transplant survival, reduces infarct expansion, and induces neovasculature formation in ischemic myocardium.* J Am Coll Cardiol, 2004. **44**(3): p. 654-60.
100. Ryu, J.H., et al., *Implantation of bone marrow mononuclear cells using injectable fibrin matrix enhances neovascularization in infarcted myocardium.* Biomaterials, 2005. **26**(3): p. 319-26.
101. Huang, N.F., et al., *Injectable biopolymers enhance angiogenesis after myocardial infarction.* Tissue Eng, 2005. **11**(11-12): p. 1860-6.
102. Akhyari, P., Fedak P.W.M., Weisel R.D., et al, *Mechanical stretch regimen enhances the formation of bioengineered autologous cardiac muscle construct.* Circolation, 2002. **106**: p. 137-42.
103. Kim, B.S., Nikolovski, J., Bonadio, J., Mooney, D.J. , *Cyclic mechanical strain regulates the developments of engineered smooth muscle tissue.* Nat Biotechnol 1999. **17**: p. 979-83.
104. Mandal B.B., K.S.C., *Non-bioengineered silk gland fibroin protein: characterization and evaluation of matrices for potential tissue engineering applications.* Biotechnol Bioeng 2008. **100**: p. 1237-50.
105. Nazarov R., J.H.J., Kaplan D.L. , *Porous 3-D scaffolds from regenerated silk fibroin.* Biomacromolecules, 2004. **5**: p. 718-26.

106. Zhang Y.Q., Z.W.L., Shen W.D., Chen Y.H., Zha X.M., Shirai K., et al. , *Synthesis, characterization and immunogenicity of silk fibroin-L-asparaginase bioconjugates.* J Biotechnol, 2005. **120**: p. 315-26.
107. Meinel L., H.S., Karageorgiou V., Kirker-Head C., McCool J., Gronowicz G., et al. , *The inflammatory responses to silk films in vitro and in vivo.* Biomaterials, 2005. **26**: p. 147-55.
108. Patra C., T.S., Novoyatleva T., Velagala S.R., Mühlfeld C.,Kundu B., Kundu S.C., Engel F.B. , *Silk protein fibroin from Antheraea mylitta for cardiac tissue engineering.* Biomaterials, 2012. **33**: p. 2673-80.
109. Laurent, T.C. and J.R. Fraser, *Hyaluronan.* FASEB Journal, 1992. **6**(7): p. 2397-404.
110. Mano, J.F., et al., *Natural origin biodegradable systems in tissue engineering and regenerative medicine: present status and some moving trends.* Journal of The Royal Society Interface, 2007. **4**(17): p. 999-1030.
111. Chang, P.L., *Microcapsules as bio-organs for somatic gene therapy.* Annals of the New York Academy of Sciences, 1997. **831**(1): p. 461-473.
112. Hagihara, Y., et al., *Transplantation of xenogeneic cells secreting beta-endorphin for pain treatment: analysis of the ability of components of complement to penetrate through polymer capsules.* Cell Transplantation, 1997. **6**(5): p. 527-30.
113. Cappai, A., et al., *Evaluation of new small barium alginate microcapsules.* Int J Artif Organs, 1995. **18**(2): p. 96-102.
114. Leor, J., et al., *Bioengineered cardiac grafts : a new approach to repair the infarcted myocardium?* Circulation, 2000. **102**(suppl 3): p. III-56-III-61.
115. Entcheva, E., et al., *Functional cardiac cell constructs on cellulose-based scaffolding.* Biomaterials, 2004. **25**(26): p. 5753-5762.
116. Märtson, M., et al., *Is cellulose sponge degradable or stable as implantation material? An in vivo subcutaneous study in the rat.* Biomaterials, 1999. **20**(21): p. 1989-1995.
117. Khor, E. and L.Y. Lim, *Implantable applications of chitin and chitosan.* Biomaterials, 2003. **24**(13): p. 2339-2349.
118. Lu, S., et al., *Both the transplantation of somatic cell nuclear transfer- and fertilization-derived mouse embryonic stem cells with temperature-responsive chitosan hydrogel improve myocardial performance in infarcted rat hearts.* Tissue Engineering Part A, 2010. **16**(4): p. 1303-15.
119. Lu, W.N., et al., *Functional improvement of infarcted heart by co-injection of embryonic stem cells with temperature-responsive chitosan hydrogel.* Tissue Engineering Part A, 2009. **15**(6): p. 1437-47.
120. Wang, H., et al., *Improved myocardial performance in infarcted rat heart by co-injection of basic fibroblast growth factor with temperature-responsive chitosan hydrogel.* J Heart Lung Transplant, 2010. **29**(8): p. 881-7.
121. Blan, N.R. and R.K. Birla, *Design and fabrication of heart muscle using scaffold-based tissue engineering.* J Biomed Mater Res A, 2008. **86**(1): p. 195-208.
122. Mi, F.-L., et al., *Fabrication and characterization of a sponge-like asymmetric chitosan membrane as a wound dressing.* Biomaterials, 2001. **22**(2): p. 165-173.
123. Francis Suh, J.K. and H.W.T. Matthew, *Application of chitosan-based polysaccharide biomaterials in cartilage tissue engineering: a review.* Biomaterials, 2000. **21**(24): p. 2589-2598.
124. Muzzarelli, R.A., *Human enzymatic activities related to the therapeutic administration of chitin derivatives.* Cell Mol Life Sci, 1997. **53**(2): p. 131-40.
125. VandeVord, P.J., et al., *Evaluation of the biocompatibility of a chitosan scaffold in mice.* J Biomed Mater Res, 2002. **59**(3): p. 585-90.
126. Onishi, H. and Y. Machida, *Biodegradation and distribution of water-soluble chitosan in mice.* Biomaterials, 1999. **20**(2): p. 175-182.
127. Lee, K.Y., W.S. Ha, and W.H. Park, *Blood compatibility and biodegradability of partially N-acylated chitosan derivatives.* Biomaterials, 1995. **16**(16): p. 1211-1216.
128. Stern, R., A.A. Asari, and K.N. Sugahara, *Hyaluronan fragments: an information-rich system.* European Journal of Cell Biology, 2006. **85**(8): p. 699-715.
129. Zhu, H., et al., *The role of the hyaluronan receptor CD44 in mesenchymal stem cell migration in the extracellular matrix.* Stem Cells, 2006. **24**(4): p. 928-35.
130. Khademhosseini, A., et al., *Microfluidic patterning for fabrication of contractile cardiac organoids.* Biomedical Microdevices, 2007. **9**(2): p. 149-157.

131. Fan, H., et al., *Cartilage regeneration using mesenchymal stem cells and a PLGA–gelatin/chondroitin/hyaluronate hybrid scaffold.* Biomaterials, 2006. **27**(26): p. 4573-4580.
132. Lisignoli, G., et al., *Hyaluronan-based polymer scaffold modulates the expression of inflammatory and degradative factors in mesenchymal stem cells: Involvement of Cd44 and Cd54.* Journal of Cellular Physiology, 2006. **207**(2): p. 364-373.
133. Bursac, N., et al., *Cardiac muscle tissue engineering: toward an in vitro model for electrophysiological studies.* American Journal of Physiology - Heart and Circulatory Physiology, 1999. **277**(2): p. H433-H444.
134. Ke, Q., et al., *Embryonic stem cells cultured in biodegradable scaffold repair infarcted myocardium in mice.* Acta Physiologica Sinica, 2005. **57**(6): p. 673-81.
135. McDevitt, T.C., et al., *In vitro generation of differentiated cardiac myofibers on micropatterned laminin surfaces.* J Biomed Mater Res, 2002. **60**(3): p. 472-479.
136. Zong, X., et al., *Electrospun fine-textured scaffolds for heart tissue constructs.* Biomaterials, 2005. **26**(26): p. 5330-8.
137. Shin, M., et al., *Contractile cardiac grafts using a novel nanofibrous mesh.* Biomaterials, 2004. **25**(17): p. 3717-3723.
138. Ishii, O., et al., *In vitro tissue engineering of a cardiac graft using a degradable scaffold with an extracellular matrix-like topography.* Journal of Thoracic and Cardiovascular Surgery, 2005. **130**(5): p. 1358-1363.
139. Piao, H., et al., *Effects of cardiac patches engineered with bone marrow-derived mononuclear cells and PGCL scaffolds in a rat myocardial infarction model.* Biomaterials, 2007. **28**(4): p. 641-649.
140. Brown, D.A., et al., *Modulation of gene expression in neonatal rat cardiomyocytes by surface modification of polylactide-co-glycolide substrates.* Journal of Biomedical Materials Research Part A, 2005. **74A**(3): p. 419-429.
141. Tay, C.Y., et al., *Micropatterned matrix directs differentiation of human mesenchymal stem cells towards myocardial lineage.* Experimental Cell Research, 2010. **316**(7): p. 1159-1168.
142. Rai, R., et al., *Synthesis, properties and biomedical applications of poly(glycerol sebacate) (PGS): A review.* Progress in Polymer Science, 2012. **37**(8): p. 1051-1078.
143. Chen, Q.-Z., et al., *Characterisation of a soft elastomer poly(glycerol sebacate) designed to match the mechanical properties of myocardial tissue.* Biomaterials, 2008. **29**(1): p. 47-57.
144. Stuckey, D.J., et al., *Magnetic resonance imaging evaluation of remodeling by cardiac elastomeric tissue scaffold biomaterials in a rat model of myocardial infarction.* Tissue Eng Part A, 2010. **16**(11): p. 3395-402.
145. Yang, J., A.R. Webb, and G.A. Ameer, *Novel citric acid-based biodegradable elastomers for tissue engineering.* Advanced Materials, 2004. **16**(6): p. 511-516.
146. Hidalgo-Bastida, L.A., et al., *Cell adhesion and mechanical properties of a flexible scaffold for cardiac tissue engineering.* Acta Biomater, 2007. **3**(4): p. 457-62.
147. Lamba, N.M.K., K.A. Woodhouse, and S.L. Cooper, *Polyurethanes in biomedical applications.*1998, USA: CRC Press.
148. Castonguay, M., et al., *Synthesis, physicochemical and surface characteristics of polyurethanes*, in *Biomedical Applications of Polyurethanes*, P. Vermette, et al., Editors. 2001, Landes Bioscience: Texas (USA). p. 1-21.
149. Guelcher, S.A., *Biodegradable polyurethanes: synthesis and applications in regenerative medicine.* Tissue Engineering Part B Reviews, 2008. **14**(1): p. 3-17.
150. Rechichi, A., et al., *Degradable block polyurethanes from nontoxic building blocks as scaffold materials to support cell growth and proliferation.* Journal of Biomedical Materials Research Part A, 2008. **84**(4): p. 847-55.
151. Zhang, J.Y., et al., *A new peptide-based urethane polymer: synthesis, biodegradation, and potential to support cell growth in vitro.* Biomaterials, 2000. **21**(12): p. 1247-1258.
152. Zhang, J.Y., et al., *Three-dimensional biocompatible ascorbic acid-containing scaffold for bone tissue engineering.* Tissue Eng, 2003. **9**(6): p. 1143-57.
153. Guan, J., et al., *Synthesis, characterization, and cytocompatibility of elastomeric, biodegradable poly(ester-urethane)ureas based on poly(caprolactone) and putrescine.* Journal of Biomedical Materials Research, 2002. **61**(3): p. 493-503.

154. Fujimoto, K.L., et al., *In vivo evaluation of a porous, elastic, biodegradable patch for reconstructive cardiac procedures.* Annals of Thoracic Surgery, 2007. **83**(2): p. 648-654.
155. Fujimoto, K.L., et al., *An elastic, biodegradable cardiac patch induces contractile smooth muscle and improves cardiac remodeling and function in subacute myocardial infarction.* Journal of the American College of Cardiology, 2007. **49**(23): p. 2292-2300.
156. Ciardelli, G., et al. *Biomimetic polyurethanes for regenerative medicine*. in *Nanotech Conference & Expo 2011*. 2011. Boston.
157. Weiss, L., *The adhesion of cells*, in *International Review of Cytology*, G.H. Bourne and J.F. Danielli, Editors. 1960, Academic Press: New York. p. 187-225.
158. McDevitt, T.C., et al., *Spatially organized layers of cardiomyocytes on biodegradable polyurethane films for myocardial repair.* Journal of Biomedical Materials Research Part A, 2003. **66A**(3): p. 586-595.
159. Siepe, M., et al., *Construction of skeletal myoblast-based polyurethane scaffolds for myocardial repair.* Artif Organs, 2007. **31**(6): p. 425-33.
160. Mukherjee, S., et al., *Evaluation of the biocompatibility of PLACL/collagen nanostructured matrices with cardiomyocytes as a model for the regeneration of infarcted myocardium.* Advanced Functional Materials, 2011. **21**(12): p. 2291-2300.
161. Rosellini, E., et al., *Engineering of multifunctional scaffolds for myocardial repair through nanofunctionalization and microfabrication of novel polymeric biomaterials.* , in *Myocardial Tissue Engineering*, A.R. Boccaccini and S.E. Harding, Editors. 2011, Springer Berlin Heidelberg: Berlin. p. 187-214.
162. Rosellini, E., et al., *New bioartificial systems and biodegradable synthetic polymers for cardiac tissue engineering: a preliminary screening.* Biomed Eng Appl Basis Comm, 2010. **22**(6): p. 497-507.
163. Guimard, N.K., N. Gomez, and C.E. Schmidt, *Conducting polymers in biomedical engineering.* Progress in Polymer Science, 2007. **32**(8–9): p. 876-921.
164. Pedrotty, D.M., et al., *Engineering skeletal myoblasts: roles of three-dimensional culture and electrical stimulation.* American Journal of Physiology: Heart and Circulatory Physiology, 2005. **288**(4): p. H1620-H1626.
165. Zhao, M., et al., *Electrical stimulation directly induces pre-angiogenic responses in vascular endothelial cells by signaling through VEGF receptors.* J Cell Sci, 2004. **117**(Pt 3): p. 397-405.
166. Kern, H., et al., *Recovery of long-term denervated human muscles induced by electrical stimulation.* Muscle Nerve, 2005. **31**(1): p. 98-101.
167. Genovese, J.A., et al., *Electrostimulation induces cardiomyocyte predifferentiation of fibroblasts.* Biochem Biophys Res Commun, 2008. **370**(3): p. 450-5.
168. Bidez, P.R., 3rd, et al., *Polyaniline, an electroactive polymer, supports adhesion and proliferation of cardiac myoblasts.* Journal of Biomaterials Science, Polymer Edition, 2006. **17**(1-2): p. 199-212.
169. Li, M., et al., *Electrospinning polyaniline-contained gelatin nanofibers for tissue engineering applications.* Biomaterials, 2006. **27**(13): p. 2705-2715.
170. Fernandes, E.G.R., V. Zucolotto, and A.A.A. De Queiroz, *Electrospinning of hyperbranched poly-L-lysine/polyaniline nanofibers for application in cardiac tissue engineering.* Journal of Macromolecular Science Part A, 2010. **47**(12): p. 1203-1207.
171. Stout, D.A., B. Basu, and T.J. Webster, *Poly(lactic–co-glycolic acid): aarbon nanofiber composites for myocardial tissue engineering applications.* Acta Biomaterialia, 2011. **7**(8): p. 3101-3112.
172. Yang, M.C., et al., *The cardiomyogenic differentiation of rat mesenchymal stem cells on silk fibroin-polysaccharide cardiac patches in vitro.* Biomaterials, 2009. **30**(22): p. 3757-65.
173. *Solvent casting and particulate leaching* Available from: http://en.wikipedia.org/wiki/Solvent_casting_and_particulate_leaching.
174. Subia B, K.J., Kundu SC, *Biomaterial scaffold fabrication techniques for potential tissue engineering applications*, in *Tissue engineering*, D. Eberli, Editor 2010, InTech: Vukovar (Croatia). p. 141-158.
175. Lee, S.H., et al., *Elastic biodegradable poly(glycolide-co-caprolactone) scaffold for tissue engineering.* J Biomed Mater Res A, 2003. **66**(1): p. 29-37.
176. Radisic, M., et al., *Pre-treatment of synthetic elastomeric scaffolds by cardiac fibroblasts improves engineered heart tissue.* Journal of Biomedical Materials Research Part A, 2008. **86A**(3): p. 713-724.
177. Gao, J., P. Crapo, and Y. Wang, *Macroporous elastomeric scaffolds with extensive micropores for soft tissue engineering.* Tissue Engineering, 2006. **12**(4): p. 917-925.

178. Camelliti, P., T.K. Borg, and P. Kohl, *Structural and functional characterisation of cardiac fibroblasts.* Cardiovascular Research, 2005. **65**(1): p. 40-51.
179. Kohl, P., *Heterogeneous cell coupling in the heart.* Circulation Research, 2003. **93**(5): p. 381-383.
180. Park, H., et al., *A novel composite scaffold for cardiac tissue engineering.* In Vitro Cellular & Developmental Biology - Animal, 2005. **41**(7): p. 188-196.
181. Chi, N.H., et al., *Cardiac repair achieved by bone marrow mesenchymal stem cells/silk fibroin/hyaluronic acid patches in a rat of myocardial infarction model.* Biomaterials, 2012. **33**(22): p. 5541-51.
182. *Freeze-drying* Available from: http://en.wikipedia.org/wiki/Freeze-drying.
183. Leor, J., Y. Amsalem, and S. Cohen, *Cells, scaffolds, and molecules for myocardial tissue engineering.* Pharmacology and Therapeutics, 2005. **105**(2): p. 151-163.
184. Cohen, S. and J. Leor, *Rebuilding broken hearts. Biologists and engineers working together in the fledgling field of tissue engineering are within reach of one of their greatest goals: constructing a living human heart patch.* Scientific American, 2004. **291**(5): p. 44-51.
185. Sapir, Y., O. Kryukov, and S. Cohen, *Integration of multiple cell-matrix interactions into alginate scaffolds for promoting cardiac tissue regeneration.* Biomaterials, 2011. **32**(7): p. 1838-1847.
186. Perets, A., et al., *Enhancing the vascularization of three-dimensional porous alginate scaffolds by incorporating controlled release basic fibroblast growth factor microspheres.* J Biomed Mater Res A, 2003. **65**(4): p. 489-97.
187. Shapiro, L. and S. Cohen, *Novel alginate sponges for cell culture and transplantation.* Biomaterials, 1997. **18**(8): p. 583-590.
188. Dvir, T., et al., *Prevascularization of cardiac patch on the omentum improves its therapeutic outcome.* Proceedings of the National Academy of Sciences of the United States of America, 2009. **106**(35): p. 14990-5.
189. Shi, C., et al., *Stem-cell-capturing collagen scaffold promotes cardiac tissue regeneration.* Biomaterials, 2011. **32**(10): p. 2508-2515.
190. Li, R.K., et al., *Construction of a bioengineered cardiac graft.* Journal of Thoracic and Cardiovascular Surgery, 2000. **119**(2): p. 368-75.
191. Miyagi, Y., et al., *Surgical ventricular restoration with a cell- and cytokine-seeded biodegradable scaffold.* Biomaterials, 2010. **31**(30): p. 7684-7694.
192. Vu, D.T. and T. Kofidis, *Myocardial restoration: is it the cell or the architecture or both?* Cardiology research and practice, 2012. **2012**: p. 240497.
193. Grover, C.N., R.E. Cameron, and S.M. Best, *Investigating the morphological, mechanical and degradation properties of scaffolds comprising collagen, gelatin and elastin for use in soft tissue engineering.* J Mech Behav Biomed Mater, 2012. **10**: p. 62-74.
194. Patra, C., et al., *Silk protein fibroin from Antheraea mylitta for cardiac tissue engineering.* Biomaterials, 2012. **33**(9): p. 2673-2680.
195. Itoh, H., et al., *A Honeycomb Collagen Carrier for Cell Culture as a Tissue Engineering Scaffold.* Artificial Organs, 2001. **25**(3): p. 213-217.
196. Guo, Z., et al., *Three-Dimensional Geometry of Honeycomb Collagen Promotes Higher Beating Rate of Myocardial Cells in Culture.* Artificial Organs, 2012. **12**(10): p. 1525-1594.
197. Guan, J., et al., *Preparation and characterization of highly porous, biodegradable polyurethane scaffolds for soft tissue applications.* Biomaterials, 2005. **26**(18): p. 3961-3971.
198. *Tissue Engineering* Available from: http://en.wikipedia.org/wiki/Tissue_engineering.
199. Kai, D., et al., *Guided orientation of cardiomyocytes on electrospun aligned nanofibers for cardiac tissue engineering.* Journal of Biomedical Materials Research, Part B: Applied Biomaterials, 2011. **98B**(2): p. 379-386.
200. Rockwood, D.N., et al., *Culture on electrospun polyurethane scaffolds decreases atrial natriuretic peptide expression by cardiomyocytes in vitro.* Biomaterials, 2008. **29**(36): p. 4783-91.
201. Fromstein, J.D., et al., *Seeding bioreactor-produced embryonic stem cell-derived cardiomyocytes on different porous, degradable, polyurethane scaffolds reveals the effect of scaffold architecture on cell morphology.* Tissue Eng Part A, 2008. **14**(3): p. 369-78.
202. Prabhakaran, M.P., et al., *Electrospun composite scaffolds containing poly(octanediol-co-citrate) for cardiac tissue engineering.* Biopolymers, 2012. **97**(7): p. 529-38.
203. Stankus, J.J., et al., *Microintegrating smooth muscle cells into a biodegradable, elastomeric fiber matrix.* Biomaterials, 2006. **27**(5): p. 735-744.

204. Guan, J., et al., *The stimulation of the cardiac differentiation of mesenchymal stem cells in tissue constructs that mimic myocardium structure and biomechanics.* Biomaterials, 2011. **32**(24): p. 5568-80.
205. Kenar, H., G. Kose, and V. Hasirci, *Design of a 3D aligned myocardial tissue construct from biodegradable polyesters.* J Mater Sci Mater Med, 2010. **21**(3): p. 989-997.
206. Agarwal, S., J.H. Wendorff, and A. Greiner, *Use of electrospinning technique for biomedical applications.* Polymer, 2008. **49**(26): p. 5603-5621.
207. Kumbar, S.G., et al., *Electrospun nanofiber scaffolds: engineering soft tissues.* Biomed Mater, 2008. **3**(3): p. 034002.
208. Genovese, J.A., et al., *Electrospun nanocomposites and stem cells in cardiac tissue engineering*, in *Myocardial Tissue Engineering*, A.R. Boccaccini and S.E. Harding, Editors. 2011, Springer Berlin Heidelberg: Berlin. p. 215-242.
209. Lannutti, J., et al., *Electrospinning for tissue engineering scaffolds.* Materials Science and Engineering: C, 2007. **27**(3): p. 504-509.
210. Heydarkhan-Hagvall, S., et al., *Three-dimensional electrospun ECM-based hybrid scaffolds for cardiovascular tissue engineering.* Biomaterials, 2008. **29**(19): p. 2907-2914.
211. Kuhlmann, M.T., et al., *G-CSF/SCF reduces inducible arrhythmias in the infarcted heart potentially via increased connexin43 expression and arteriogenesis.* The Journal of Experimental Medicine, 2006. **203**(1): p. 87-97.
212. Kuwabara, M., et al., *Granulocyte colony-stimulating factor activates Wnt signal to sustain gap junction function through recruitment of β-catenin and cadherin.* FEBS Letters, 2007. **581**(25): p. 4821-4830.
213. Spadaccio, C., et al., *A G-CSF functionalized scaffold for stem cells seeding: a differentiating device for cardiac purposes.* Journal of Cellular and Molecular Medicine, 2011. **15**(5): p. 1096-1108.
214. Ravichandran, R., et al., *Poly(Glycerol sebacate)/gelatin core/shell fibrous structure for regeneration of myocardial infarction.* Tissue Engineering Part A, 2011. **17**(9-10): p. 1363-73.
215. Ravichandran, R., et al., *Expression of cardiac proteins in neonatal cardiomyocytes on PGS/fibrinogen core/shell substrate for Cardiac tissue engineering.* International Journal of Cardiology, 2012. **5**: p. 5.
216. Norman, J. and T. Desai, *Methods for fabrication of nanoscale topography for tissue engineering scaffolds.* Annals of Biomedical Engineering, 2006. **34**(1): p. 89-101.
217. Motlagh, D., et al., *Microtextured substrata alter gene expression, protein localization and the shape of cardiac myocytes.* Biomaterials, 2003. **24**(14): p. 2463-76.
218. Rosellini, E., et al., *Three-dimensional microfabricated scaffolds with cardiac extracellular matrix-like architecture.* International Journal of Artificial Organs, 2010. **33**(12): p. 885-94.
219. Cristallini, C., et al., *Novel biodegradable, biomimetic and functionalised polymer scaffolds to prevent expansion of post-infarct left ventricular remodelling.* J Mater Sci Mater Med, 2012. **23**(1): p. 205-16.
220. Srinivasan, A. and P.K. Sehgal, *Characterization of biocompatible collagen fibers--a promising candidate for cardiac patch.* Tissue Eng Part C Methods, 2010. **16**(5): p. 895-903.
221. Srinivasan, A., et al., *Collagen 3 D fleece as scaffold for cardiac tissue engineering.* Indian Journal of Thoracic and Cardiovascular Surgery, 2012. **28**(1): p. 1-5.
222. Leong, K.F., C.M. Cheah, and C.K. Chua, *Solid freeform fabrication of three-dimensional scaffolds for engineering replacement tissues and organs.* Biomaterials, 2003. **24**(13): p. 2363-2378.
223. Yeong, W.-Y., et al., *Rapid prototyping in tissue engineering: challenges and potential.* Trends in Biotechnology, 2004. **22**(12): p. 643-652.
224. Abdelaal, O.A. and S.M. Darwish, *Fabrication of tissue engineering scaffolds using rapid prototyping techniques.* Int J Chem Environ Eng, 2011. **59**: p. 577-585.
225. Weigel, T., G. Schinkel, and A. Lendlein, *Design and preparation of polymeric scaffolds for tissue engineering.* Expert Rev Med Devices, 2006. **3**(6): p. 835-51.
226. Sachlos, E. and J.T. Czernuszka, *Making tissue engineering scaffolds work. Review: the application of solid freeform fabrication technology to the production of tissue engineering scaffolds.* Eur Cell Mater, 2003. **5**: p. 29-40.
227. De Mulder, E.L., P. Buma, and G. Hannink, *Anisotropic porous biodegradable scaffolds for musculoskeletal tissue engineering.* Materials, 2009. **2**(4): p. 1674-1696.
228. Patel, H., M. Bonde, and G. Srinivasan, *Biodegradable polymer scaffold for tissue engineering.* Trends Biomater Artif Organs, 2011. **25**(1): p. 20-29.
229. Yeong, W.-Y., et al., *Porous polycaprolactone scaffold for cardiac tissue engineering fabricated by selective laser sintering.* Acta Biomater, 2010. **6**(6): p. 2028-34.

230. Murry, C.E., H. Reinecke, and L.M. Pabon, *Regeneration gaps: observations on stem cells and cardiac repair.* Journal of the American College of Cardiology, 2006. **47**(9): p. 1777-1785.
231. Gittard, S.D. and R.J. Narayan, *Laser direct writing of micro- and nano- scale medical devices.* Expert Rev Med Devices, 2010. **7**: p. 343-356.
232. Patz, T.M., et al., *Two-dimensional differential adherence and alignment of C2C12 myoblasts.* Materials Science and Engineering: B, 2005. **123**(3): p. 242-247.
233. Guillemette, M.D., et al., *Combined technologies for microfabricating elastomeric cardiac tissue engineering scaffolds.* Macromolecular Bioscience, 2010. **10**(11): p. 1330-1337.
234. Choi, H.W., et al., *Structuring electrospun polycaprolactone nanofiber tissue scaffolds by femtosecond laser ablation.* J Laser Appl 2007. **19**: p. 225-231.
235. Park, H., et al., *The significance of pore microarchitecture in a multi-layered elastomeric scaffold for contractile cardiac muscle constructs.* Biomaterials, 2011. **32**(7): p. 1856-1864.
236. Freed, L.E., et al., *Advanced material strategies for tissue engineering scaffolds.* Advanced Materials, 2009. **21**(32-33): p. 3410-3418.
237. Engelmayr, G.C., et al., *Accordion-like honeycombs for tissue engineering of cardiac anisotropy.* Nat Mater, 2008. **7**(12): p. 1003-1010.
238. Mattioli-Belmonte, M., et al., *Rapid-prototyped and salt-leached PLGA scaffolds condition cell morpho-functional behavior.* Journal of Biomedical Materials Research Part A, 2008. **85A**(2): p. 466-476.
239. Vozzi, G., et al., *Microsyringe-based deposition of two-dimensional and three-dimensional polymer scaffolds with a well-defined geometry for application to tissue engineering.* Tissue Engineering, 2002. **8**(6): p. 1089-98.
240. Vozzi, G., et al., *PAM-microfabricated polyurethane scaffolds: in vivo and in vitro preliminary studies.* Macromol Biosci, 2008. **8**(1): p. 60-8.
241. Lionetti, V., et al., *Hyaluronan mixed esters of butyric and retinoic acid affording myocardial survival and repair without stem cell transplantation.* Journal of Biological Chemistry, 2010.
242. Vindigni, V., et al., *Hyaluronan Benzyl Ester as a Scaffold for Tissue Engineering.* International Journal of Molecular Sciences, 2009. **10**(7): p. 2972-2985.
243. Gallina, C., et al., *Development of morphology and function of neonatal mouse ventricular myocytes cultured on a hyaluronan-based polymer scaffold.* Journal of Cellular Biochemistry, 2012. **113**(3): p. 800-7.
244. Fiumana, E., et al., *Localization of mesenchymal stem cells grafted with a hyaluronan-based scaffold in the infarcted heart.* Journal of Surgical Research, 2012. **27**: p. 27.
245. Kai, D., et al., *Polypyrrole-contained electrospun conductive nanofibrous membranes for cardiac tissue engineering.* Journal of Biomedical Materials Research Part A, 2011. **99A**(3): p. 376-385.
246. Mooney, E., et al., *Carbon Nanotubes and Mesenchymal Stem Cells: Biocompatibility, Proliferation and Differentiation.* Nano Letters, 2008. **8**(8): p. 2137-2143.
247. Mackle, J.N., et al., *In vitro Characterization of an Electroactive Carbon-Nanotube-Based Nanofiber Scaffold for Tissue Engineering.* Macromolecular Bioscience, 2011. **11**(9): p. 1272-1282.
248. Mooney, E., et al., *The electrical stimulation of carbon nanotubes to provide a cardiomimetic cue to MSCs.* Biomaterials, 2012. **33**(26): p. 6132-9.
249. Dvir, T., et al., *Nanowired three-dimensional cardiac patches.* Nat Nano, 2011. **6**(11): p. 720-725.
250. Siedle, B., et al., *Sesquiterpene lactones as inhibitors of human neutrophil elastase.* Bioorg Med Chem, 2002. **10**(9): p. 2855-61.
251. Brown, D.A., et al., *Modulation of gene expression in neonatal rat cardiomyocytes by surface modification of polylactide-co-glycolide substrates.* J Biomed Mater Res A, 2005. **74**(3): p. 419-29.
252. Shachar, M., et al., *The effect of immobilized RGD peptide in alginate scaffolds on cardiac tissue engineering.* Acta Biomater, 2011. **7**(1): p. 152-62.
253. Rowley, J.A. and D.J. Mooney, *Alginate type and RGD density control myoblast phenotype.* J Biomed Mater Res, 2002. **60**(2): p. 217-23.

CHAPTER 2
Fabrication of myocardial patches based on synthetic biodegradable polyurethanes

Abstract

The production of efficient heart patches for myocardium repair requires the use of biomaterials with high elastomeric properties and controllable biodegradability. In this chapter, biodegradable poly(ester urethanes) and poly(ether ester urethanes) are proposed as scaffolding polymeric materials for MTE. They were synthesized from poly(ε-caprolactone) (PCL) and poly(ethylene glycol) (PEG) as macrodiols, 1,4-diisocyanatobutane (BDI) as diisocyanate, L-Lysine Ethyl Ester and Alanine-Alanine-Lysine (AAK) as chain extenders. This peptide was used to tune biodegradability, since the Alanine-Alanine sequence is a target for the elastase enzyme. Two formulations were processed into scaffolds by Thermally Induced Phase Separation (TIPS). Scanning Electron Microscopy (SEM) micrographs revealed promising microstructures, which mimicked the striated muscle tissue.

2.1 Introduction: Polyurethanes

Polyurethanes (IUPAC abbreviation PUR, but commonly abbreviated PU) are a large family of polymeric materials which are characterized by a large diversity of chemical compositions, mechanical properties, tissue-specific biocompatibility and biodegradability, with mechanical flexibility and moderate blood compatibility. Thanks to their variable composition and mechanical properties, PURs are among the most extensively used synthetic polymers in biomedical applications after half a century of use in the healthcare system [1]. These polymers played a major role in the development of durable cardiovascular devices since the 1980s, such as blood bags, vascular catheters, bladders of the left ventricle assist device (LVAD), the total artificial heart (TAH) and small caliber grafts for vascular access and bypass surgery [2]. However, they also showed some problems in long-term stability applications, such as pacemaker leads and breast implant coatings [3]. During the next decade, researchers focused their attentions on PURs susceptibility to biodegradation. Research efforts towards understanding their biodegradation have yielded novel PURs with improved stability for long-term implantable devices, as well as an entirely new class of bioresorbable PURs .

2.1.1 Synthesis of PURs

Polyurethanes belong to the group of block copolymers and are characterized by the presence of a significant number of urethane groups. The urethane-forming reaction involves the

isocyanate and the hydroxyl group OH, as illustrated in figure 2.1. As a consequence, the synthesis of PURs requires two essential components: isocyanate (typically diisocyanate) and a bi- or multi-functional polyol with two or more hydroxyl terminal groups.

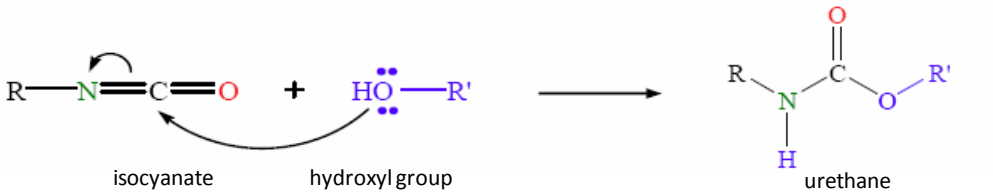

Fig. 2.1 Urethane-forming reaction.

The use of a diisocyanate and a bi-functional polyol (or macrodiol) results in thermoplastic polymers without covalent crosslinking, whereas the use of components with more than two functional groups (e.g., triisocyanate or a multi-hydroxyl polyol) determines PUR three-dimensional networks.

The third important reagent for PUR synthesis is the chain extender. The reaction of a diisocyanate with a polyol usually produces a soft polymer with a low molecular weight. A chain extender, which may be a diol or a diamine with lower molecular weight with respect to long chain diols, can be added in order to produce a higher molecular weight PUR. A polyurethane-urea is obtained if a diamine is used, while if a diol is used a polyurethane is produced (see figure 2.2). The chain extender may be added and react after the low molecular weight PUR (prepolymer) formation (two steps synthesis) or in a single step with the diisocyanate and the macrodiol (one step synthesis).

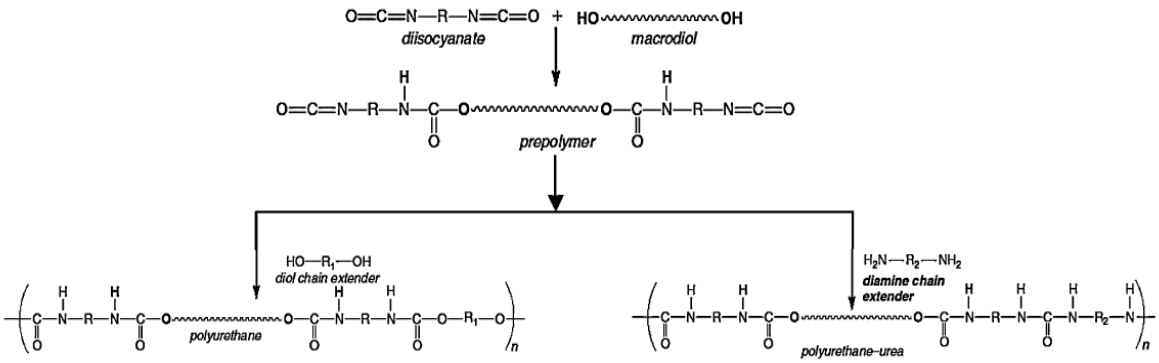

Fig. 2.2 Two steps synthesis of polyurethane and polyurethane-urea.

The properties of the final PUR are primarily dependent on the chemical nature (type of diol, diamine, or diisocyanate) of these three building blocks, and the relative proportions used during synthesis [4]. In tables 2.1 and 2.2 are collected the most common macrodiols and diisocyanates used.

Table 2.1 Typical macrodiols for PUR synthesis.

Name	Chemical Structure
Poly(ethylene oxide) (PEO)	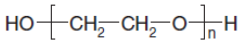
Poly(propylene oxide) (PPO)	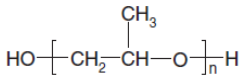
Poly(ε-caprolactone) (PCL)	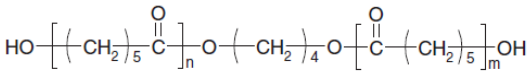
Poly(D,L-lactide)	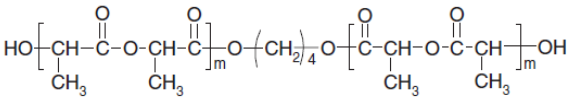
Poly(glycolide)	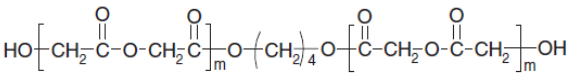

Table 2.2 Typical diisocyanates for PUR synthesis.

Name	Chemical Structure
1,6-Diisocyanatohexane (HDI)	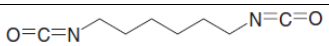
1,4-Diisocyanatobutane (BDI)	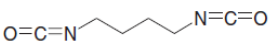
Isophorone diisocyanate (IPDI)	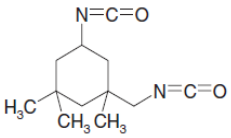
Dicyclohexylmethane diisocyanate (H12MDI)	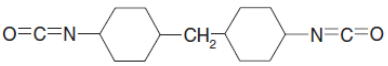
Lysine methyl ester diisocyanate (LDI)	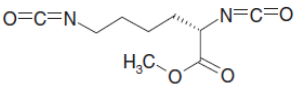
4,4′-Diphenylmethane diisocyanate (MDI)	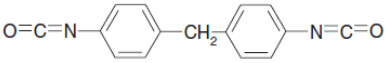

2.1.2 Phase segregation of PURs

Hydrogen bonding can occur between the isocyanate-derived groups (urethanes and ureas) of different polymeric chains. Because of these bonds and the differences in polarity between the segments, PURs can undergo microphase separation to form hard, pseudo-crystalline domains and soft domains [5] (see figure 2.3). The soft domains of PURs are generally composed of long chain polyols and result amorphous and elastomeric at room temperature because the glass transition temperature is below room temperature. PURs can exhibit rubber-like behavior since the hard domains, made of segments resulting from the linking of diisocyanates and chain extender molecules, act as physical crosslinks that fix each soft

segment at its two ends and thus prevent the chains from flowing apart when they are stretched under applied stress. Without flow, the stretched polymer segments can then reshape elastically when stress is released [6].

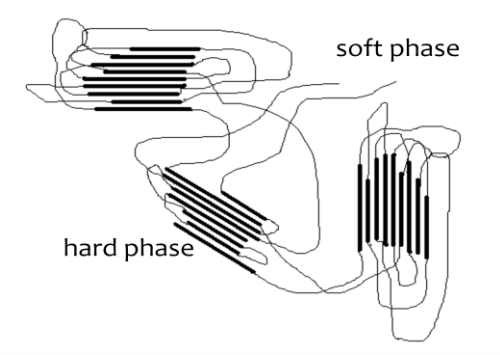

Fig. 2.3 Microphase separation of PURs

Unlike chemical crosslinks, these physical crosslinks are not thermally stable. Subject to sufficient heat treatment, the semi-crystalline hard phase can be melted as for any other thermoplastic polymer. Consequently, segmented PURs are typical thermoplastic elastomers, exhibiting rubber-like mechanical properties and thermo-plastic characteristics.

2.1.3 Biocompatibility of PURs

The biocompatibility of several type of PURs has been widely studied both in vitro and in vivo for a wide range of applications, from durable medical devices (such as vascular catheters, the total artificial heart and small diameter vascular grafts for artificial reconstruction or bypass surgery) [3] to biodegradable implants for tissue engineering [6].
The cell types used to assess the biocompatibility of PURs in vitro are often fibroblasts and endothelial cells, which are among the most commonly used cell types for cytotoxicity tests of biomaterials. Other types of cells used include specific types of leukocytes, as well as specific epithelial cells depending on the targeted site of implantation (e.g., skin, blood vessel, tympanum and cornea [4]). In general, PURs are recognized to have good biocompatibility, maintaining sufficient cell adhesion and proliferation rates in vitro [7], however this short-term cytocompatibility (several days) does not assure a longer-term efficacy and safety of PURs in vivo (weeks to months).
While PURs were recognized in the 1970s and 1980s as stable materials for blood contact, and had been applied in a wide range of cardio-vascular devices [3, 8], their application in long-term implants fell under discussion because of the failure of pacemakers and breast implants [9]. The biological toxicity of degradation products of PURs was also investigated. Aromatic diisocyanates (e.g., 4,4-methylenediphenyl diisocyanate (MDI) and toluene diisocyanate (TDI)) revealed as potentially source of carcinogenic by-products of PUs [10]. As a consequence, aliphatic diisocyanate such as lysine diisocyanates (LDI) and 1,4-diisocyanatobutane (butyl diisocyanate, BDI), have often replaced the use of aromatic diisocyanates [11] for the synthesis

of biodegradable PURs. These polymers exhibit better blood and tissue compatibility, showing no adverse tissue reaction both in vitro and in vivo in comparison to those made using aromatic [2].

2.1.4 Degradability of PURs

As mentioned, PURs were traditionally developed as long-term implant materials, and many attempts were made to create formulations resisting to biodegradation processes [3]. Since the late 1990s attempts have been made to enhance the biodegradability of PURs for applications in tissue engineering [12]. The susceptibility of biodegradable PURs lies in macrodiol components of the polymer, which is generally a polyester. They are degraded by hydrolytic mechanisms (see figure 2.4) and have been made with varied molecular structure to allow controlled hydrolysis rates.

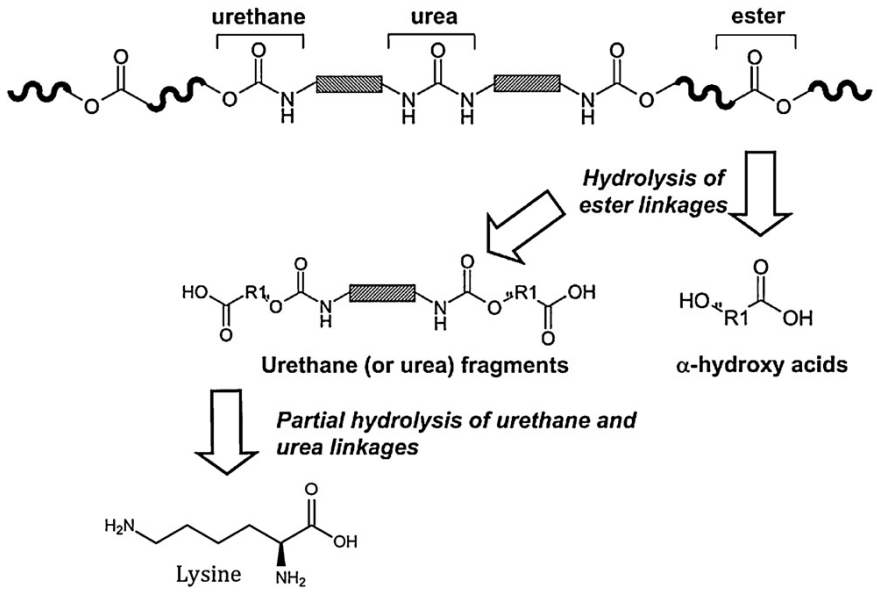

Fig. 2.4 Scheme showing the sites of attack and possible by-products following breakdown of l-lysine-based poly(ester-urethane) by hydrolysis [1].

Along with hydrolysis of ester bonds, several degradation mechanisms have been identified in PURs including oxidation, environmental stress cracking (ESC) and enzymatic degradation [13]. (i) Environmental stress cracking: Poly(ether urethane) materials are susceptible to a degradation phenomenon involving crack formation and propagation. This micro-cracking phenomenon is probably due to residual polymer surface stress, which may have been introduced during fabrication process. (ii) Oxidation: Implanted poly(ether urethane) devices containing metallic components have been subject to bulk oxidation, catalyzed by the aqueous ionic environment of the implant site. (iv) Enzymatic degradation: PUR degradation can also take place because of water soluble enzymes present in the physiological environment. While most enzymes have evolved with highly specific affinities for particular biological substrates, some appear capable of recognizing and acting upon no specific substrates, including synthetic

PURs. (iv) Mineralization/calcification: Calcification (deposition of calcium-containing apatite minerals) has also been reported to occur in cardiovascular and non-cardiovascular medical devices. Calcification is the leading macroscopic cause of failure for most prosthetic heart valves and blood pumps, limiting the functional lifetime of the device by loss of elasticity in the PUR parts [1]. Among these mechanisms, ESC, oxidation and calcification show evident effects only after a long-term implantation of several years. For biodegradable PURs, which are designed to degrade in a relative short period (several months), the main degradation mechanisms are hydrolysis with or without the enzymatic catalysis [14]. As shown in figure 2.4, ester linkages have been believed to hydrolyze both in vitro and in vivo, yielding hydroxy-acid degradation products, as well as urethane and urea fragments with terminal acid groups [14]. The further degradation of urethane and urea fragments to free polyamines is currently under discussion. For lysine-derived polyisocyanates, hydrolysis of urethane linkages to lysine has been reported [15].

2.1.5 Biodegradable PURs for Tissue Engineering

Polyurethanes for tissue engineering applications and drug delivery systems are designed to undergo faster or modulated hydrolytic degradation to non cytotoxic decomposition products in vivo. A very common strategy for achieving biodegradation of PURs is to incorporate a polyester macrodiol that hydrolyzes in vitro and in vivo, such as poly(lactic acid) (PLA), poly(glycolic acid) (PGA) [16] and polycaprolactone (PCL). Poly(ester urethane ureas) (PEUUs) synthesized from 1,4-diisocyanatohexane (BDI) and PCL have been reported to be completely resorbed in rats after only 12 weeks [17]. Biodegradation of PURs can be tuned by enhancing degradation of hard segments through the incorporation of a chain extender that is recognizable by enzymes [18, 19]. In PUR elastomers having Alanine-Alanine-Lysine (AAK) peptide as chain extender, the linkage between two alanine units can be cleaved by a specific elastase. PURs synthesized from the AAK chain extender have shown a significantly faster degradation with respect to those synthesized from a putrescine chain extender, with no cytotoxic products [19].

2.1.6 Thermal properties and processability of PURs

While chemical crosslinking makes materials insoluble and unable of being further shaped by heat and pressure, physically crosslinked PUR elastomers have a good processibility [20], since they can be easily melted around 50 °C. They can be fabricated into different shapes, such as fibers, sheets, and highly porous scaffolds by a number of techniques, such as extrusion [21], wet spinning [22], electrospinning [23, 24], thermally induced phase separation [25] and salt leaching/freeze-drying [26, 27]. Depending on the particular fabrication technique, different porosities, surface-to-volume ratios and three dimensional structures may be obtained. Consequently, modulation in mechanical properties can be achieved to meet the requirements of a wide range of tissue engineering applications, including repair of cardiovascular, muscular and neuronal tissue.

2.2.7 Polyurethane synthesis and scaffold fabrication in the present work

In this chapter the synthesis and characterization of poly(ester urethanes) and poly(ether ester urethanes) biodegradable biomaterials for MTE scaffolds are described. The proposed formulations are based on poly(ε-caprolactone) (PCL) and poly(ethylene glycol) (PEG) as macrodiols, 1,4-diisocyanatobutane (BDI) as diisocyanate component, L-Lysine Ethyl Ester and Alanine-Alanine-Lysine as chain extenders. PCL was selected since it can confer biodegradability to the final PUR, while PEG was added in low amounts to tune mainly wettability, mechanical and biological properties of the final constructs. BDI was chosen because it is an aliphatic diisocyanate, which is used due to its corresponding, non-toxic, biodegradation products [2].
Amino acids-based chain extenders were used for their biocompatibility. Alanine-Alanine-Lysine peptide was selected especially to tune biodegradability properties, since, as it has been discussed previously, the Alanine-Alanine sequence may be cleaved by the elastase enzyme.
The obtained polymers were processed into films and tridimensional porous scaffolds. The latter were prepared by the Thermally Induced Phase Separation technique, with the application of a thermal gradient. It allows the formation of oriented stretched pores with a resulting anisotropic structure that confers to the substrates a remarkable similarity to the streaked muscle tissue [28].

2.2 Materials and methods

2.2.1 Polyurethane synthesis

PURs were synthesized through a two steps procedure [29, 30]. Poly(ε-caprolactone) diol (Polysciences, M_w=1250 g/mol) and Poly(ethylene glycol) (Sigma-Aldrich, M_w=1500g/mol) were used as macrodiols and dissolved in 1,2-dichloethane (DCE, Sigma-Aldrich). The solution was azeotropically dried by refluxing under nitrogen over molecular sieves. 1,4-diisocyanatobutane (BDI, Aldrich) was reacted (2:1 molar ratio) with the macrodiols in presence of the catalyst (Dibutyltindilaureate, Fluka) to form the prepolymer. At the end of this first step (150 min, 80°C), the chain extender (L-Lysine Ethyl Ester (Sigma-Aldrich) or AAK (Advanced ChemTech) and Lysine Ethyl Ester 50/50), was dissolved in anhydrous DCE with Triethylamine (TEA, Sigma-Aldrich) and added at 1:1 molar ratio with respect to macrodiols at room temperature. Chain extension reaction was stopped after 16 hours by the addition of methanol (MeOH, Sigma-Aldrich). The polymers were collected by precipitation in petroleum ether (Sigma-Aldrich) and purified by dissolution in dimethylformamide (DMF, Sigma-Aldrich) followed by precipitation in methanol. The obtained powder was dried under vacuum at 40°C for 72h.
The code name used for PCL-based PURs is XBC1250-type, where X, B, C1250 respectively indicate: the chain extender (K for Lysine ethyl ester and A for Alanine-Alanine-Lysine/ Lysine 50/50), the diisocyanate (BDI), the macrodiol (PCL) and its molecular weight (1250 g/mol). For PCL-PEG based PURs the code name is KBC1250-E1500-N'-type, where E1500 corresponds to the PEG macrodiol and its molecular weight (1500 g/mol), while N' indicates

the weight percentage of PEG with respect to PCL mass. Codes and compositions of all synthesized PURs have been reported in table 2.3.

Tab. 2.3 Polyurethanes Composition

PURs CODES	PEG M_w(g/mol)	% PEG w/w	Chain Extender
KBC1250	-	-	Lysine Ethyl Ester
KBC1250-E1500-10	1500	10	Lysine Ethyl Ester
KBC1250-E1500-20	1500	20	Lysine Ethyl Ester
ABC1250	-	-	Lysine Ethyl Ester/Alanine-Alanine-Lysine

2.2.2 Polymer characterization and processing

PURs were chemically characterized through ATR-IR (Attenuated Total Reflection Infrared Spectroscopy) by using a Perkin Elmer Spectrum 100 equipped with an ATR attachment (UATR KRS5) with Diamond crystal.
Number average molecular weights (M_n) and molecular weight distributions (M_w/M_n) of PURs were measured by Size Exclusion Chromatography (SEC) using an Agilent Technologies instrument (1200 Series) equipped with a RI detector and two Waters styragel columns at 35°C. The measurements were performed using Tetrahydrofuran (THF, Sigma-Aldrich) as eluent (0.4 ml/min) and narrow polystyrene standards for calibration.
Thermal characterization was performed by Differential Scanning Calorimetry (DSC), using a TA Instrument DSC Q20. The thermal curves were obtained heating samples from -60°C to 150°C under nitrogen flow, cooling from 150°C to -60°C and heating again from -60°C to 150°C, with 10°C/min heating/cooling rate. For PCL based PURs the crystallinity grade has been calculated from DSC first cycle curves, through the formula:

$$C\% = (\Delta H_m \cdot 100)/(w \cdot \Delta H^\circ_m) \quad (1)$$

Where ΔH_m is the heat of fusion of the material, ΔH°_m is the heat of fusion of the starting PCL diol (70,7 J/g) and w is the PCL weight fraction in the copolymer [31].
Films of the synthesized PURs were obtained by hot pressing and mechanically characterized in triplicate by stress-strain tests, performed by using a MTS QTest/10 Elite Controller. The displacement rate was 10 mm/min and the load limit of the sensor was 500 N. Static Contact Angle measurements were carried out on films (three points for each sample) in order to study their hydrophylicity, by a KSV INSTRUMENT CAM2000 and water as test liquid (5 µl of drop volume).

Hydrolytic and Enzymatic degradation tests

Hydrolytic and enzymatic degradation tests with Elastase (from porcine pancreas, Sigma Aldrich) were carried out on square 0.3 mm thick films of ABC1250 and KBC1250 as control.

Hydrolytic and enzymatic tests with Lipase (from porcine pancreas, Sigma Aldrich) were performed on both square 0.3 mm thick films and square 1 mm thick scaffolds of KBC1250.
Both degradation tests were carried out at 37°C. The samples were placed in vials containing 0.1 ml of phosphate buffer (PBS, pH = 7.6)/mg of PUR (hydrolytic tests) and 0,3 mg of enzyme/ml of PBS solution (enzymatic tests).
The degradation medium was renewed every 3 days and three samples were taken once a week (for five weeks), washed with distilled water and then vacuum dried at 40°C for three days.
At every time interval, % weight loss of the specimens was evaluated according to the formula:

$$\% \text{ weight loss} = [(W_0\text{-}W)/W_0] \text{ x}100 \quad (2)$$

where W_0 is the initial weight of the sample, while W is its weight after degradation, at a particular time interval.

Scaffold preparation and characterization

Polyurethanes were processed in scaffolds by Thermally Induced Phase Separation (TIPS) according to the following procedure. The polymers were dissolved in dimethyl sulfoxide (DMSO, Sigma-Aldrich) (7% w/v) at 80°C. The solutions were poured in parallelepiped stainless steel molds (55mm x 20mm x 25mm) and quenched at -80°C for 3h. The frozen solutions were then washed in ethanol/water (90/10 v/v) for 5 days and finally lyophilized. In order to obtain scaffolds with oriented pore structures, a thermal gradient was applied during the freezing-phase of TIPS [28].
The resulting microstructures were characterized by Static Contact Angle measurements, by the same instrument and test parameters used for PUR films, and Scanning Electron Microscopy (SEM), by a LEO 1420 microscope (Zeiss). Stress-strain tests were performed using the MTS QTest/10 Elite Controller. The displacement rate was 10 mm/min and the load limit of the sensor was 500 N.
Image data were imported into ImageJ software for analysis. The average pore size was obtained by measuring the maximum and minimum diameter of 20 pores chosen at random throughout the central section of the samples.

Cell viability (MTS assay)

Cell viability tests were performed on films and scaffolds (1 x 1 cm^2), that were previously sterilized through immersion in ethanol/water (70/30) solution and UV treatment (10 min), using a rat heart cell line (H_9C_2cardiomyoblasts). Cells were cultured in DMEM (Dulbecco's Modified Eagle Medium, Gibco) enriched with 10% fetal bovine serum (FBS), glutamine (2mM), penicillin (100 U/ml) and streptomycin (100 μg/ml) (Euroclone, Italy). Cells were maintained at 37° C in a humidified atmosphere with 5% CO_2 and used at 10^5 x cm^2 on the samples' surfaces. To evaluate cell viability, MTS assay was performed (CellTiter 96® Aqueous Non-Radioactive Cell Proliferation Assay, Promega, Italy). It is a colorimetric assay for measuring cellular metabolic activity via NAD(P)H-dependent cellular oxido-reductase

enzymes that reduce the tetrazolium dye, MTS, to its insoluble formazan, giving a purple color with an absorbance maximum at 490-500 nm in phosphate-buffered saline.
Cells were cultured on the different surfaces for 24 and 72h. A MTS solution was added to the culture medium. After 3h, the culture medium was removed and the solution was read in UV-VIS spectroscopy (V-630 UV-Vis Spectrophotometer, Jasco, USA) at 490 nm. The absorbance was directly proportional to viable cells amount. Cells seeded on cell culture Petri dishes were used as positive control.

Western Blot (Vinculin, Myf5, PCNA)

H_9C_2 cardiomyoblasts were cultured for 24 and 72 hours on different materials. Culture medium was then discarded and a lysis solution (SDS 2.5%, Tris-HCl pH 7.4, 0.25 M in bidistilled water) was placed on the different samples. Cell proteins were quantified through BCA assay (Thermo Scientific, USA). For electrophoresis, 10 μg of total proteins were used. Samples were diluted with Laemmli reducing buffer (60 mM Tris-Cl pH 6.8, 2% SDS, 10% glycerol, 5% β-mercaptoethanol, 0.01% bromophenol blue), and electrophoresed on 7.5% sodium dodecylsulfate polyacrylamide gels (SDS-PAGE). The proteins were blotted onto nitrocellulose membranes. The membranes were incubated for 1 h in 5% blocking solution (non-fat dry milk in PBS), then incubated overnight with 1:500 dilution of primary antibodies (Vinculin – Calbiochem, USA-, PCNA and Myf5 – Millipore, Italy), followed by incubation with appropriate secondary antibody HRP-conjugated (Perkin-Elmer). Proteins were detected by Western Lightning plus-ECL (Perkin-Elmer, USA), and protein bands were then visualized by Bio-Rad VersaDoc™ imaging system.

Statistical Analysis

Data obtained from stress-strain tests, contact angle measurements and cell viability test were investigated for statistical significance using one-way analysis of variance (ANOVA). A *p*-value less than 0.05 was considered significant.

2.3 Results and discussion

2.3.1 Polyurethane synthesis

All PURs formulations were successfully synthesised, as demonstrated by ATR-IR spectroscopy. The spectra of the polyurethanes are reported in Figure 2.5. The peak observable in the region between 1630 and 1640 cm^{-1} corresponds to the stretching of the urethane C=O (amide I) and the peak at 1530 cm^{-1} represents N-H bending vibrations (amide II), which indicates the formation of urethane linkages. The absorption at 1721cm^{-1} represents the stretching of the carboxyl group (C=O) due to ester groups.
The N-H stretching of the urethane group can be observed at 3330 cm^{-1}. The absorption at 1106 cm^{-1} can be ascribed to the stretching of the C-O-C linkage of both urethane and ether groups. This peak is more intense for KBC1250-E1500-20 due to the higher PEG content

into this polymeric formulation. The spectra of ABC1250 showed a broad peak in the region of the N-H bending (amide I): multiple signals overlapped, due to the absorption of peptide groups (at higher frequencies) and urethane groups (at lower frequencies).

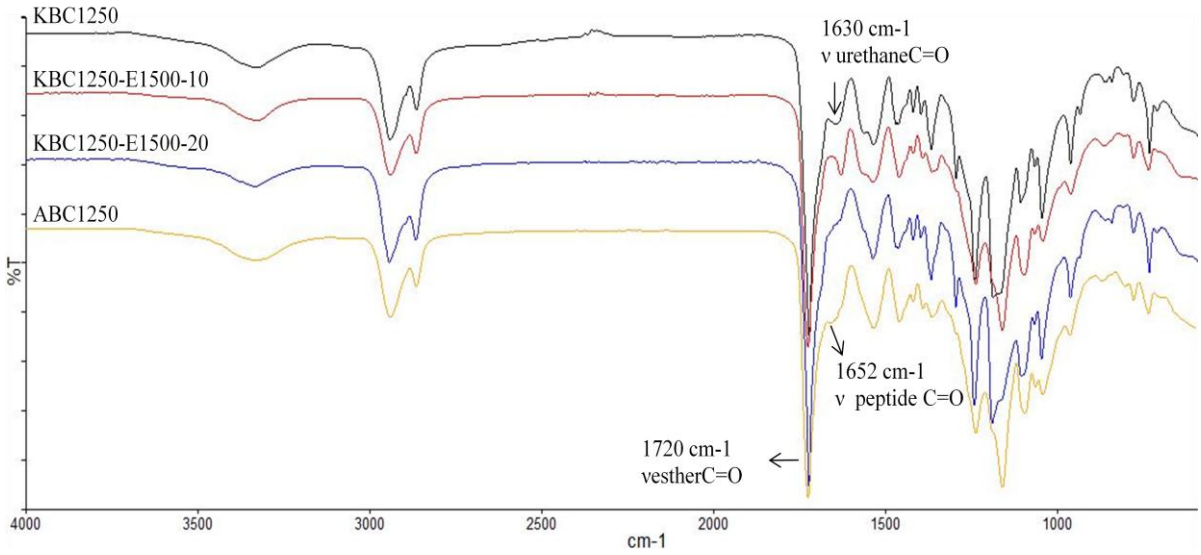

Fig. 2.5 FT-ATR spectra of KBC1250, KBC1250-E1500-10, KBC1250-E1500-20 and ABC1250.

Average numeral molecular weights (M_n) and polydispersity indexes (M_w/M_n) of the synthesised polymers, obtained by SEC analysis, are collected in Table 2.4.

Tab. 2.4 Polyurethane average numeral molecular weights (M_n) and polydispersity indices (M_w/M_n)

PURs	$M_n \times 10^3$ (g/mol)	M_w/M_n
KBC1250	20	1.6
KBC1250-E1500-10	41	1.3
KBC1250-E1500-20	43	1.2
ABC1250	41	1.7

2.3.2 Thermal and mechanical properties of the synthesized PURs

DSC characterization showed different thermal properties for the PURs obtained. The thermograms of the samples are compared in Figure 2.6 a (first cycle) and 2.6 b (third cycle) together with the curves of the PCL diol. Experimental data are collected in Table 2.5.
The first heating cycle shows a broad exothermic peak between -50°C and 0°C for all the compositions. This transition could be attributed to a cold crystallization, due to the rearrangement of the amorphous regions into a crystalline phase during heating [32]. These crystallization temperatures (T_c) decrease by increasing PEG content. This trend could be linked to the presence of PEG blocks: with increasing PEG amount, polymeric chains become more flexible and able to crystallize or rearrange themselves at lower temperatures. For mixed PCL-PEG based PURs, melting peaks appear lower and broader with respect to KBC1250. Broad peaks are the result of crystals with different sizes, since polyurethane chains have a

more irregular chemical structure because of the presence of PEG segments. However, all the samples show two melting peaks in the first heating cycle, due to the presence of two different crystalline domains for PCL segments. The existence of these two domains appears clear in the first heating cycle of the PCL diol alone, containing two well defined melting peaks at 36 and 55°C. In the third cycle, all the samples (except PCL diol) show one melting peak, probably because the fast cooling and heating do not allow the rearrangement of the polymer chains into two crystalline phases .

The cristallinity grade of KBC1250 and ABC1250 was calculated using formula (1), starting from their overall melting enthalpies in the first cycle (26 and 21 J/g, respectively). The result was 53% for KBC1250 and 41% for ABC1250. The cristallinity grade was not calculated for the mixed PCL-PEG based PURs because the formula applied in the calculation does not take into account the possible contribution of PEG segments in the formation of crystalline domains. Glass transitions cannot be observed because they are outside of the range considered (T_g of the oligomeric PCL diol is at -70.3 °C [33]).

Tab. 2.5 PUR Crystallization and melting temperatures

PURs	**T_c(°C)**		**T_m(°C)**		
	I cycle	**III cycle**	**I cycle**		**III cycle**
KBC1250	-5	15	36	56	42
KBC1250-E1500-10	-19	-2	20	63	36
KBC1250-E1500-20	-24	-	21	48	36
ABC1250	-16	6	31	57	40

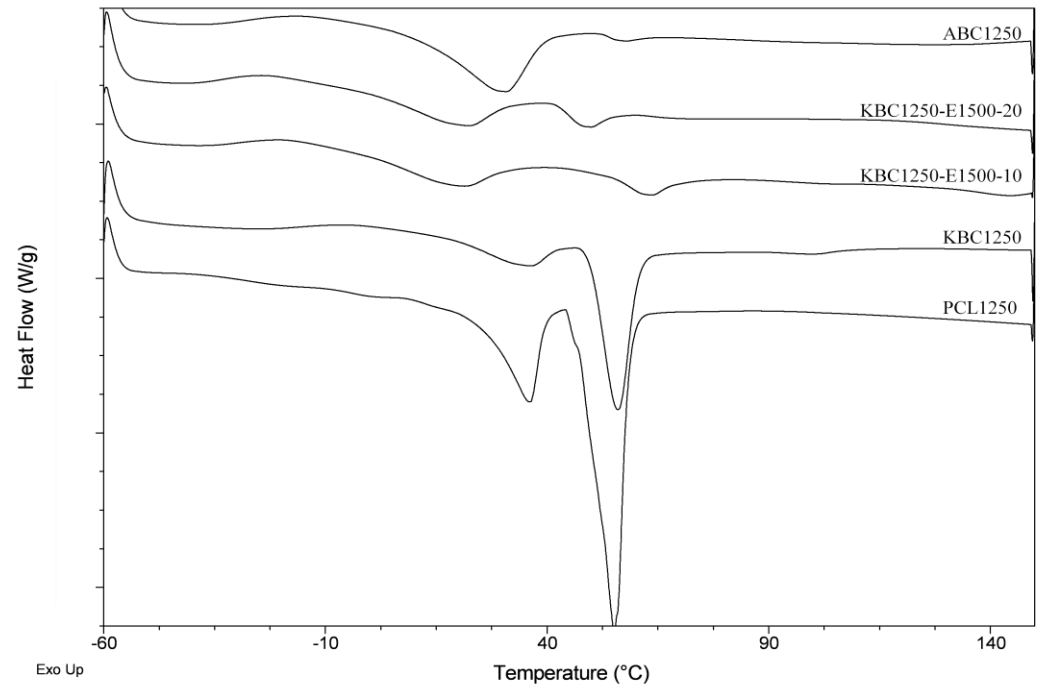

(a)

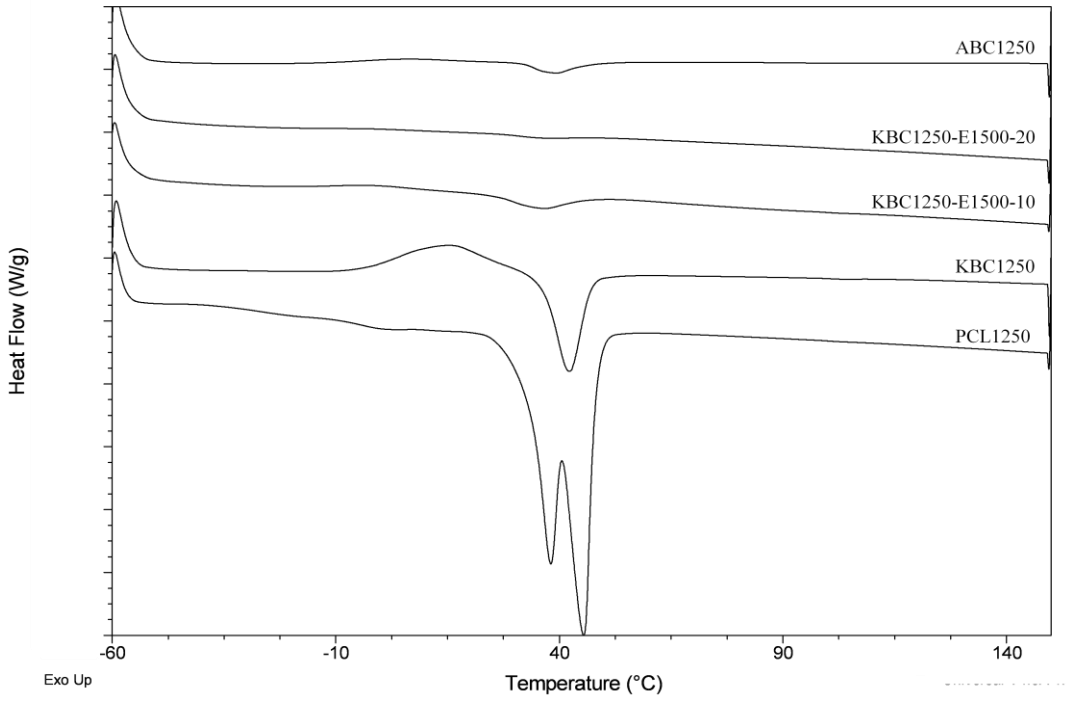

(b)

Fig. 2.6 DSC curves of the synthesised PURs: (a) I cycle, (b) III cycle.

PUR films were characterized by stress strain tests and results are collected in Table 4. All the curves, shown in Figure 2.7, present a typical elastic behaviour up to 20% of strain approximately, followed by a short plastic deformation. An increase in the stress response can be observed, probably due to the strain-induced crystallization of the macrodiols [34]. This behaviour is marked for the PURs containing PEG.

Data in Table 2.6 show that the polymers have Young Moduli encompassing from 7 to 14 MPa and the elastic modulus decreases with increasing PEG content. The stress-strain curves, shown in Figure 3, and the histograms, shown in Figure 4, highlight that the maximum stress and the corresponding strain increase with increasing PEG content. In detail, the statistical analysis (one-way ANOVA) showed that there are significant differences on elastic moduli for KBC1250 and KBC1250-E1500-20, KBC1250-E1500-10 and KBC1250-E1500-20 ($p<0.05$). In addition, the differences on stress values are all significant, while those on % strain are not significant for KBC1250 and KBC1250-E1500-10, and KBC1250 and ABC1250.
These results demonstrate the possibility of tuning the mechanical properties of PURs by slightly varying the PEG content.

Tab. 2.6 Experimental mechanical data of the synthesized PURs.

PURs	Young Modulus (MPa)	Average Max Stress (MPa)	Average Max % Strain
KBC1250	14.3 ± 1.1	5.0 ± 0.4	515± 81
KBC1250-E1500-10	12.2 ± 1.6	9.9 ± 1.0	596 ± 90
KBC1250-E1500-20	7.2 ± 1.8	16.9 ± 0.9	1081 ± 84
ABC1250	9.4 ± 1.5	2.0 ± 0.3	453± 80

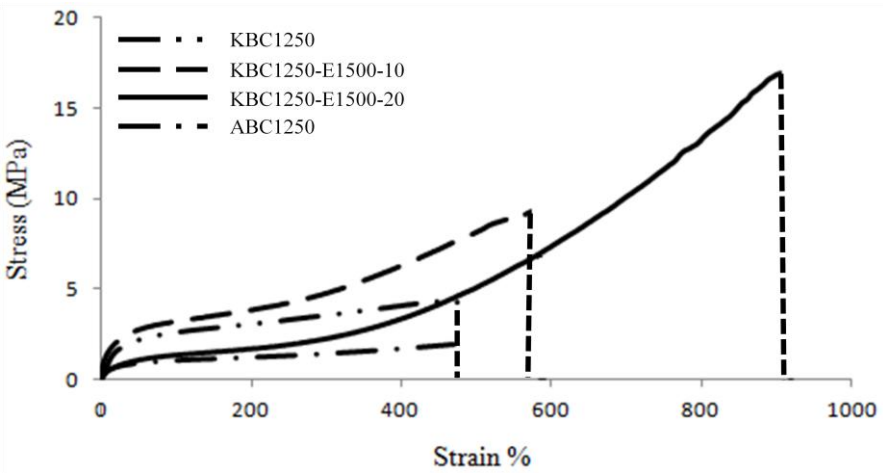

Fig. 2.7 Stress-strain curves of PURs.

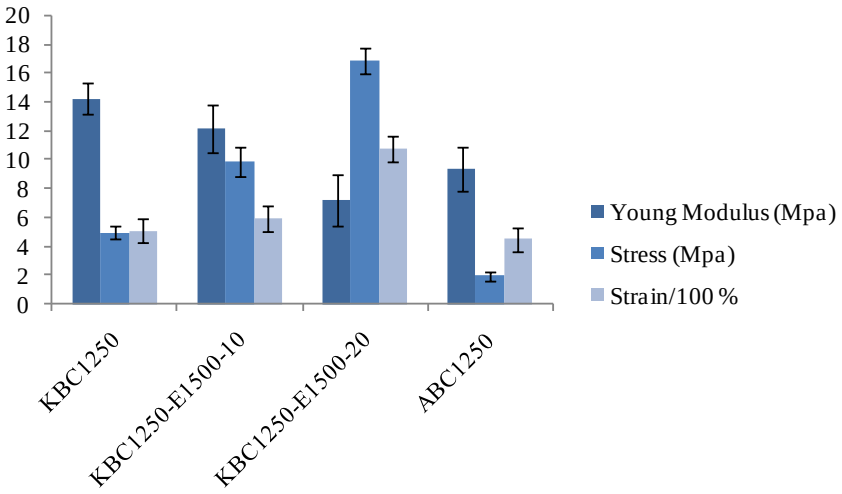

Fig. 2.8 Comparison of mechanical parameters of the KBC-series of PURs.

2.3.3 Surface properties of PUR films

Contact angle measurements, whose results are collected in Table 2.7, demonstrated a low hydrophobicity for all the polyurethane films. No significant differences in contact angle can be observed between KBC1250, KBC1250-E1500-10 and KBC1250-E1500-20, probably due to the low difference in the PEG content.

Tab. 2.7 Contact Angle values for PUR films.

PUR FILMS	Contact Angle (°)
KBC1250	78 ± 2
KBC1250-E1500-10	81 ± 2
KBC1250-E1500-20	81 ± 1
ABC1250	94 ± 1

Nevertheless, after about one month of film ageing at room temperature in air, a significant decrease in contact angle value has been observed, particularly for mixed PCL-PEG PURs, that reached a contact angle vale of about 40°. The observed increase in hydrophilicity is probably due to a slow process of surface segregation, typical of multiconstituent systems, such as polyurethanes, characterized by the presence of a two-microphase structure with regions enriched in either hard or soft segments. This phase separation generates a dynamic system that tends to segregate on the surface the lowest surface energy component in order to decrease the surface energy [35]. A second contribute to this change in hydrophilicity could be given by another typical process for polyurethanes: water adsorption from air, which causes the hydrolysis of ester bonds in the polymeric chain and a slow surface degradation [36].

2.3.4 Enzymatic (elastase) and hydrolytic degradation tests

The results obtained by the elastase degradation test, carried out on ABC1250 and KBC1250 films, are shown in Figure 2.9. After the first week of incubation, where no degradation effects were observable for both samples, ABC1250 exhibited a progressive weight loss, up to about 5% after 5 weeks. KBC1250, used as control, showed a more constant weight loss of about 2% during the whole degradation test. These data reveal a significant effect of the presence of the AAK peptide introduced into the PUR backbone on the enzymatic degradation behaviour. Guan and co-workers obtained 2-25% weight loss for similar polyurethane films having 100% AAK peptide in the chemical composition in analogous enzymatic degradation tests (elastase concentration 0,3 mg/ml) [19]. Our results demonstrate that the replacement of 50% AAK peptide with Lysine in the PUR backbone leads to a fine tuning of the enzymatic degradation behaviour, resulting in a plain slowing down of the degradation process.

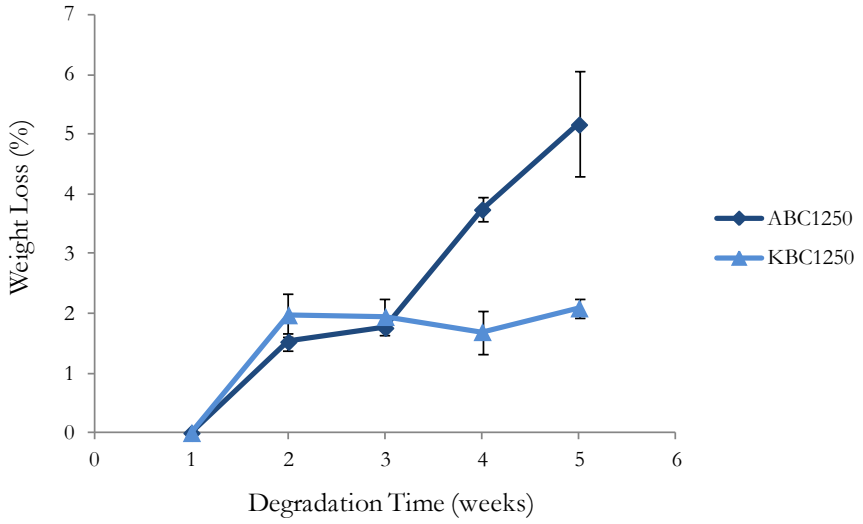

Fig. 2.9 Weight loss of ABC1250 and KBC1250 films in PBS with 0,3 mg/ml elastase.

2.3.5 Morphological, thermal and mechanical properties of the scaffolds

Based on the observations that KBC1250-E1500-20 showed the mechanical properties closest to those required for the perspective application (the lowest Elastic Modulus and the highest Maximum % Strain), this polymer was selected to prepare porous scaffolds. Scaffolds with KBC1250 were also prepared as reference for materials without PEG.
SEM micrographs of the scaffolds produced by TIPS are collected in Figure 6. The longitudinal and cross sections showed a porous microstructure characterized by long and stretched pores. The pores are oriented in one direction in accordance to the thermal gradient applied during the quenching step of scaffolds preparation. The resulting anisotropic structure (Figure 6a and 6c) seems to mimic the striated muscle tissue. Guan and colleagues reported that a similar structural biomimicry promotes adhesion and proliferation of muscle cells [28]. SEM micrographs elucidated also differences in the porous structures of the two materials.

The scaffold fabricated from KBC1250 has interconnected porosity and pores of 98 ± 14 μm (see Figure 2.10 a and 2.10 b), while the scaffold obtained by the PCL-PEG based PUR is characterized by well aligned tubes with smooth walls and pore size of 15 ± 2μm (see Figure 6c and 6d). The formation of these two micro-architectures could be linked to the different molecular weight of the two formulations (20000 g/mol for KBC1250 and 43000 g/mol for KBC1250-E1500-20), as observed also by other authors [37]. However, they can promote different processes: it is known that large pores favour cell colonization, cell migration and nutrients supply, while small pores (tens μm) can promote vascularization [38, 39].

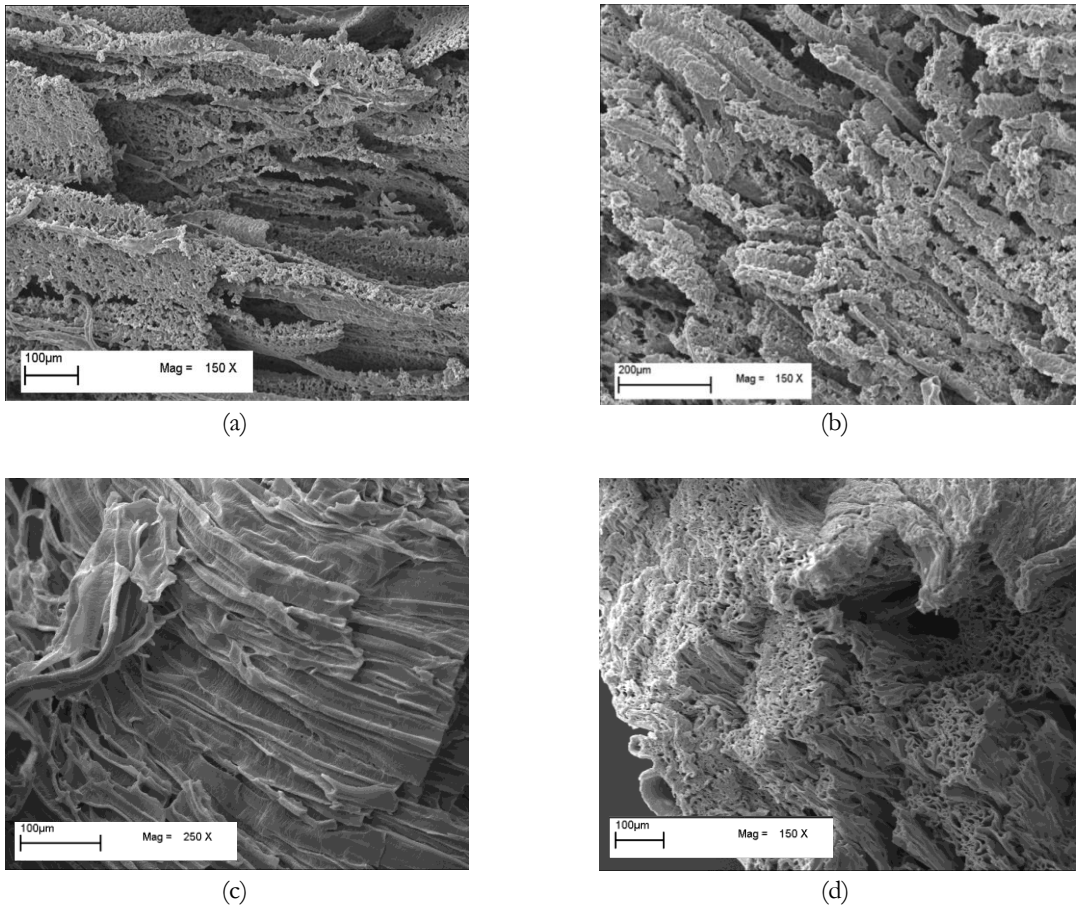

Fig. 2.10 SEM images of: longitudinal (a) and cross (b) sections of KBC1250 and longitudinal (c) and cross (d) sections of KBC1250-E1500-20.

Thermal and mechanical properties of the prepared scaffolds have been evaluated. For both KBC1250 and KBC1250-E1500-20 scaffolds, the first heating cycle is characterized by a melting peak at 58 and 55°C, respectively (see Table 2.8 and Figure 2.11). In the third cycle a melting peak is observable at lower temperatures and a very low crystallization peak is present for KBC1250 scaffold. In the third cycle the thermal behavior of processed and non-processed materials result similar (see Figure 2b) as a consequence of thermal history removal.

Tab. 2.8 Scaffold crystallization and melting temperatures.

PUR SCAFFOLDS	T_c(°C)		T_f (°C)	
	I cycle	III cycle	I cycle	III cycle
KBC1250	-	-7	58	37
KBC1250-E1500-20	-	-	55	36

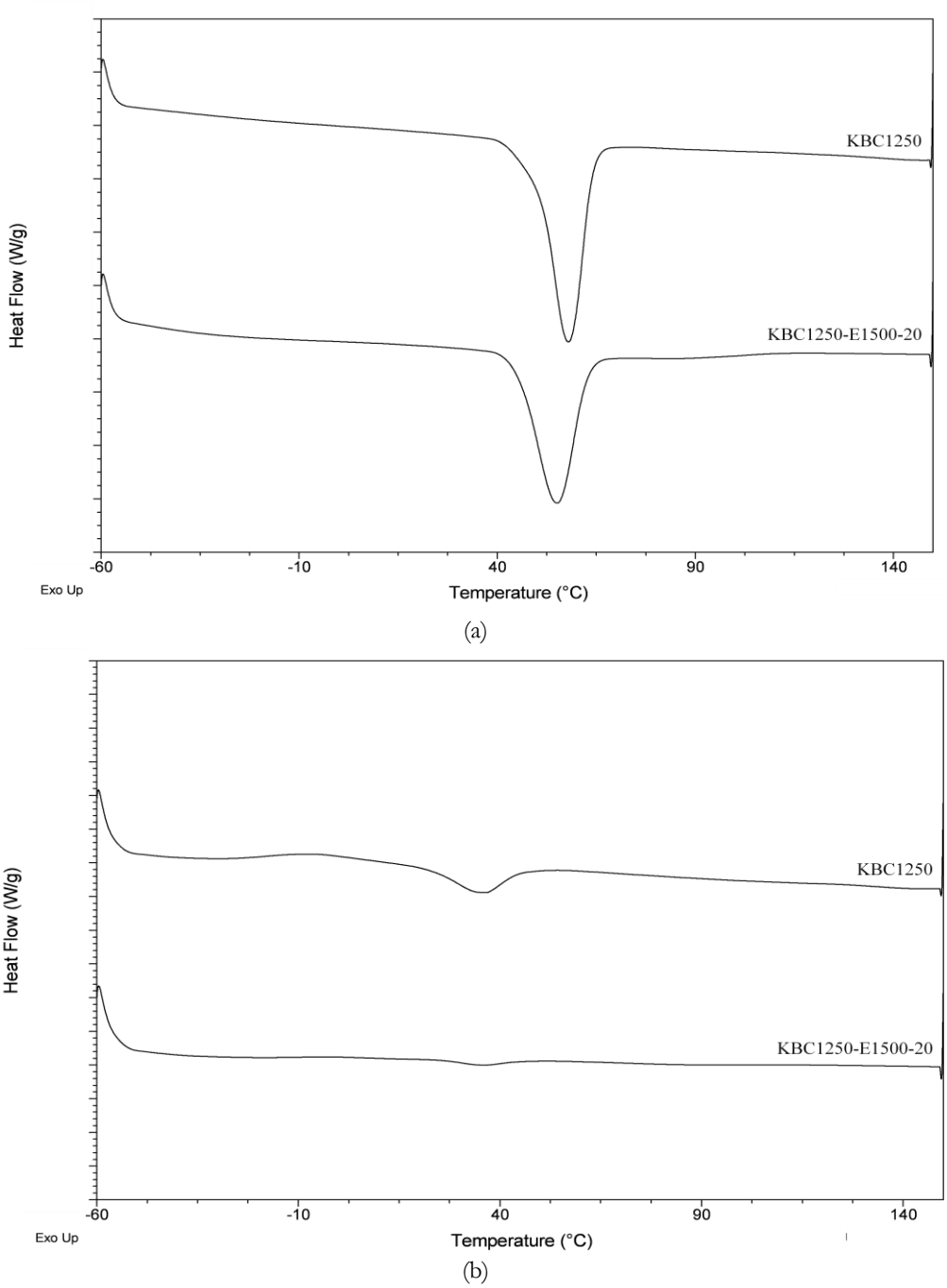

Fig. 2.11 DSC curves of KBC1250 and KBC1250-E1500-20 based scaffolds: (a) I cycle, (b) III cycle.

DSC characterization revealed satisfactory thermal properties for the porous scaffolds, because they both show melting temperatures significantly higher than the physiological temperature. This aspect has to be taken into account since the mechanical performance of the myocardial patch can be affected by the melting or softening of parts or domains of the materials.

The crystallinity grade for KBC1250, which was calculated by the enthalpies in the first heating cycle (ΔH_m= 45J/g), is 90%. It is much higher than the crystallinity percentage obtained for non porous KBC1250 (40%, see Table 3). This significant difference is probably due to the high level of order of the polymeric chains in the scaffold microstructure, where they tend to align to form long oriented pores, as a consequence of the thermal treatment during TIPS.

Tensile tests were performed on scaffolds along the direction of the stretched pores. As shown in Figure 2.12, the resultant Stress-Strain curves present an initial elastic deformation, followed by a plastic behavior.

Tab. 2.9 Experimental mechanical data of the prepared PUR scaffolds.

PUR SCAFFOLDS	Young Modulus (MPa)	Average Max Stress (MPa)	Average Max % Strain
KBC1250	2,8 ± 0,9	0,6 ± 0,2	155 ± 56
KBC1250-E1500-20	1,6 ± 0,3	0,3 ± 0,1	126 ± 25

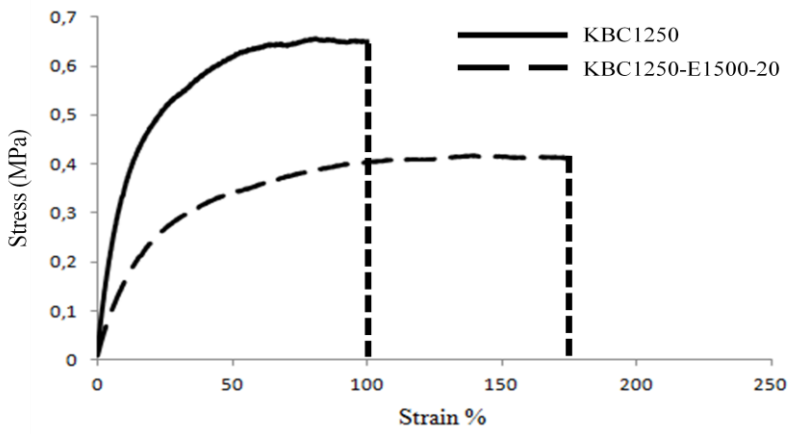

Fig. 2.12 Stress strain curves of KBC1250 and KBC1250-E1500-20 based scaffolds.

The statistical analysis showed that there are no significant differences on the elastic modulus, and stress and strain behaviour for the two scaffolds. Therefore, the addiction of a low percentage of PEG seems not to significantly affect the mechanical behaviour of the porous substrates, where the higher influence on mechanical performance is probably given by the similar microstructure with respect to the chemical compositions of the polymers.

It is known that a heart patch should be able to mimic the mechanical behaviour of myocardial tissue and to withstand the strain due to cardiac beating [40-44]. The stiffness (Young Modulus) of myocardial tissue was evaluated in the range 10–20 kPa at the beginning and 200–500 kPa at the end of diastole, and the stress and strain at break respectively in the

ranges 3-15 kPa and 22-90% [45-48]. As a consequence, an ideal heart patch should be characterized by Young Moduli encompassing from tens of kPa to 1 MPa and by an elastomeric mechanical behaviour, able to withstand the contractile and expansive forces originated during the cardiac cycle [49]. Based on these considerations, proposed scaffolds seem to be suitable as cardiac patches, even though characterized by a lower elastic modulus, maximum stress and strain with respect to the corresponding films (see Table 4 and 7). Their elastic response corresponds to about 20% of deformation, maximum stress and strain are significantly higher than stress and strain at break of the myocardium and elastic moduli are closer to that of native tissue.

2.3.6 Surface properties of scaffolds

As shown from data collected in Table 2.10, PUR scaffolds are more hydrophobic with respect to the corresponding films (see Table 2.7). Several authors showed that submicron roughness makes an inherently hydrophobic material highly hydrophobic [50, 51]. This higher hydrophobicity can be attributed also to the scaffold higher crystallinity and aligned fiber-like structure. The correlation between crystallinity and wettability was observed for other types of polymeric materials by Pittman [52] and Areias [53]. In particular, Areias also observed the increase of surface hydrophobicity with increasing fiber orientation of poly(L-lactide) electrospun mats, which suggests that the orientated long tubes of PUR scaffolds can produce a similar effect.
In addition, a significant hydrophilicity increase ($p<0.05$) for the scaffold based on the PUR containing PEG is observable, probably as a results of material transformation following the TIPS procedure. The formation of scaffold microstructure takes place in DMSO and the following washings are made with a solution of ethanol and water. The contact of the material with these polar solvents could induce a sort of segregation of the polar PEG segments on the exposed surfaces of the porous structure.

Tab. 2.10 Contact Angle values for PUR scaffolds.

PUR SCAFFOLDS	Contact Angle (°)
KBC1250	137 ± 2
KBC1250-E1500-20	123 ± 2

2.3.7 *In vitro* biological characterization of films and scaffolds

Results of viability tests (MTS), performed with H_9C_2 rat heart cells (Figure 2.13), showed unaltered cell viability after 24 hours with respect to the control when seeded on porous and dense KBC1250. After 72 hours porous KBC1250 showed a significant increased cell viability with respect to the control and the other samples ($p<0.0001$).
These results are in agreement with the observation [38, 39] that interconnected microstructure with pore sizes of about 100 μm can favor cell colonization. An opposite trend

was observed for KBC1250-E1500-20 film and its porous scaffolds. While cell viability on KBC1250-E1500-20 films was acceptable and only slightly decreased with respect to control, cells showed a significantly decreased viability after both 24 and 72 hours seeding on porous scaffolds. KBC1250-E1500-20 scaffold microstructure is characterized by very small pores that probably inhibit H_9C_2 cell attachment and proliferation. In this case the high hydrophobicity of the sample is not compensated by a suitable microstructure for cell adhesion.
The increased cell viability after 72 hours indicated the cell ability to proliferate on all the samples with duplication rates comparable to control, with the exception of porous KBC1250-E1500-20.

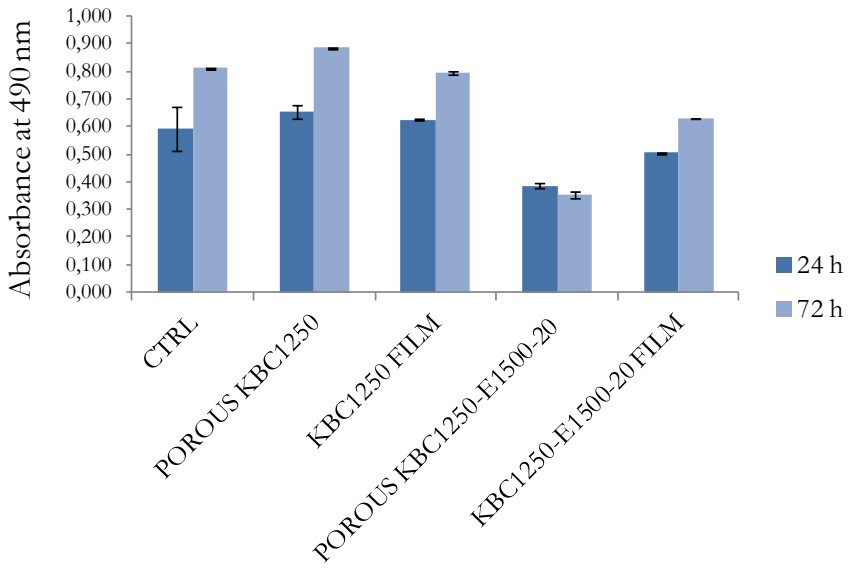

Fig. 2.13 Results of viability MTS tests performed on KBC1250 film and porous scaffold, KBC1250-E1500-20 film and porous scaffolds using H_9C_2 rat heart cell line.

Results from Western Blot are shown in Figure 2.14. Vinculin expression has been evaluated after 24h and 72h of cell culture on different materials. After 24h all samples displayed no significant changes in the expression of the adhesion protein when compared to the control. A significant up-regulation has been shown on porous KBC1250. The study conducted by Arai and co-workers demonstrated the existence of a correlation between substrate pore size and cardiac myocytes response [54]. They considered honeycomb-patterned substrates with subcellular, cellular and overcellular pore sizes. The best results in terms of cellular adhesion and spreading were obtained with overcellular pores, probably because cells are forced to stretch along the edges of the pores. If we consider that myocardial cells have typically dimensions encompassing from 10 to 100 μm [55][43], we can hypothesize that the larger pores of KBC1250 can favor cardiomyocytes attachment. However, in this work, Western Blot data show that after 72h, both porous materials revealed superior cell compatibility (stable cell adhesion) with respect to the corresponding films, and displayed vinculin expression comparable to control.

Concerning cell differentiation through a contractile phenotype, Myf5 protein expression has been analyzed. After 24h and 72h porous KBC1250 enhanced the contractile ability, while in all the other cases Myf5 expression resulted comparable to the control.
Eventually, cell proliferation has been evaluated by PCNA expression. These data confirmed the cell viability data showing that KBC1250-E1500-20 inhibited cell proliferation when compared to both control and KBC1250 surfaces. However, the unaltered expression of adhesion and differentiation proteins demonstrated the presence of viable cells on all the studied surfaces.

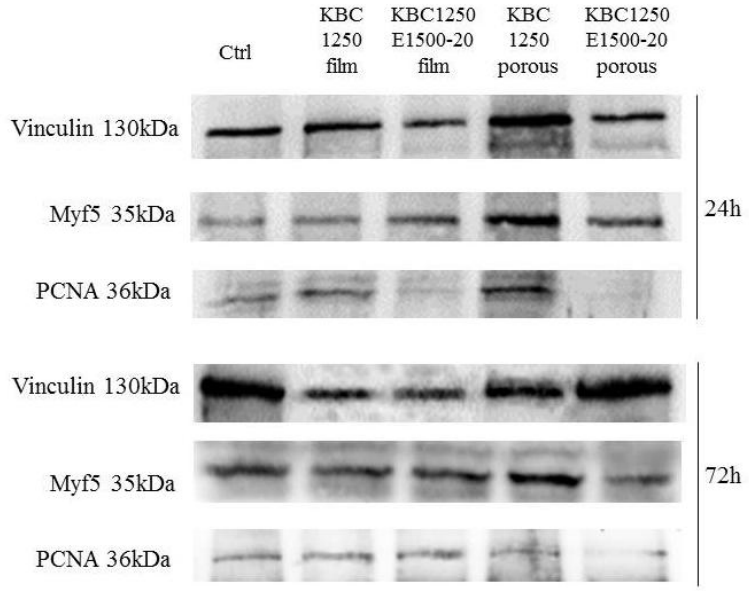

Fig. 2.14 Results of Western Blot performed on KBC1250 film and porous scaffold, KBC1250-E1500-20 film and porous scaffolds using H_9C_2 rat heart cell line.

The presence of PEG in the polyurethane composition seems not to show any positive effect on film and porous scaffold biocompatibility, indicating that H_9C_2 adhesion and proliferation are not strictly affected by substrate hydrophobicity.

2.3.8 Lipase and hydrolytic degradation of KBC1250 films and scaffolds

Degradation properties of KBC1250 films and scaffolds in presence of lipase enzyme were investigated, since lipases are a subclass of esterases, which catalyze the hydrolysis of ester bonds in lipids. Hydrolytic degradation of the polymer was taken as control.
As shown in figure 2.15 a and b, weight loss during enzymatic degradation appears faster and more pronounced with respect to hydrolytic degradation, for both dense and porous KBC1250. These results were expected, since KBC1250 is characterized in its polymeric chains by polyester (PCL) blocks that are susceptible to lipase activity.
If results of hydrolytic degradation of dense and porous constructs are compared (see figure 2.16 a), weight loss of films appears faster than weight loss of porous scaffolds. The opposite can be observed in the case of lipase degradation of KBC1250 films and scaffolds. As shown

in figure 2.16 b, a more pronounced weight loss after 2 weeks takes place for the porous sample, with respect to its corresponding film. This different behavior between dense and porous constructs in both degradation processes, could be due the different mechanism of hydrolytic and enzymatic degradation. Generally PCL has a mass hydrolytic degradation while a surface one in presence of an enzyme [56]. If we consider that KBC1250 has PCL blocks in its polymeric chains, a mass degradation process can be hypothesized in PBS solution, while a surface mechanism in lipase solution. Probably hydrolytic degradation is slower for porous samples because the mass mechanism is delayed by the "hydrophobic effect" of the scaffolds, while lipase degradation is faster for these type of constructs since they exhibit a larger amount of surface area, allowing for a more intense surface degradation process.

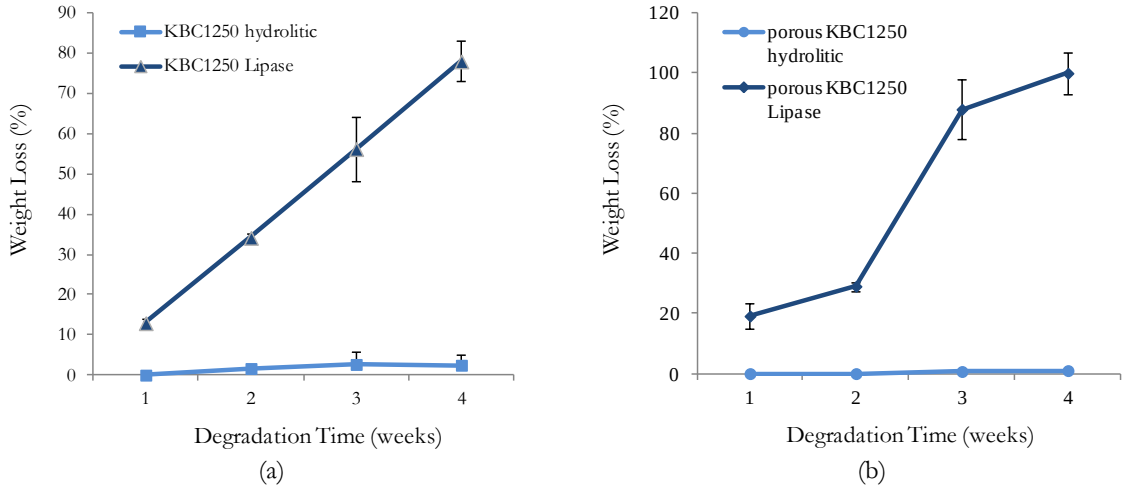

Fig. 2.15 Weight loss of KBC1250 films (a) and scaffolds (b) in PBS with 0,3 mg/ml lipase.

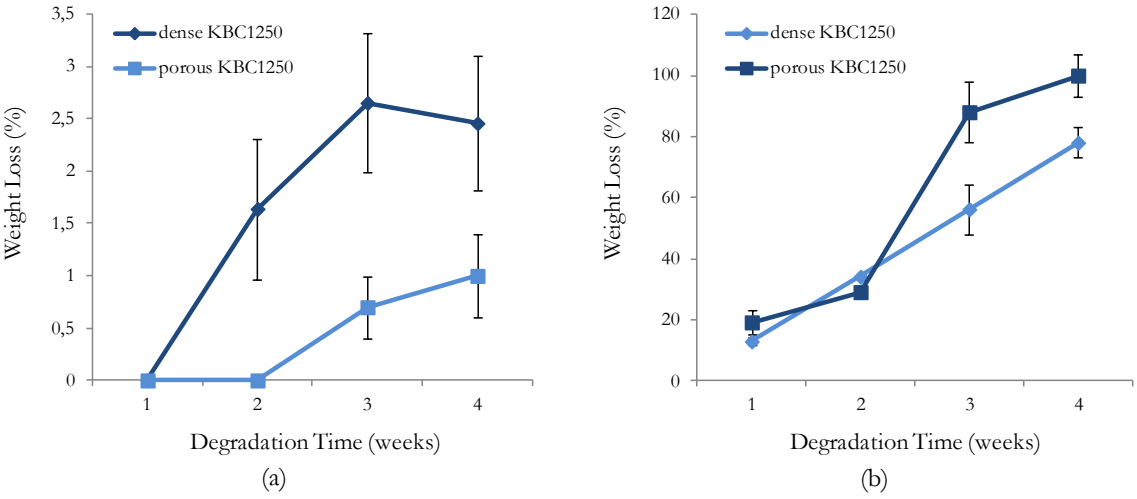

Fig. 2.16 Weight loss of KBC1250 film and porous scaffold after hydrolytic (a) and lipase (b) degradation.

2.4 Conclusions

The chemical, thermal and mechanical characterizations of the synthesized PURs clearly indicate the successful preparation of new polymeric materials with the desired physical-chemical properties for myocardial TE applications.
In addition, polymers could be easily processed in dense films and porous scaffolds. The latter showed a microstructure with elongated and unidirectional pores, which conferred to the substrates a remarkable similarity to the streaked muscle tissue. A "structural biomimicry", one of the key requirements for applications of biomaterials in tissue engineering, was achieved. Concerning thermal properties, porous substrates showed melting temperatures well above the physiological one, an important aspect for implantable devices.
Mechanical tests have revealed that, although KBC1250-E1500-20 showed the mechanical properties closest to those required for cardiac repair, all the dense films have elastomeric behavior, high toughness and appropriate values of elastic modulus. Porous devices showed mechanical properties lower than the corresponding films that however do not hinder their potential application as heart patches, since they keep an elastomeric behavior with mechanical parameters very close to the required ones.
In addition, although a fine tuning and control on mechanical (films) and surface properties (scaffolds) was obtained by introducing PEG segments in PUR polymeric chain, this effect was not completely reflected in an improvement of cell behavior as measured by biological tests. Both porous structures, with and without PEG segments, showed a good biological response in terms of cardiomyoblast adhesion. Nevertheless, the best response in terms of cell viability was registered for dense and porous KBC1250 substrates, with a higher value for the porous structure, as it is expected in view of the morphological features that are known to better perform in in vitro cell culture tests [18]. Hydrolytic and lipase degradation tests showed a different behavior for dense and porous KBC1250, with a faster weight loss for the scaffold in the presence of the enzyme.
Finally, elastase degradation tests demonstrated the possibility to finely tune biodegradation rate of PURs through a partial introduction of an enzyme-target peptide as chain extender.

References

1. Chena Q., L.S., Thouas G.A., *Elastomeric biomaterials for tissue engineering* Progress in Polymer Science, 2012 in press: p. 88.
2. Zdrahala, R.J. and I.J. Zdrahala, *Biomedical applications of polyurethanes: a review of past promises, present realities, and a vibrant future.* J Biomater Appl, 1999. **14**(1): p. 67-90.
3. Zdrahala, R.J., *Small caliber vascular grafts. Part II: Polyurethanes revisited.* J Biomater Appl, 1996. **11**(1): p. 37-61.
4. Vermette P., G.H.J., Laroche G., Guidoin R., , *Biomedcial applications of polyurethanes*2001. 273.
5. Aldenhoff, Y.B., et al., *Performance of a polyurethane vascular prosthesis carrying a dipyridamole (Persantin) coating on its lumenal surface.* J Biomed Mater Res, 2001. **54**(2): p. 224-33.
6. Guelcher, S.A., *Biodegradable polyurethanes: synthesis and applications in regenerative medicine.* Tissue Eng Part B Rev, 2008. **14**(1): p. 3-17.
7. Zdrahala, R.J., *Small caliber vascular grafts. Part I: state of the art.* J Biomater Appl, 1996. **10**(4): p. 309-29.

8. Fromstein, J.D. and K.A. Woodhouse, *Elastomeric biodegradable polyurethane blends for soft tissue applications.* J Biomater Sci Polym Ed, 2002. **13**(4): p. 391-406.
9. Santerre, J.P., et al., *Understanding the biodegradation of polyurethanes: from classical implants to tissue engineering materials.* Biomaterials, 2005. **26**(35): p. 7457-70.
10. Cardy, R.H., *Carcinogenicity and chronic toxicity of 2,4-toluenediamine in F344 rats.* J Natl Cancer Inst, 1979. **62**(4): p. 1107-16.
11. Lamba N., W.K., Cooper S., Lelah M. , *Polyurethanes in biomedical applications*1998.
12. Borkenhagen, M., et al., *In vivo performance of a new biodegradable polyester urethane system used as a nerve guidance channel.* Biomaterials, 1998. **19**(23): p. 2155-65.
13. Pinchuk, L., *A Review of the Biostability and Carcinogenicity of Polyurethanes in Medicine and the New-Generation of Biostable Polyurethanes.* Journal of Biomaterials Science-Polymer Edition, 1994. **6**(3): p. 225-267.
14. A., G.S., *Biodegradable polyurethanes: synthesis and applications in regenerative medicine.* Tissue Engineering Part B, 2008. **14**: p. 3-17.
15. Zhang J.Y., D.B.A., Beckman E.J., Hollinger J.O., *Three-dimensional biocompatible ascorbic acid-containing scaffold for bone tissue engineering.* Tissue Engineering Part B, 2003. **9**: p. 1143–57.
16. Bruin P., V.G.J., Nijenhuis A.J., Pennings A.J. , *Design and synthesis of biodegradable poly(ester-urethane) elastomer networks composed of non-toxic building-blocks.* Die Makromolekulare Chemie Rapid Communications, 1988. **9**: p. 589–94.
17. Fujimoto K.L., G.J.J., Oshima H., Sakai T., Wagner W.R., *In vivo evaluation of a porous, elastic, biodegradable patch for reconstructive cardiac procedures.* Annals of Thoracic Surgery, 2007. **83**: p. 648–54.
18. Elliott, S.L., et al., *Identification of biodegradation products formed by L-phenylalanine based segmented polyurethaneureas.* J Biomater Sci Polym Ed, 2002. **13**(6): p. 691-711.
19. Guan, J. and W.R. Wagner, *Synthesis, characterization and cytocompatibility of polyurethaneurea elastomers with designed elastase sensitivity.* Biomacromolecules, 2005. **6**(5): p. 2833-42.
20. Krol, P., *Synthesis methods. chemical structures and phase structures of linear polyurethanes. Properties and applications of linear polyurethanes in polyurethane elastomers, copolymers and ionomers.* Progress in Materials Science, 2007. **52**: p. 915–1015.
21. Richardson T.B., M.M.A., Uzunpinar C., Marcovich N.E., Aranguren M.I., Kilinc-Balci F., Broughton Jr R.M., Auad M.L., *Study of nanoreinforced shape memory polymers processed by casting and extrusion.* Polymer Composites, 2011. **32**: p. 455–63.
22. Gisselfalt, K., B. Edberg, and P. Flodin, *Synthesis and properties of degradable poly(urethane urea)s to be used for ligament reconstructions.* Biomacromolecules, 2002. **3**(5): p. 951-8.
23. Stankus, J.J., J. Guan, and W.R. Wagner, *Fabrication of biodegradable elastomeric scaffolds with sub-micron morphologies.* J Biomed Mater Res A, 2004. **70**(4): p. 603-14.
24. Stankus, J.J., et al., *Fabrication of cell microintegrated blood vessel constructs through electrohydrodynamic atomization.* Biomaterials, 2007. **28**(17): p. 2738-46.
25. Guan, J., et al., *Preparation and characterization of highly porous, biodegradable polyurethane scaffolds for soft tissue applications.* Biomaterials, 2005. **26**(18): p. 3961-71.
26. Gogolewski, S., K. Gorna, and A.S. Turner, *Regeneration of bicortical defects in the iliac crest of estrogen-deficient sheep, using new biodegradable polyurethane bone graft substitutes.* J Biomed Mater Res A, 2006. **77**(4): p. 802-10.
27. Gogolewski, S. and K. Gorna, *Biodegradable polyurethane cancellous bone graft substitutes in the treatment of iliac crest defects.* J Biomed Mater Res A, 2007. **80**(1): p. 94-101.
28. Guan, J., K.L. Fujimoto, and W.R. Wagner, *Elastase-sensitive elastomeric scaffolds with variable anisotropy for soft tissue engineering.* Pharmaceutical Research, 2008. **25**(10): p. 2400-2412.
29. Rechichi, A., et al., *Degradable block polyurethanes from nontoxic building blocks as scaffold materials to support cell growth and proliferation.* J Biomed Mater Res A, 2008. **84**(4): p. 847-55.
30. Ciardelli G, S.S., Serafini P, Boffito M, Caporale A, Silvestri A, et al. Nanotech Conference & Expo 2011, *Biomimetic polyurethanes for regenerative medicine.* Nanotech Conference & Expo 2011, Boston, 2011. **3**: p. 155-158.
31. Penco M., S.L., Bignotti F., D'Antone S., Di Landro L. , *Thermal properties of a new class of block copolymers based on segments of poly(D,L-lactic-glycolic acid) and poly(e-caprolactone)* European Polymer Journal, 2000. **36**: p. 901-908.

32. Wellen R.M.R., R.M.S., *The kinetics of isothermal cold crystallizationand tensile properties of poly(ethyleneterephthalate).* Journal of Materials Science, 2005. **40**: p. 6099–6104.
33. Penco M., S.L., Bignotti F., D'Antone S., Di Landro L., *Thermal properties of a new class of block copolymers based on segments of poly(D,L-lactic-glycolic acid) and poly(e-caprolactone)* European Polymer Journal, 2000. **36**: p. 901-908.
34. Seymour R.W., A.A.E.J., Cooper S.L. , *Segmental Orientation Studies of Block Polymers Hydrogen-Bonded Polyurethanes.* Macromolecules 1973. **6**(6): p. 896–902.
35. Vermette P., G.H.J., Laroche G., Guidoin R., *Biomedical Applications of Polyurethanes*2001, Texas (USA): Landes Bioscience.
36. Lamba N.M.K., W.K.A., Cooper S.L. , *Polyurethanes in biomedical applications*1998, USA: CRC Press.
37. Guan, J.J., et al., *Preparation and characterization of highly porous, biodegradable polyurethane scaffolds for soft tissue applications.* Biomaterials, 2005. **26**(18): p. 3961-3971.
38. Cohen, S. and J. Leor, *Rebuilding broken hearts. Biologists and engineers working together in the fledgling field of tissue engineering are within reach of one of their greatest goals: constructing a living human heart patch.* Sci Am, 2004. **291**(5): p. 44-51.
39. Causa, F., P.A. Netti, and L. Ambrosio, *A multi-functional scaffold for tissue regeneration: the need to engineer a tissue analogue.* Biomaterials, 2007. **28**(34): p. 5093-9.
40. Mirsky, I., D.N. Ghista, and H. Sandler, *Cardiac mechanics: physiological, clinical, and mathematical considerations*1974, New York: John Wiley & Sons Ltd. 510.
41. Hidalgo-Bastida, L.A., et al., *Cell adhesion and mechanical properties of a flexible scaffold for cardiac tissue engineering.* Acta Biomater, 2007. **3**(4): p. 457-62.
42. Bouten, C.V.C., et al., *Substrates for cardiovascular tissue engineering.* Advanced Drug Delivery Reviews, 2011. **63**(4–5): p. 221-241.
43. McDevitt, T.C., et al., *Spatially organized layers of cardiomyocytes on biodegradable polyurethane films for myocardial repair.* Journal of Biomedical Materials Research Part A, 2003. **66A**(3): p. 586-595.
44. Christman, K.L. and R.J. Lee, *Biomaterials for the Treatment of Myocardial Infarction.* Journal of the American College of Cardiology, 2006. **48**: p. 907-913.
45. Bouten, C.V., et al., *Substrates for cardiovascular tissue engineering.* Adv Drug Deliv Rev, 2011. **63**(4-5): p. 221-41.
46. Christman, K.L. and R.J. Lee, *Biomaterials for the treatment of myocardial infarction.* J Am Coll Cardiol, 2006. **48**(5): p. 907-13.
47. Chen Q.Z., H.S.E., Ali N.N., Lyon A.R., Boccaccini A.R. , *Biomaterials in cardiac tissue engineering: Ten years of research survey.* Mater Sci Eng R, 2008. **59**: p. 1-37.
48. Jawad, H., et al., *Myocardial tissue engineering.* Br Med Bull, 2008. **87**: p. 31-47.
49. Jawad, H., et al., *Myocardial tissue engineering.* British Medical Bulletin, 2008. **87**(1): p. 31-47.
50. Ballester-Beltran J., R.P., Moratal D., Song W., Mano J. F., Salmeron-Sanchez M. , *Role of superhydrophobicity in the biological activity of fibronectin at the cell-material interface.* Soft Matter, 2011. **7**: p. 10803–10811.
51. Erbil H. Y., D.A.L., Avci Y., Mert O., *Adhesion Mechanism of Water Droplets on Hierarchically Rough Superhydrophobic Rose Petal Surface.* Science, 2003. **299**: p. 1377–1380.
52. Pittman A. G., L.B.A., *Effect of polymer crystallinity on the wetting properties of certain fluoroalkyl acrylates.* Journal of Polymer Science Part A-1: Polymer Chemistry, 1969. **7**(11): p. 3053-3056.
53. Areias A. C., R.C., Sencadas V., Garcia-Giralt N., Diez-Perez A., Gómez Ribelles J. L., Lanceros-Méndez S. , *Influence of crystallinity and fiber orientation on hydrophobicity and biological response of poly(L-lactide) electrospun mats.* Soft Matter, 2012. **8**(21): p. 5818-5825.
54. Arai K., T.M., Yamamoto S., Shimomura M. , *Effect of pore size of honeycomb films on the morphologym, adhesion and cytoskeletal organization of cardiac myocytes.* Colloids and Surfaces A: Physicochemical and Engineering Aspects, 2008. **313**: p. 530-535.
55. Davis, M.E., et al., *Custom design of the cardiac microenvironment with biomaterials.* Circ Res, 2005. **97**(1): p. 8-15.
56. Herzog K., M.l.R.J., Deckwer W. D., *Mechanism and kinetics of the enzymatic hydrolysis of polyester nanoparticles by lipases.* Polymer Degradation and Stability 2006. **91**: p. 2486-2498.

CHAPTER 3
Surface modification of polyurethane films and scaffolds

Abstract

Materials and their constructs used as bioartificial tissues should not just be passively tolerated by the cells but should actively promote specific cell responses, acting as analogous of the natural ECM. To improve cell adhesion to biomaterials, a suitable method consists in functionalizing their surface by grafting pro-adhesive ligands, corresponding to the amino acid active sequences of the adhesion ECM proteins, such as fibronectin and laminin. In this part of the work, RGD peptides were covalently attached, following plasma assisted activation, to the surfaces of PUR films and scaffolds, in order to promote cardiomyocyte adhesion. ATR-IR and XPS spectroscopy, Static Contact Angle measurements and chemical quantification methods were used to verify the success of peptide grafting. The evaluation of the biological properties of the modified surfaces, that was performed by MTS assay and SEM micrographs, demonstrated that the presence of RGD sequences on PUR films promoted cell adhesion and viability. A significant peptide-effect on cell viability was not observed for porous constructs, although vinculin expression was slightly higher on modified scaffolds with respect to the unmodified ones.

3.1 Introduction: modification of biomaterial surfaces

The interactions between cells and their environments are mediated by the "bio-recognition processes", that consist in specific binding of the receptors on cell surface with their corresponding ligands, as it will be thoroughly described in section 3.1.2. In native tissues in vivo, cells attached on the extracellular matrix (ECM) are mediated by the binding between integrins (receptors on cell surfaces) and ECM adhesion proteins such as fibronectin, vitronectin, laminin and collagen. In addition to the function of a physical support, native ECM regulates cell behaviors by presenting various kinds of growth factors to the cells. On biomaterial surfaces, the same mechanisms also take place. When foreign materials come into contact with body fluid or cell culture medium, the initial response is protein adsorption on the materials' surfaces [1].

Therefore, the materials interact with the cells through the adsorbed protein layer. The composition and structure of this protein layer play a critical role in determining subsequent cell behaviors. Based on the understanding of the biorecognition process on cell behaviors, two main strategies in surface engineering of biomaterials are considered. Firstly, the material surface properties such as chemical composition, hydrophilicity/hydrophobicity (wettability), surface charge and roughness, etc. are modulated to allow the adsorbed proteins to maintain their normal conformation and bioactivity [1]. Particular attention is given to surface wettability, which is generally measured as the contact angle between the material surface and

a liquid [2]. A low contact angle (<90°) between the material and water indicate good spreading of water on the material surface (hydrophilicity of the material), while a high water contact angle (>90°) is a sign of an hydrophobic material surface.
Synthetic polymers used in biotechnologies and in medicine are usually too hydrophobic in their pristine state, showing water contact angles of about 100° or more and resulting unsuitable for cellular colonization. If the material is too hydrophobic, proteins which are spontaneously adsorbed to the materials from the culture media, blood and other body fluids, acquire a denatured and rigid state and the resulting conformation is inappropriate for binding to cells, because specific sites (e.g. RGD-containing oligopeptides) are less accessible to cell adhesion receptors (e.g. integrins). On the other hand, on highly hydrophilic surfaces cell attachment and spreading is limited or completely disabled. Highly hydrophilic surfaces bind proteins with weak forces, which could lead to their detachment especially at later culture intervals, when they bind a large number of cells. An optimal cell adhesion occurs only to moderately hydrophilic surfaces [3]. The wettabilty of polymeric surfaces can be modulated by physical methods, e.g. by irradiation by ions, plasma or ultraviolet light. These methods are safer than chemical methods, since they are not associated with potential retention of cytotoxic chemicals and their subsequent release from the material [4] [5]. This method, however, cannot induce specific cell behaviors due to the nonspecific protein absorption.
The second strategy is to directly immobilize certain biomolecules on the biomaterial surfaces to induce specific cellular responding. Biomolecules attachment can also be performed through an initial physical treatment of the biomaterial surface.

3.1.1 Plasma technique

Plasma state can be considered as a high energy state of matter, in which a gas is partially ionized into charged particles, electrons, and neutral molecules due to high energy radiation or strong electric field. Plasma states can be divided in two main categories: hot plasmas (near-equilibrium plasmas) and cold plasmas (non-equilibrium plasmas). Hot plasmas are characterized by very high temperatures of electrons and heavy particles, both charged and neutral, and they are close to 100% degree of ionization. Cold plasmas are composed of low temperature particles, such as charged and neutral molecular and atomic species, and relatively high temperature electrons and they are characterized by low degrees of ionization (less than 10%). Hot plasmas include electrical arcs, plasma jets of rocket engines, thermonuclear reaction generated plasmas, etc. while cold plasmas include low-pressure direct current (DC) and radio frequency (RF) discharges (silent discharges), discharges from fluorescent (neon) illuminating tubes and corona discharges [6].
DC, RF, or microwave (MW) power of low-pressure non-equilibrium discharges (cold plasmas) is transferred to a low-pressure gas environment, with or without an additional electric or magnetic field. Ultimately, all these discharges are initiated and sustained through electron collision processes under the action of the specific electric or electromagnetic fields. Accelerated electrons (energetic electrons) induce ionization, excitation and molecular fragmentation processes leading to a complex mixture of active species, which undergo

recombination processes in the presence or absence of the plasma. The recombination reaction mechanisms are very different from those for conventional chemical processes [6].
High frequency (RF) plasmas can be electrodeless or electrode discharges with capacitive or inductive coupling configurations. In the case of electrodeless discharges, the electrodes are not in contact with the plasma gas and are usually located outside the plasma chamber. The reaction chambers employed in these cases are manufactured using nonporous insulating materials (e.g. glass, quartz, ceramics). Electrode discharge chambers are usually grounded, metallic containers where the power is transferred to the plasma gas by electrodes inserted into the discharge chamber through insulating, vacuum-tight, metal/ceramic feed-throughs [6].

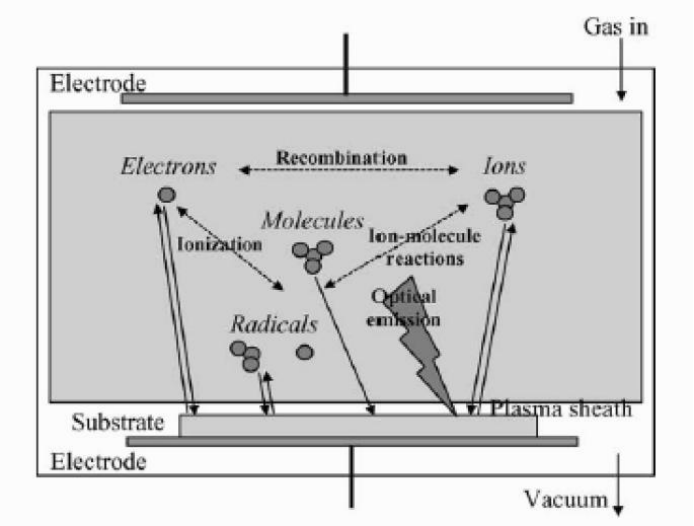

Fig. 3.1 A schematic diagram showing a capacitively coupled RF-plasma reactor and the interaction of plasma species with the substrate [6].

RF discharges gained their name from the frequency range, which is employed to produce the plasma (RF band: 1 kHz–1 GHz). Although these plasmas have been investigated over the entire frequency range, most of the RF-installations use the standard 13.56 MHz frequency (or its harmonies) in order to avoid interference with communication networks. These discharges usually are characterized by low degrees of ionization, and operate in relatively high pressure environments (10–500 mTorr); they are non-equilibrium plasmas and are often called glow discharges. A schematic diagram of a capacitively coupled RF-plasma reactor, and the interaction of plasma species with the substrate are presented in figure 3.1. RF-plasmas are the most common choice for the microelectronic industry, since they have several advantages with respect to DC discharges: they can operate at lower pressures and their ionization mechanism is more efficient [6].

3.1.1.1 Plasma for biomaterials

Plasma surface treatments are attractive for biomaterials thanks to: (i) their ability of changing surface chemistry and material properties in a controlled way; (ii) their inherent sterility; (iii) the possibility to modify the "final" substrates (webs, tubes, fabrics etc) [7].

The idea of employing non-equilibrium plasmas to improve biomaterial performances was applied first in the early 1970s [8, 9]. Since then, low-pressure plasma deposition (plasma enhanced chemical vapor deposition, PE-CVD), treatment (grafting of chemical functionalities, cross-linking) and etching processes have been widely used, and can now be considered as mature technologies for biomedical applications. Several processes, that employ radio- (RF, mainly 13.56 MHz) rather than audio-frequency (kHz) or microwaves (GHz), have been imported from microelectronics or developed ex novo, in order to improve the biocompatibility of several implantable devices, such as vascular prostheses, heart valves, intra-ocular and contact lenses, catheters and sensors [7]. The plasma is able to exert mainly four effects: (i) surface cleaning, (ii) surface ablation or etching, (iii) surface crosslinking, and (iv) modification of the surface chemical structure. Recently, plasma has also be optimized to transfer geometric micro-patterns at the surface of biomedical polymers, with the aim of driving the behavior of cells in tissue engineering (see section 3.1.2) [7].
From a chemical point of view, the interaction between the ionized or high energy particles and the material surface leads to the cleavage of C-C and C-H bonds present in the polymer chains. Consequently, macromolecules split and free radicals and conjugated double bonds are generated on the polymer chain. The resultant radicals and functional groups may react with the oxygen (if present in the chamber atmosphere) and create oxidized structures, e.g. carbonyl, carboxyl and ester groups, which increase the polarity and wettability of the polymer surface [10]. Oxygen plasma is often used to impart oxygen containing functional groups to polymer surfaces such as poly(ε-caprolactone) (PCL), poly(ethylene glycol) (PE), and poly(ethylene therephthalate) (PET). In addition to oxygen, carbon dioxide plasma has been used to introduce carboxyl groups on polypropylene (PP), polystyrene (PS) and PE, and air plasma has been used to oxidize poly(methyl methacrylate) (PMMA). Ammonia and nitrogen plasmas have been used to impart amine groups to the surface of poly(tetrafluoro ethylene) (PTFE) and PS, respectively. Inert gases can be used to introduce radical sites on the polymer surface for subsequent graft copolymerization [10].
Plasma can provide modification of the top nanometer of a polymer surface without using solvents or generating chemical waste and with less degradation and roughening of the material than many wet chemical treatments. The type of functionalization imparted can be varied by selection of plasma gas (Ar, N_2, O_2, H_2O, CO_2, NH_3), as just described, and operating parameters (pressure, power, time, gas flow rate) [10].

3.1.2 Micro- and nano-patterning

During the last decade, surface micro- and nano-patterning became a very important and promising approach to affect cell behaviors on biomaterial surfaces. Micro- or nano-scaled surface patterns, either topographic or chemical ones, seem to have significant influence on cell behaviors in terms of cell shapes and migration, protein synthesis and gene expressions [1]. Several methods exist for patterning molecules and polymers with different chemical domains and/or topographic (tracks, grooves, pits, etc.) or random features; highly resolved lithography (e-beam, scanning probe microscopy) can develop nanometric features, while 'soft'

lithography (microcontact printing, embossing, casting) and other techniques can pattern polymers at a micrometric scale [1].
The topographic surface pattern produced on a silicon wafer can be easily replicated onto a polymeric material surface to form regular physical topographies. Grooves and ridges are among the most studied topographical patterns related to cell morphology control, since microgroove/ridge surfaces have shown significant control over cellular behaviors. Cell spreading, alignment, and migration can be oriented along these grooves/ridges. One theory that accounts for these phenomena is called "contact guide effect", in which cell integrin receptors in focal contact transfer the variable degrees of tension or compression into the cytoskeleton, and cell stretch receptors subject to these stresses will be activated and reorganize the cytoskeleton according to the surface topography [11]. The cellular response to the surface topographies is also influenced by the dimensions of the surface features, ranging from nano, submicron to micro-scales, depending on the cell types, cell-cell interaction, as well as substrate composition and topography type [1].
Besides physical topography patterns, chemical patterns were also fabricated to affect cell behaviors. Microcontact printing (μCP) developed by Whitesides's group enables translation of topographic surface patterns to chemical surface patterns on biomaterial surfaces [12]. Typically, a siloxane stamp with desired physical surface patterns is coated with a solution containing the substance to be printed, such as adhesion proteins. By contacting the stamp and the substrate, the substance can be printed on the substrate with the same patterns of the siloxane template. The patterning of proteins using μCP on biomaterial surfaces is an effective approach to control cell adhesion, spreading, orientation, and to obtain cell micropatterns. Different chemical domains (hydrophilic/hydrophobic, acid/base, fouling/non-fouling) can be created at the surface of polymers by means of plasma processes performed through 'physical masks', that are micron-thick polymer or metal foils where a proper pattern is drilled (e.g. by laser techniques). When properly positioned (close contact) at the surface of the polymer under modification, and utilized with selected plasma processes, physical masks allow to transfer their pattern with the best reported resolution of a few microns [7]. As an example, Favia and co-workers combined the plasma process with the use of a copper grid (mask or stencil) to develop cell adhesive tracks alternated with non-fouling (PEO-like coatings) domains at the surface of polystyrene (PS) substrates. A first plasma process (H_2 followed by NH_3 plasma treatment) was applied to the substrates, then the masks were applied, finally a PEO-like non-fouling coating was plasma-deposited. The effect of the patterns and of the different chemical domains was evaluated on cellular adhesion, spreading and growth. Keratinocytes adhered and grew aligned along the uncoated PS zones corresponding to the border and the bars of the mask, while the wider PEO-like areas were free from cells [7].

3.1.3 Surfaces modified with RGD peptides

In multicellular organisms contacts of cells with neighboring cells and the surrounding ECM are mediated by cell adhesion receptors. The integrins are the most numerous and versatile adhesion receptors. They play an important role also in processes like embryogenesis, cell differentiation, immune response, wound healing and haemostasis [13] [14]. Integrins consist

of two non-covalently associated transmembrane subunits, called α and β (see figure 3.2). To date, 18 α and 8 β subunits are known, that form 24 different heterodimers [15]. The combination of the particular α and β subunits determines the ligand specificity of the integrin. Some integrins, however, are highly promiscuous, binding to vitronectin, fibronectin, von Willebrand factor, osteopontin, tenascin, bone sialoprotein and thrombospondin. Vice versa, ECM molecules like fibronectin are ligands for several integrins [15].
The tripeptide RGD was identified 18 years ago by Pierschbacher and Rouslahti as the minimal essential cell adhesion sequence in fibronectin [16]. Then, RGD sites were identified in many other ECM proteins, including vitronectin, fibrinogen, von Willebrand factor, collagen, laminin, osteopontin, tenascin and bone sialoprotein as well as in membrane proteins, in viral and bacterial proteins, and in snake venoms. However, RGD sequence is not the "universal cell recognition motif", but it is nevertheless unique with respect to its broad distribution and usage. The conformation of the RGD containing loop and its flanking amino acids in the respective proteins are mainly responsible for their different integrin affinity [17].

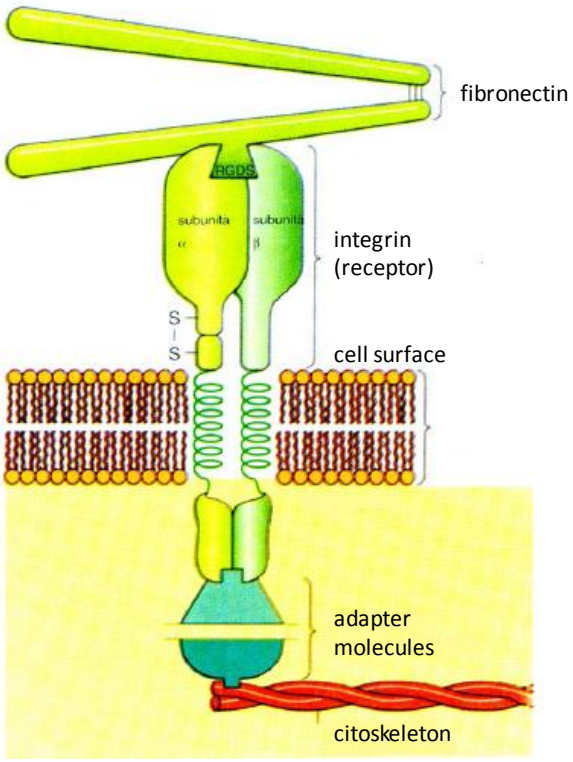

Fig. 3.2 Cell adhesion mechanism to the ECM.

The process of integrin mediated cell adhesion involves a sequence of four partly overlapping events [18]: cell attachment, cell spreading, organization of actin cytoskeleton, and formation of focal adhesions. In the initial attachment step the cell contacts the surface and some ligand binding occurs that allows the cell to withstand gentle shear forces. Secondly, the cell body begins to flatten and its plasma membrane spreads over the substratum. Thirdly, actin organization into microfilament bundles occurs. In the last step the formation of focal adhesions takes place, which link the ECM to molecules of the actin cytoskeleton. Clustered integrins and more than 50 other transmembrane, membrane associated and other cytosolic

molecules are involved in focal adhesion (tetraspanins, growth factors receptors, syndecans, lipids, tensin, talin, vinculin, paxillin, and focal adhesion kinase) [19-21].
It is well established that integrin-mediated cell spreading and focal adhesion are crucial for cell survival and proliferation [22]. On the other hand, loss of attachment may cause apoptosis in many cell type ("anoikis"). It can be even induced in the presence of immobilized ECM molecules when non immobilized soluble ligands (such as RGD peptides) are added [23-25]. While immobilized ligands act as agonists of the ECM, leading to cell adhesion and survival, non-immobilized ones act as antagonists, leading to cell detachment , a round shape and apoptosis.
Since RGD peptides have been found to promote cell adhesion in 1984 [26], numerous materials have been RGD functionalized for academic studies or medical applications. Nevertheless, RGD peptides do not only trigger cell adhesion but can also be used to address selectively certain cell lines and promote specific cell responses [27].
In the last decades researchers attempted to functionalize polymers to obtain specific cell surface interactions. They started to experiment coatings with cell adhesive proteins like fibronectin, collagen, or laminin [28-30]. However, the use of proteins bears some disadvantages in the view of medical applications. At first the proteins have to be isolated from other organisms and purified, increasing the risk of undesirable immune responses and infections [27]. In addition, proteins are object of proteolytic degradation and needed to be refreshed continuously and inflammation and infection can even accelerate this degradation [27]. Furthermore, only a part of the proteins have proper orientation for cell adhesion [31] and surface properties may influence their conformation and/or the orientation [32]. As already stated, on hydrophobic surfaces proteins are generally subjected to denaturation, since they tend to maximize interaction with hydrophobic amino acid side chains [27]. Most of the described problems can be overcome by using the single cell recognition motifs as small immobilized peptides. They show higher stability towards sterilization conditions, heat treatment and pH-variation [33], storage [34] and conformational shifting as well as easier characterization and cost effectiveness [35]. In addition, while ECM proteins contain normally several different cell recognition motives, small peptides represent only one single motif, which may selectively address one particular type of cell adhesion receptors. Sometimes linear peptides are subjected to slow enzymatic degradation while cyclic peptides are known to exhibit high long time stability [27].

3.1.3.1 Immobilization of RGD peptides on biomaterial surfaces

Stable linking of RGD peptides to a biomaterial surface is essential to promote strong cell adhesion, since formation of focal adhesions occurs if the ligands withstand the cells contractile forces. Weakly adsorbed ligands lead only to weak fibrillar adhesions and cells can remove mobile integrin ligands by internalization [27].
Therefore, RGD peptides should be covalently attached to the polymer, e.g. via functional groups like hydroxyl-, amino-, or carboxyl groups. Since these functional groups are not present in all polymers, they have to be introduced by blending, co-polymerization, chemical or physical treatment.

Concerning co-polymerization, one example is given by the introduction of the RGD sequence into a polyurethane (PUR) backbone [36, 37]. This bulk modification has two disadvantages: only a small fraction of the peptides can be detected by cells on the device surface and the sequences may be fixed in a conformation that is less active in integrin binding. As a consequence, a surface attachment is often preferred. It can be achieved by chemical and physical treatment, e.g. alkaline hydrolysis, reduction, oxidation, track-etching, or plasma deposition [27].

In most cases RGD peptides are linked to polymers via a stable covalent amide bond. This is usually done by reacting an activated surface carboxylic acid group with the nucleophilic N-terminus of the peptide. Carboxylic acid groups may be generated grafting acrylic acid olygomers in a plasma chamber and can be activated by using a peptide coupling reagent, e.g. 1-ethyl-3-(3-dimethylaminopropyl)-carbodiimide (EDC, also referred to as water soluble carbodiimide, WSC), dicyclohexyl-carbodiimide (DCC) or carbonyl diimidazole (CDI). Two problems may arise by this coupling method. Firstly, there are other reactive functional groups in the RGD peptide, such as carboxyl groups at the C-terminus and in the aspartic acid side chain and the nucleophilic guanidino group of the arginine side chain (see figure 3.3). Secondly, the coupling reagent and the activated carboxyl groups can be deactivated quickly by hydrolysis [27].

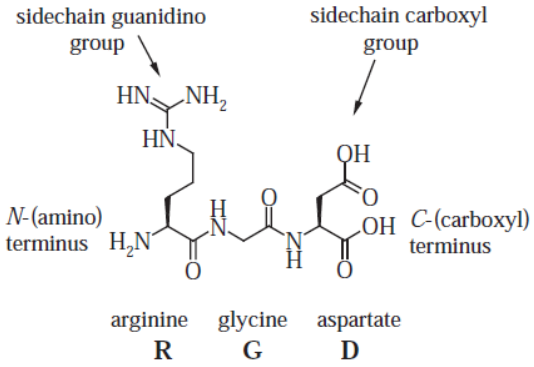

Fig. 3.3 The RGD molecular formula and nomenclature [27].

One possibility to overcome these problems is to block the reactive amino acid side chains with protecting groups and to use other solvents than water (e.g. DMF, dichloromethane or acetone). A significant drawback of this strategy is the need of harsh conditions to remove the protecting groups [27]. Alternatively coupling of unprotected RGD peptides in water can be employed by a two step procedure: first, activation of the surface carboxyl group as an active ester, that is less prone to hydrolysis, e.g. N-hydroxysuccinimide (NHS) esters in presence of EDC, and second coupling of the peptide in water (see figure 3.4) [38].

Best conditions for coupling the RGD peptide to the NHS active ester are pH 8–9 in phosphate or sodium bicarbonate buffer with a reaction time of 1–2 h. More elevated pH values and high concentrations of buffer or salts can reduce the half lifetime of the NHS active ester down to less than 1 min. Following this protocol there is no need for protecting groups, since in the two step procedure, the aspartate side chain carboxyl group is not activated for coupling, and due to protonation in water the nucleophilicity of the arginine side

chain is nearly abolished [27]. In some cases coupling was performed at lower pH and/or lower temperatures with longer coupling times resulting in higher yields. A yield increase can be obtained also with an excess of the peptide [39, 40].

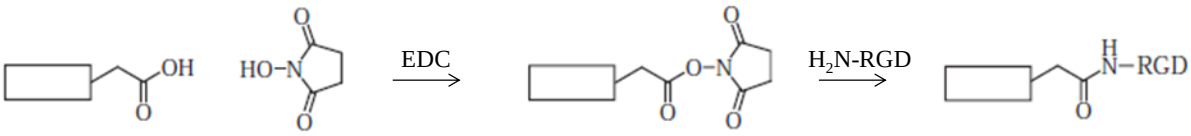

Fig. 3.4 Coupling of unprotected RGD peptides in water

3.1.3.2 RGD modified surfaces in Myocardial Tissue Engineering

The influence of the presence of adhesion proteins, such as fibronectin and laminin, on biomaterial surfaces for myocardium repair, has been widely investigated [41-43]. Although the influence of their surface micropatterning on cell response [44, 45] has been less studied, the promising results obtained and the discover on the bioactive properties of some ECM proteins-derived peptides has incited MTE researchers to modify biomaterials with cell binding domains, especially those based on the RGD sequence. In 2001 Rowley and co-workers (as already described in Chapter 1) covalently modified alginates of varying monomeric ratio with RGD based ligands through carbodiimide chemistry in order to promote cell adhesion to these polymers. They investigated a range of surface density (1-100 fmol/cm^2) on alginate substrates and observed that C2C12 skeletal myoblast proliferation and differentiation could be tuned by varying RGD density and the alginate monomeric ratio [46]. More recently, Shachar and colleagues also studied a macroporous alginate scaffold functionalized with RGD motif as substrate for cardiac repair. The immobilized RGD peptide promoted cell adhesion and prevented cell apoptosis. In addition, it accelerated cardiac tissue regeneration, since, within 6 days, the cardiomyocytes reorganized their myofibrils and reconstructed myofibers composed of multiple cardiomyocytes in a typical myofiber bundle. The non-myocyte cell population (cardiofibroblasts) also benefited from the presence of RGD modified matrix and consequently supported the cardiomyocytes [47].
The group of Schussler functionalized a collagen porous scaffold with RGDS peptide for MTE applications through a hetero bifunctional cross-linker reagent (Sulfosuccinimidyl 6-[3-(2-pyridyldithio)-propionamido] hexanoate). They analyzed cardiomyocites contractile performance, viability and differentiation and observed an increased viability and a good cell contractile apparatus for RGDS scaffolds, with cross-striation of cardiac myocytes (not found in the control constructs) [48].
Guan and colleagues surface modified biodegradable polyurethane films using radio frequency glow discharge followed by coupling of RGDS with glutaraldehyde [49]. They tested endothelial cell adhesion on pristine surfaces and on RGDS-modified surfaces. It revealed higher (>140% and >200%, respectively) with respect to tissue culture polystyrene.
The work of Guan is an optimal starting point for a study on RGD surface modification of PURs for myocardial tissue engineering. The need to investigate RGD surface effects on PURs arises from the consideration that these polymers are suitable candidates for contractile

tissue regeneration (especially when processed into porous structures), due to their finely modulated elastomeric and degradability properties. Their biocompatibility has been proved, too [50, 51]. Nevertheless, it is fundamental and crucial their chemical functionalization, in order to stimulate specific cardiomyocites and stem cells response.

3.1.4 Surface Modification in the present work

Based on the results obtained mainly by the biological characterization of PUR films and scaffolds (as discussed in Chapter 2), KBC1250-based dense and porous constructs were selected for a biochemical surface modification. In detail, RGD functionalization was performed in order to improve biocompatibility of the constructs and promote cell adhesion and proliferation. An initial plasma treatment was carried out to graft acrylic acid oligomers. Their terminal acidic carboxylic groups were activated in order to allow the subsequent covalent attachment of the peptide, trough the formation of an amide bond. On PUR films RGD was attached both homogenously and with a linear micropattern, in order to investigate its effect on cardiomyocytes response, in terms of adhesion and viability.

3.2 Materials and methods

3.2.2 Surface modification by Radio Frequency Plasma

Plasma treatment was performed in two phases in a RF plasma reactor (Diener electronic - Plasma Surface Tecnology, Germany) on KBC1250 films and scaffolds. During the first phase, an Argon plasma, which was performed for 5 min with a gas pressure of 0.7 mbar, was used to produce active radicals on material surfaces, which were necessary for the subsequent graft copolymerization of acrylic acid monomers. During the second phase, a plasma treatment was performed in presence of acrylic acid vapours (from distilled liquid) for 15 min with a gas pressure of 0.1 mbar, to allow the formation of a poly (acrylic acid) (PAA) layer on the surface of the samples. Films and scaffolds were then washed 3 times with distilled water to remove any unreacted monomer.

3.2.3 RGD attachment

PAA grafted polyurethane constructs were placed in an aqueous solution with 5 mg/ml of 1-ethyl-3-(3-dimethylaminopropyl) carbodiimide (EDC, Sigma Aldrich) and 1,25 mg/ml of N-hydroxysuccinimide (NHS, Sigma Aldrich) (pH 5.0) at 4 °C for 20 h, to activate the carboxyl acidic groups of the grafted PAA chains. Films and scaffolds were than washed 3 times with distilled water and dried in vacuum oven at 50°C for 24 h.
After activation reaction, the samples were immersed into a Phosphate Buffer Saline Solution containing RGD peptide (Creo Salus, USA) 1 μM for 2 h at ambient temperature. A siloxane stencil, which was fabricated through Soft Lithography by Ing. Gianni Orsi from University of

Pisa, was applied during RGD reaction on one film (2 x 5 cm^2), in order to create a linear chemical micropattern on film surface. This mask contains siloxane strips 100 µm wide at 50 µm intervals (see Figure 3.5). As a consequence, RGD lines should be 50 µm wide.
All samples were finally washed several times with distilled water and dried in vacuum oven at 50°C for 24 h.

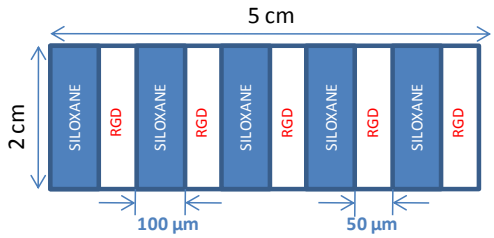

Fig. 3.5 Schematic structure of the siloxane mask that was used to create a linear RGD micropattern on film surface.

3.2.4 Modified surface characterization

Modified constructs were chemically characterized through ATR-IR (Attenuated Total Reflection Infrared Spectroscopy) by using a Perkin Elmer Spectrum 100 equipped with an ATR attachment (UATR KRS5) with Germanium crystal. KBC1250 films were also analyzed by XPS (X-Ray Photoelectron Spectroscopy), using a PHI 5000 Versaprobe.
Variations in surface wettability after plasma treatments and RGD attachment were evaluated through Static Contact Angle measurements using a KSV INSTRUMENT CAM2000 and 5 µl of water drop volume.
Quantification of the acidic COOH groups on PAA modified surfaces were carried out by Toluidine colorimetric assay (TBO). In detail, samples(1 x 1 cm^2) were immersed into 0.05 mM TBO aqueous solution (pH 10). The formation of ionic complexes between COOH groups and the cationic dye was allowed to proceed for 12 hours at room temperature. The samples surface was rinsed with 0.1 mM NaOH solution to remove the unbound TBO molecule. The bonded TBO was desorbed by incubation in 50% acetic acid solution (2 ml) for 10 min. The absorbance at 632,8 nm was recorded by a UV–vis spectrophotometer (PerkinElmer, Lambda 25). The amount of carboxyl groups was calculated by referring to a calibration curve from 0,005% wt/v to 0.0035% wt/v of TBO/acetic acid solution (50%/50%) recorded at the same conditions. The calculation was based on the assumption that 1 mol TBO corresponds exactly with 1 mol carboxyl groups.

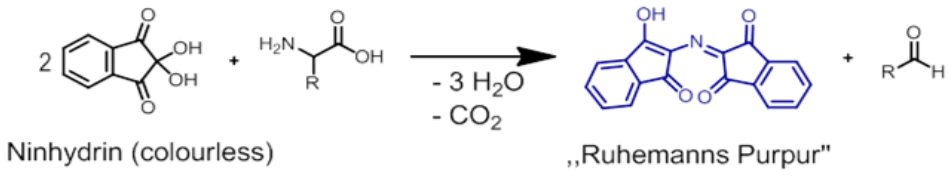

Fig. 3.6 Reaction of Nynhydrin with amino groups, resulting in a purple compound.

Quantification of the attached RGD was performed by Kaiser Test, that is based on Nynhydrin reaction with NH_2 terminal groups of the peptides, that leads to the formation of a purple compound (see Figure 3.6).
In detail, the Kaiser reagents were added to squared samples (1 x 1 cm^2) of functionalized films and scaffolds in the following order and amounts: 75 µl of Phenol, 100 µl of KCN, 75 µl of Ninhydrin. The mixture was heated at 95°C for 5 min and then diluted with ethanol/water 60/40 v/v. The obtained solution were filtered by using GHP membrane filters (pores diameter 0,45 µm) in order to avoid light scattering phenomena, due to the presence of polymer particles inside the solution, that can cause a significant shift of the baseline during the UV test. The maximum absorbance (A) of the Kaiser product was observed at 570 nm. The measurements were taken over three replicate samples and then averaged. Starting from the averaged absorbance value, the molar extinction coefficient ε (15000 M^{-1} cm^{-1}) and the path length b (1 cm), the molar concentration of the diluted solution was obtained through Lambert Beer low:

$$A = \varepsilon \cdot b \cdot C$$

From this molar concentration and the final volume (after dilution), the number of RGD moles on surface samples was calculated.

Cell Viability (MTS assay)

Cell viability tests were performed on functionalized and not functionalized films and scaffolds (1 x 1 cm^2), using H_9C_2 cardiomyoblasts, as described in Chapter 2. Briefly, cells were cultured in DMEM (Dulbecco's Modified Eagle Medium, Gibco) enriched with 10% fetal bovine serum (FBS), glutamine (2mM), penicillin (100 U/ml) and streptomycin (100 µg/ml) (Euroclone, Italy). Cells were maintained at 37° C in a humidified atmosphere with 5% CO_2 and used at 10^5 x cm^2 on the samples' surfaces. MTS assay (CellTiter 96® Aqueous Non-Radioactive Cell Proliferation Assay, Promega, Italy) was used to evaluate cell viability. Cells were cultured on the different surfaces for 1, 3 and 7 days. A MTS solution was added to the culture medium. After 3h, the culture medium was removed and the solution was read in UV-VIS spectroscopy (V-630 UV-Vis Spectrophotometer, Jasco, USA) at 490 nm. Cells seeded on cell culture Petri dishes were used as positive control.

Cell adhesion (SEM and Western Blot)

Cell adhesion was qualitatively investigated through SEM micrographs after 1 and 3 day culture on dense samples, while through the evaluation of vinculin expression (Western Blot) on scaffolds.
H_9C_2 cardiomyoblasts were cultured for 7 days on the porous constructs. Culture medium was then discarded and a lysis solution (SDS 2.5%, Tris-HCl pH 7.4, 0.25 M in bidistilled water) was placed on the different samples. Cell proteins were quantified through BCA assay (Thermo Scientific, USA). For electrophoresis, 10 µg of total proteins were used. Samples were diluted with Laemmli reducing buffer (60 mMTris-Cl pH 6.8, 2% SDS, 10% glycerol, 5% β-mercaptoethanol, 0.01% bromophenol blue), and electrophoresed on 7.5% sodium

dodecylsulfate polyacrylamide gels (SDS-PAGE). The proteins were blotted onto nitrocellulose membranes. The membranes were incubated for 1 h in 5% blocking solution (non-fat dry milk in PBS), then incubated overnight with 1:500 dilution of primary antibodies (Vinculin – Calbiochem, USA), followed by incubation with appropriate secondary antibody HRP-conjugated (Perkin-Elmer). Proteins were detected by Western Lightning plus-ECL (Perkin-Elmer, USA), and protein bands were then visualized by Bio-Rad VersaDoc™ imaging system.

Statistical Analysis

Data obtained from MTS assay were investigated for statistical significance using one-way analysis of variance (ANOVA). A *p*-value less than 0.05 was considered significant.

3.3 Results and Discussion

3.3.1 Characterization of functionalized films

3.3.1.1 ATR-IR and XPS

ATR-IR spectroscopy and XPS demonstrated that surface modification of KBC1250 films was obtained successfully. In figure 3.7 ATR spectra of the pristine film, the sample modified with PAA and that after RGD attachment are collected. For PAA-KBC1250, an enlargement of the intense band at about 1720 cm^{-1} is observable. In detail, a shoulder, that is not present in KBC1250 spectrum and that can be ascribable to the presence of COOH functional groups, appears on the right side of this band. In RGD-PAA-KBC1250 spectrum, a peak at 1656 cm^{-1}, that is ascribable to the stretching of peptide bonds, indicates the presence of RGD sequences covalently attached to the PUR surface. The spectrum registered for the sample functionalized with the linear chemical micropattern is not reported, since it does not show the diagnostic peptide peak. This could be explained with the lower amount of RGD groups on PUR surface (see 3.3.1.3 section: "COOH and NH_2 quantification").

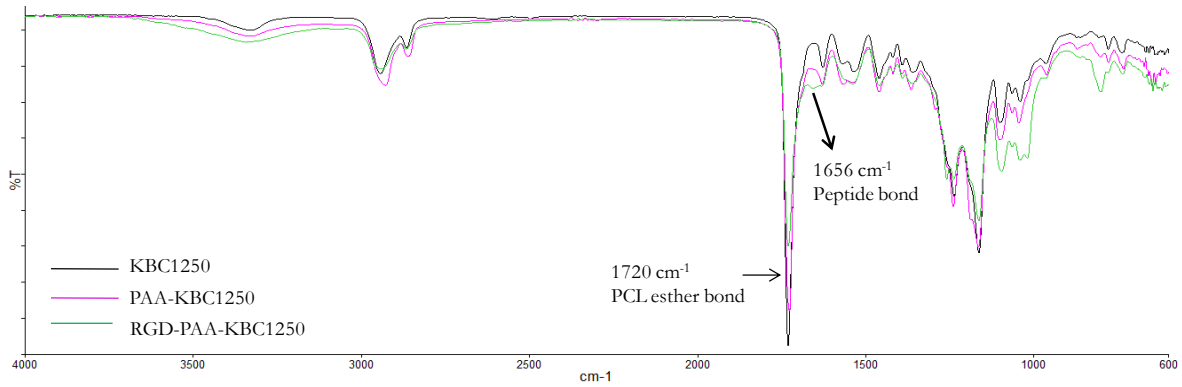

Fig. 3.7 ATR-IR spectra of KBC1250, PAA-KBC1250, RGD-PAA-KBC1250 films.

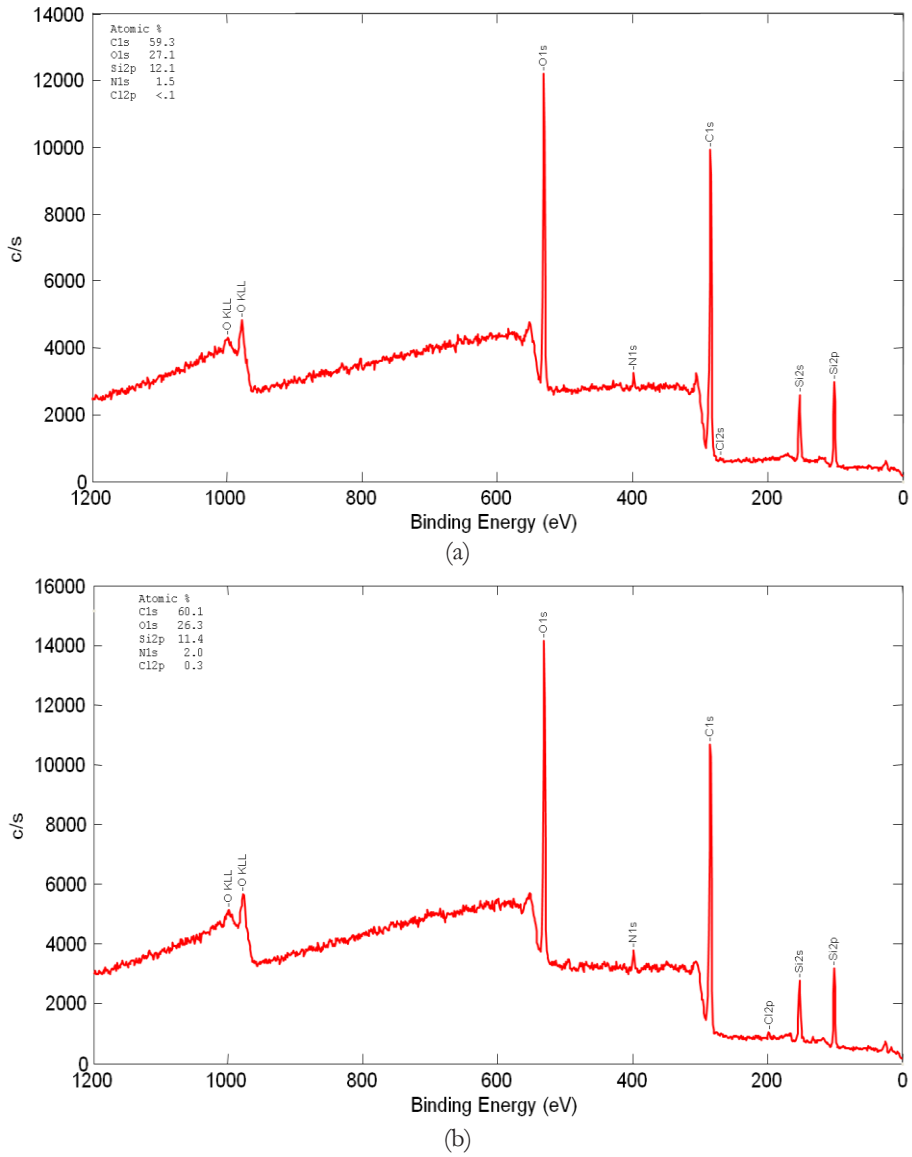

Fig. 3.8 XPS spectra of KBC1250 (a) and RGD-PAA-KBC1250 (b) films.

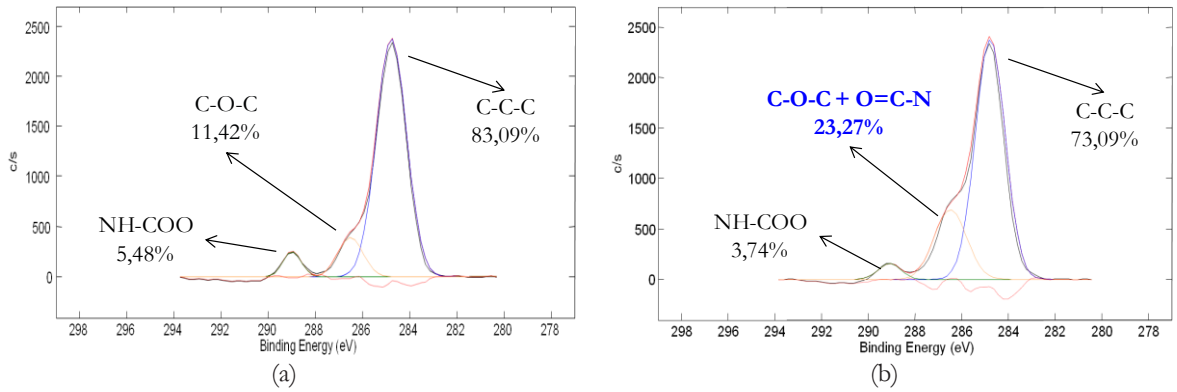

Fig. 3.9 Deconvolution of the carbon peak in XPS spectra of KBC1250 (a) and RGD-PAA-KBC1250 (b) films.

XPS spectra of KBC1250 and RGD-PAA-KBC1250 are reported in figure 3.8. The validation of the peptide functionalization of films was obtained by the analysis of the atomic surface composition and of the carbon peak in both spectra. An increase of 0.5% of N amount is observable passing from the pristine PUR to the modified one (figure 3.8). By the deconvolution of the carbon peak, three contributions may be detected: the main peak at 284 eV corresponds to aliphatic carbon atoms, that at 286 eV identifies carbon atoms linked to oxygen with ether bonds, while the one at 289 eV corresponds to carbon atoms involved in urethane functional groups (figure 3.9 a). For the functionalized surface, a redistribution of the areas of the different contribution is observable. In detail, there is an increase of 11% of the peak at 286 eV, that is associated to carbon atoms involved in both urethane and peptide bonds (figure 3.9 b) [52].

3.3.1.2 Surface wettability

The evaluation of wettability variation after plasma and RGD modification confirmed the successful surface functionalization. As it is possible to see in table 3.2, acrylic acid grafting led to a decrease of the contact angle value of about 44°, while RGD covalent attachment determined an increase of about 30° with respect to the PAA-KBC1250. The final contact angle value achieved (65°) indicates a moderate hydrophylicity for the modified surface and it is very close to 55°, that seems to be the optimal value to obtain the maximum cell adhesion and growth, regardless of the cell type [3].

Tab. 3.2 Contact Angle values for pristine KBC1250, PAA- and RGD-PAA-KBC1250 films.

PUR FILMS	Contact Angle (°)
KBC1250	79 ± 1
PAA-KBC1250	35 ± 2
RGD-PAA-KBC1250	65 ± 2

3.3.1.3 COOH and NH_2 groups quantification

Acidic and amino groups were quantified after plasma treatment and RGD reaction, respectively. Through Toluidine assay (TBO) a density of 0.003 μmol/mm^2 for COOH functional groups on dense samples was obtained. This density value was considered for the subsequent calculations of EDC and NHS amounts, in order to activate all the acidic groups. Nevertheless, RGD amounts for the subsequent reaction was calculated considering that a density of 0,01 fmol/mm^2 was reported as the minimum value for cell adhesion [53] and 1,5x10^{-3}-0,2 nmol/mm^2 seems to be the optimal range for focal adhesion of fibroblasts [54].
An RGD surface density of 3.2 and 1.7 nmol/mm^2 was calculated through the Kaiser test for the homogenously modified sample and for that modified with a linear micropattern, respectively. These results indicate that the minimum density value to promote cell adhesion was exceeded and values very close to those suggested for fibroblasts adhesion were obtained.

However, since data in literature about the optimal RGD density to promote cardiomyocyte adhesion were not found, an investigation on the ideal conditions for the focal adhesion of this type of cells are necessary as future work.

3.3.1.4 Cell viability and adhesion on functionalized films

MTS assay was performed to quantify cardiomyocyte viability on functionalized and not functionalized KBC1250 films after 1, 3 and 7 culture days. As shown in figure 3.10, after 24 h and up to 3 days, cell viability is significantly higher for the RGD modified samples, compared to KBC1250 control (not functionalized) ($p<0.05$). In particular, cell viability appears lower for the samples functionalized with the RGD linear micropattern with respect to those modified homogeneously ($p<0.05$). This trend, which is repeated after 24 and 72 h, could be explained since the amount of RGD peptides attached on the surface functionalized by the use of the siloxane stencil is lower (1.7 nmol/mm^2) with respect to the surface modified homogeneously (3.2 nmol/mm^2) and, as a consequence, a lower amount of cells attached is expected. After 3 days a general decrease in cell viability is observable for the substrates. Nevertheless, it returns to increase after the seventh day of culture, with viability values comparable to those of the control for all the samples ($p>0.05$). In conclusion, the presence of RGD peptides on PUR film surfaces seems to accelerate the positive biological response of the substrates in terms of cardiomyocyte viability.

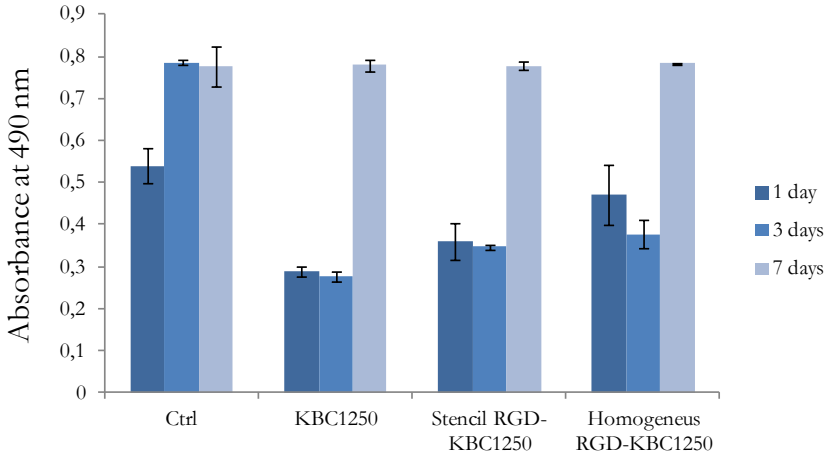

Fig. 3.10 Results of viability MTS tests performed on KBC1250 films using H_9C_2 rat heart cell line.

SEM micrographs allowed to evaluate qualitatively the effect of RGD peptides on cell adhesion after 24 and 72 culture hours. As shown in figure 3.11 a, after 24h, cardiomyocytes do not show good adhesion on KBC1250 (control), where a round cell morphology is evident. On modified samples (figure 3.11 b and c) cell morphology is slightly less spherical and characterized by the presence of filaments. After 3 culture days, cells show a clear good adhesion on functionalized surfaces, with a stretched shape and filaments, especially in the case of the homogeneously modified KBC1250. If MTS results are considered, it is possible to state that, regardless of the decreased viability observed after 3 days, survived cells are well attached to RGD modified films.

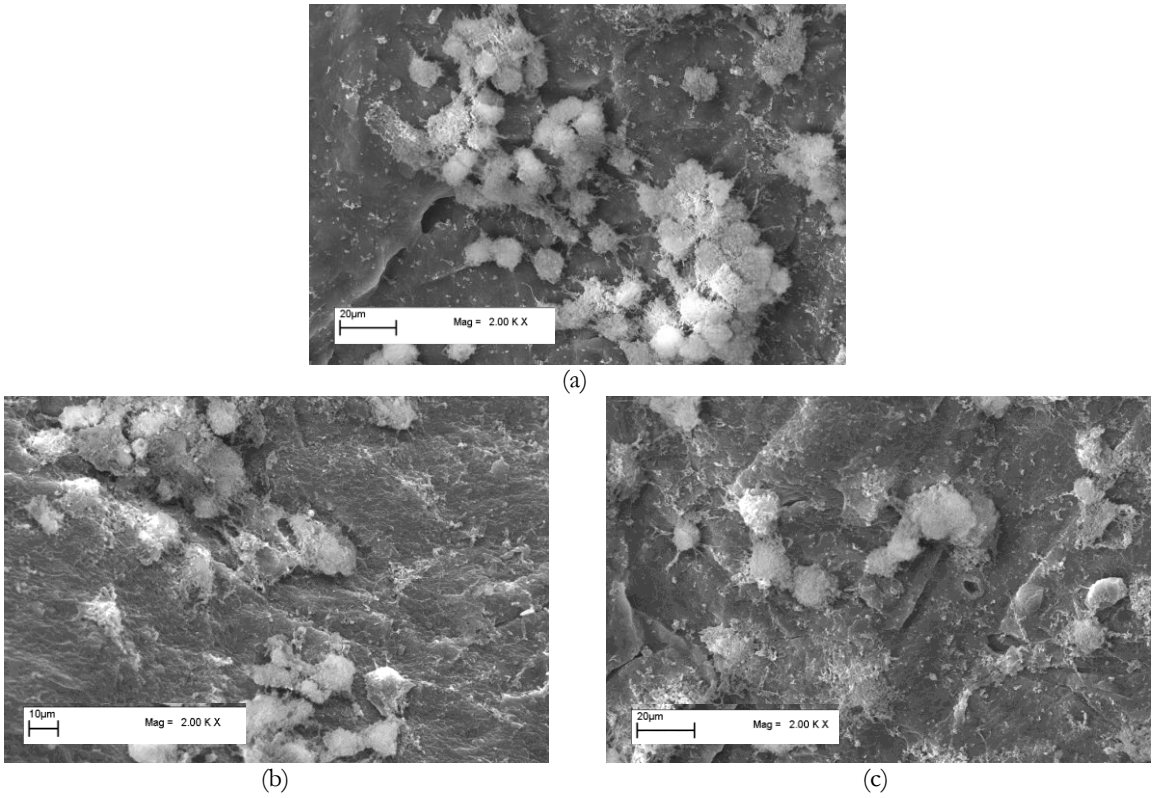

Fig. 3.11 SEM micrographs of KBC1250 (not functionalized) (a), KBC1250-RGD functionalized with a linear chemical micropattern (b) and KBC1250-RGD (c) films, after 24h of cell culture.

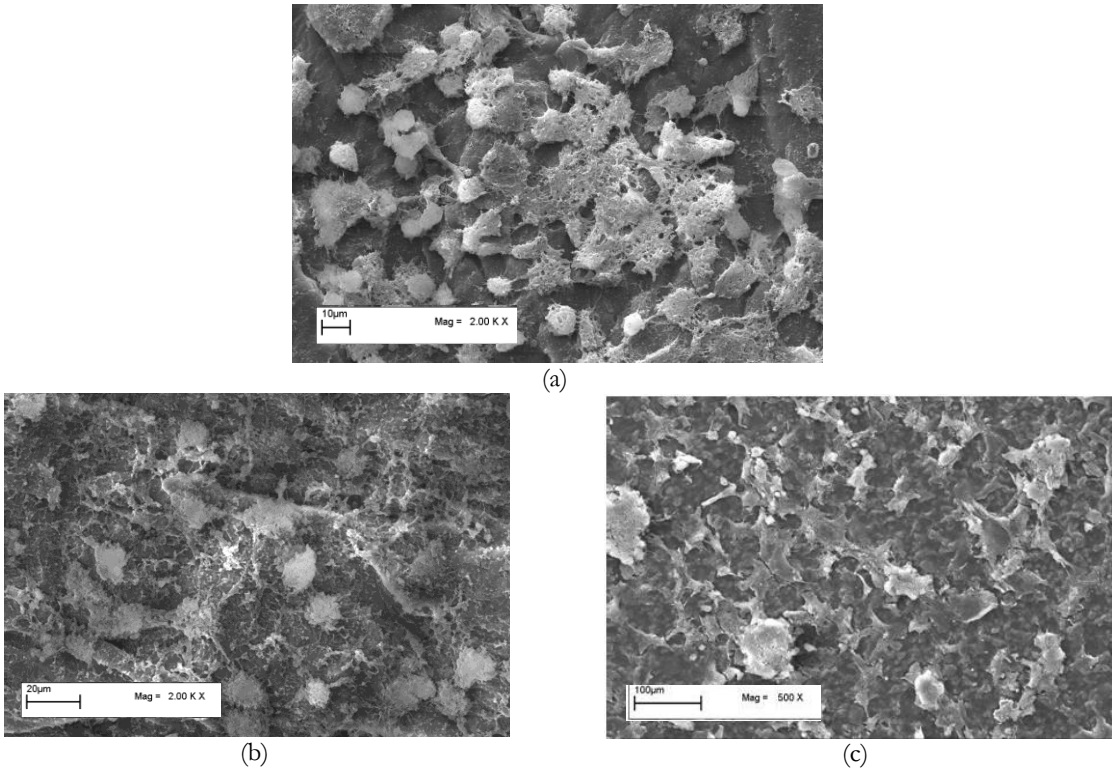

Fig. 3.12 SEM micrographs of KBC1250 (not functionalized) (a), KBC1250-RGD functionalized with a linear chemical micropattern (b) and KBC1250-RGD (c) films, after 72h of cell culture.

3.3.2 Characterization of functionalized scaffolds

3.3.2.1 ATR-IR

As for dense PUR substrates, ATR spectra demonstrated the successful surface modification of KBC1250 scaffolds, after plasma treatments and RGD covalent attachment. As shown in figure 3.13, the same enlargement of the intense band at about 1720 cm^{-1}, observed in the case of PAA-KBC1250 films and ascribable to the presence of acidic carboxyl groups is present. Concerning RGD-PAA-KBC1250 spectrum, the peak at 1656 cm^{-1}, corresponding to the stretching of peptide bonds, is observable.

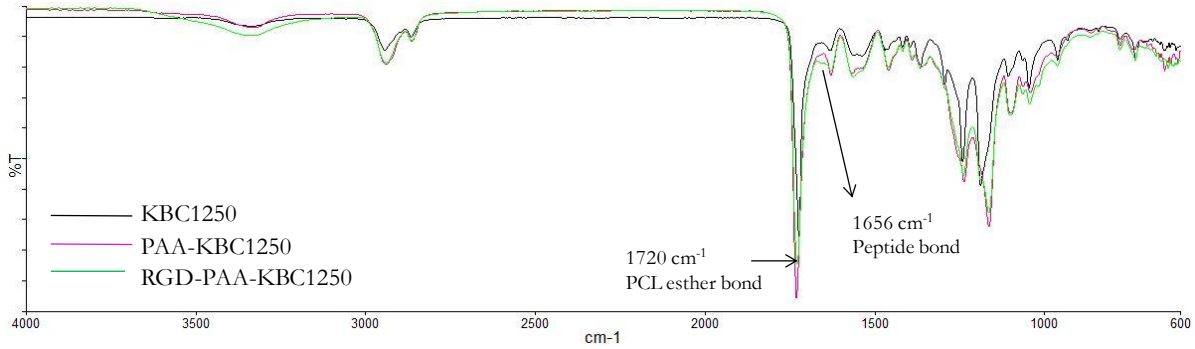

Fig. 3.13 ATR-IR spectra of KBC1250, PAA-KBC1250, RGD-PAA-KBC1250 scaffolds.

3.3.2.2 Surface wettability

Static Contact Angle measurements allowed to confirm the modification of scaffold surfaces. As shown in table 3.2, a significant increase in hydrophilicity was registered for the porous KBC1250 after acrylic acid plasma treatment. The covalent attachment of RGD peptide determined an increase of contact angle value corresponding to a decrease in wettability. Although the trend in contact angle variation was the same observed for modified PUR films, the final value achieved for scaffold surfaces (99°) was higher than films. The functionalization conditions, that were used for PUR films, modified wettability properties of scaffolds but not enough to achieve an optimal contact angle value for cell attachment. The "hydrophobic" effect of surface micro-roughness, that has been already discussed in Chapter 2, seems to be maintained.

Tab. 3.2 Contact Angle values for KBC1250 scaffold and modified PUR scaffolds.

PUR SCAFFOLDS	Contact Angle (°)
KBC1250	115 ± 1
PAA-KBC1250	80 ± 1
RGD-PAA-KBC1250	99 ± 1

3.3.2.3 COOH and NH_2 groups quantification

Acidic groups were quantified after plasma treatment through Toluidine assay, as for dense films. A COOH density of 0.004 μmol/mm^3 was obtained. As in the case of films, this density value was considered for the subsequent calculations of EDC and NHS amounts, in order to activate all the acidic groups, but not for RGD amounts in the covalent attachment reaction. For this reagent, the same data from literature that were used for dense films were considered [53, 54]. Amino groups quantification was performed thorough the Kaiser test and a final RGD surface density of 1.4 nmol/mm^3 was calculated. In this case a volume unit was considered for density calculation since during plasma treatment and, as a consequence, during the subsequent functionalization steps, reactive groups could be formed in the inner part of porous surfaces.

3.3.2.4 Cell Viability and adhesion on functionalized scaffolds

MTS assay was used to quantify cardiomyocyte viability also on functionalized and not functionalized porous constructs, after 1, 3 and 7 culture days. As shown in figure 3.14, there are no significant differences in cell viability passing from the unmodified sample to the RGD modified one ($p>0.05$), after 1 and 3 culture days. After 7 culture days, a slight viability increase can be observed for the functionalized scaffolds ($p<0.05$). In addition, Western Blot assay demonstrated a slight increase in vinculin expression at the same time interval (see figure 3.15).

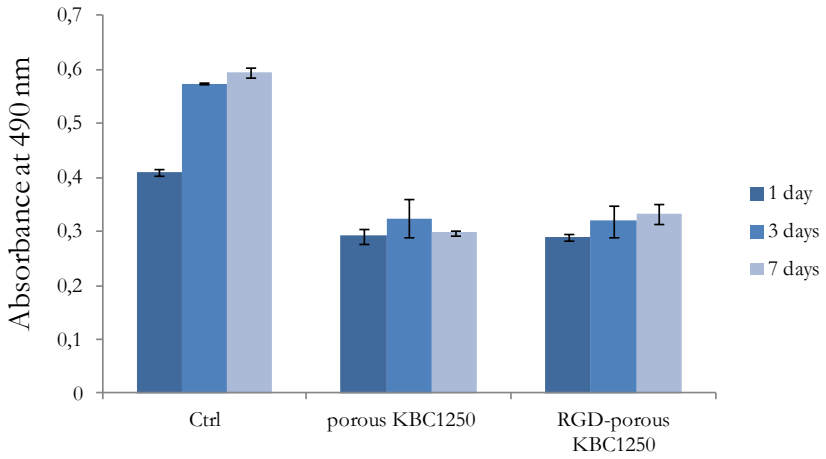

Fig. 3.14 Results of viability MTS tests performed on KBC1250 scaffolds using H_9C_2 rat heart cell line.

This overall biological response of the modified scaffolds could be ascribed to the hydrophobicity of the porous samples. Passing from the not functionalized to the functionalized porous constructs, a decrease in contact angle values of about 16° was observed, with a final value of 99°. This wettability increase after surface modification can have caused a negative effect on cardiomyocyte adhesion and viability, thus hindering the detection of any positive influence of the biomimetic surface functionalisation performed on

these samples. However, after 7 culture days, probably the effect of the suitable porous microstructure and of the attached peptides balance the negative hydrophobicity effect.
Another explanation for these biological results could be linked to the presence of some RGD peptides not covalently bonded to the inner walls of the porous microstructure. As already discussed in the Introduction section, non-immobilized peptides can lead to cell detachment, a round shape and apoptosis [23-25].

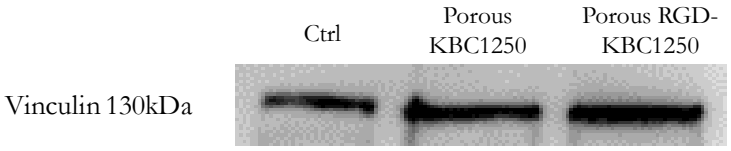

Fig. 3.15 Results of Western Blot performed on KBC1250 porous scaffold, not surface modified and modified, using H_9C_2 rat heart cell line.

3.4 Conclusions

Spectroscopic (ATR-IR and XPS) analysis, increase in surface wettability and colorimetric assays showed the successful surface modification of both KBC1250 films and scaffolds, by the covalent attachment of RGD peptides. In the case of the dense substrates, Contact Angle measurements and Kaiser Test demonstrated respectively the presence of an optimal hydrophilicity and peptide density, able to promote cell adhesion. A positive effect on cardiomyocyte viability (already after 1 and 3 culture days) and adhesion (after 3 culture days) resulted from MTS tests and SEM micrographs. Although an increase in surface wettability and a good RGD density were obtained also for the porous constructs, the biological response of this type of substrates was not significantly improved by surface modification. A slight increase in cell viability and in the expression of the vinculin protein was observed only after 7 days of culture. These results can be linked to the hydrophobicity of the porous surfaces (that was not drastically decreased after the functionalization process) or the presence of not covalently bound peptides inside the scaffold microstructure, that may prevent cell adhesion and cause cell death.

References

1. Ma, Z., Mao, Z. and Gao, C., *Surface modification and property analysis of biomedical polymers used for tissue engineering.* Colloids Surf B Biointerfaces, 2007. **60**(2): p. 137-57.
2. Youssef, W., R.R. Wickett, and S.B. Hoath, *Surface free energy characterization of vernix caseosa. Potential role in waterproofing the newborn infant.* Skin Res Technol, 2001. **7**(1): p. 10-7.
3. Lee, J.H., et al., *Interaction of Different Types of Cells on Polymer Surfaces with Wettability Gradient.* J Colloid Interface Sci, 1998. **205**(2): p. 323-330.
4. Bacakova, L., et al., *Molecular mechanisms of improved adhesion and growth of an endothelial cell line cultured on polystyrene implanted with fluorine ions.* Biomaterials, 2000. **21**(11): p. 1173-9.
5. Heitz, J., et al., *Cell adhesion on polytetrafluoroethylene modified by UV-irradiation in an ammonia atmosphere.* J Biomed Mater Res A, 2003. **67**(1): p. 130-7.

6. Denes F. S., M.S., *Macromolecular plasma-chemistry: an emerging field of polymer science.* Prog. Polym. Sci. , 2004. **29**: p. 815–885.
7. Favia P., S.E., Gristina R., D'Agostino R., *Novel plasma processes for biomaterials: micro-scale patterning of biomedical polymers.* Surface and Coatings Technology, 2003: p. 707-711.
8. Yasuda, H., et al., *Ultrathin coating by plasma polymerization applied to corneal contact lens.* J Biomed Mater Res, 1975. **9**(6): p. 629-43.
9. Chawla, A.S., *Use of plasma polymerization for preparing silicone-coated membranes for possible use in blood oxygenators.* Artif Organs, 1979. **3**(1): p. 92-6.
10. Bacakova, L., et al., *Modulation of cell adhesion, proliferation and differentiation on materials designed for body implants.* Biotechnol Adv, 2011. **29**(6): p. 739-67.
11. Curtis, A. and C. Wilkinson, *Topographical control of cells.* Biomaterials, 1997. **18**(24): p. 1573-83.
12. Singhvi, R., et al., *Engineering cell shape and function.* Science, 1994. **264**(5159): p. 696-8.
13. Ruoslahti, E. and M.D. Pierschbacher, *New perspectives in cell adhesion: RGD and integrins.* Science, 1987. **238**(4826): p. 491-7.
14. Albelda, S.M. and C.A. Buck, *Integrins and other cell adhesion molecules.* FASEB J, 1990. **4**(11): p. 2868-80.
15. van der Flier, A. and A. Sonnenberg, *Function and interactions of integrins.* Cell Tissue Res, 2001. **305**(3): p. 285-98.
16. Pierschbacher, M.D. and E. Ruoslahti, *Cell attachment activity of fibronectin can be duplicated by small synthetic fragments of the molecule.* Nature, 1984. **309**(5963): p. 30-3.
17. Pierschbacher M.D., R.E., *Cell attachment activity of fibronectin can be duplicated by small synthetic fragments of the molecule* Nature Biotechnology, 1984. **309**.
18. LeBaron, R.G. and K.A. Athanasiou, *Extracellular matrix cell adhesion peptides: functional applications in orthopedic materials.* Tissue Eng, 2000. **6**(2): p. 85-103.
19. Zamir, E. and B. Geiger, *Molecular complexity and dynamics of cell-matrix adhesions.* J Cell Sci, 2001. **114**(Pt 20): p. 3583-90.
20. Geiger, B. and A. Bershadsky, *Assembly and mechanosensory function of focal contacts.* Curr Opin Cell Biol, 2001. **13**(5): p. 584-92.
21. Petit, V. and J.P. Thiery, *Focal adhesions: structure and dynamics.* Biol Cell, 2000. **92**(7): p. 477-94.
22. Chen, C.S., et al., *Geometric control of cell life and death.* Science, 1997. **276**(5317): p. 1425-8.
23. Grano, M., et al., *Adhesion properties and integrin expression of cultured human osteoclast-like cells.* Exp Cell Res, 1994. **212**(2): p. 209-18.
24. Noiri, E., et al., *Cyclic RGD peptides ameliorate ischemic acute renal failure in rats.* Kidney Int, 1994. **46**(4): p. 1050-8.
25. Stromblad, S., et al., *Suppression of p53 activity and p21WAF1/CIP1 expression by vascular cell integrin alphaVbeta3 during angiogenesis.* J Clin Invest, 1996. **98**(2): p. 426-33.
26. Pierschbacher M.D., R.E., *Cell attachment activity of fibronectin can be duplicated by small synthetic fragments of the molecule.* Nature 1984. **309** (5963): p. 30-33.
27. Hersel, U., C. Dahmen, and H. Kessler, *RGD modified polymers: biomaterials for stimulated cell adhesion and beyond.* Biomaterials, 2003. **24**(24): p. 4385-415.
28. Miyata, T., et al., *Delayed exposure to pulsatile shear stress improves retention of human saphenous vein endothelial cells on seeded ePTFE grafts.* J Surg Res, 1991. **50**(5): p. 485-93.
29. Vohra, R., et al., *Comparison of different vascular prostheses and matrices in relation to endothelial seeding.* Br J Surg, 1991. **78**(4): p. 417-20.
30. Thomson, G.J., et al., *Adult human endothelial cell seeding using expanded polytetrafluoroethylene vascular grafts: a comparison of four substrates.* Surgery, 1991. **109**(1): p. 20-7.
31. Elbert, D.L. and J.A. Hubbell, *Conjugate addition reactions combined with free-radical cross-linking for the design of materials for tissue engineering.* Biomacromolecules, 2001. **2**(2): p. 430-41.
32. Lhoest, J.B., et al., *Fibronectin adsorption, conformation, and orientation on polystyrene substrates studied by radiolabeling, XPS, and ToF SIMS.* J Biomed Mater Res, 1998. **41**(1): p. 95-103.
33. Ito, Y., M. Kajihara, and Y. Imanishi, *Materials for enhancing cell adhesion by immobilization of cell-adhesive peptide.* J Biomed Mater Res, 1991. **25**(11): p. 1325-37.
34. Boxus, T., et al., *Synthesis and evaluation of RGD peptidomimetics aimed at surface bioderivatization of polymer substrates.* Bioorg Med Chem, 1998. **6**(9): p. 1577-95.

35. Neff, J.A., K.D. Caldwell, and P.A. Tresco, *A novel method for surface modification to promote cell attachment to hydrophobic substrates.* J Biomed Mater Res, 1998. **40**(4): p. 511-9.
36. Lin, H.B., et al., *Synthesis, surface, and cell-adhesion properties of polyurethanes containing covalently grafted RGD-peptides.* J Biomed Mater Res, 1994. **28**(3): p. 329-42.
37. Lin, H.B., et al., *Synthesis of a novel polyurethane co-polymer containing covalently attached RGD peptide.* J Biomater Sci Polym Ed, 1992. **3**(3): p. 217-27.
38. Sartori, S., Rechichi, A., Vozzi G., D'Acunto M., Heined E., Giusti P., Ciardelli G., *Surface modification of a synthetic polyurethane by plasma glow discharge: Preparation and characterization of bioactive monolayers.* Reactive and Functional Polymers, 2008. **68** (3): p. 809–821.
39. Dai, W., J. Belt, and W.M. Saltzman, *Cell-binding peptides conjugated to poly(ethylene glycol) promote neural cell aggregation.* Biotechnology (N Y), 1994. **12**(8): p. 797-801.
40. Beer, J.H., K.T. Springer, and B.S. Coller, *Immobilized Arg-Gly-Asp (RGD) peptides of varying lengths as structural probes of the platelet glycoprotein IIb/IIIa receptor.* Blood, 1992. **79**(1): p. 117-28.
41. Hidalgo-Bastida, L.A., et al., *Cell adhesion and mechanical properties of a flexible scaffold for cardiac tissue engineering.* Acta Biomater, 2007. **3**(4): p. 457-462.
42. Brown, D.A., et al., *Modulation of gene expression in neonatal rat cardiomyocytes by surface modification of polylactide-co-glycolide substrates.* J Biomed Mater Res A, 2005. **74**(3): p. 419-29.
43. Siepe, M., et al., *Construction of skeletal myoblast-based polyurethane scaffolds for myocardial repair.* Artif Organs, 2007. **31**(6): p. 425-33.
44. McDevitt, T.C., et al., *Spatially organized layers of cardiomyocytes on biodegradable polyurethane films for myocardial repair.* J Biomed Mater Res A, 2003. **66**(3): p. 586-95.
45. Tay, C.Y., et al., *Micropatterned matrix directs differentiation of human mesenchymal stem cells towards myocardial lineage.* Exp Cell Res, 2010. **316**(7): p. 1159-68.
46. Rowley, J.A. and D.J. Mooney, *Alginate type and RGD density control myoblast phenotype.* J Biomed Mater Res, 2002. **60**(2): p. 217-23.
47. Shachar, M., et al., *The effect of immobilized RGD peptide in alginate scaffolds on cardiac tissue engineering.* Acta Biomater, 2011. **7**(1): p. 152-62.
48. Schussler O., C.C., Louis-Tisserand M., Al-Chare W., Oliviero P., Menard C., Michelot R., Bochet P., Salomon D.R., Chachques J.C., Carpentier A., Lecarpentier Y., *Use of arginine-glycine-aspartic acid adhesion peptides coupled with a new collagen scaffold to engineer a myocardium-like tissue graft.* Nat Clin Pract Cardiovasc Med. , 2009. **6**(3): p. 240-9.
49. Guan, J. and W.R. Wagner, *Synthesis, characterization and cytocompatibility of polyurethaneurea elastomers with designed elastase sensitivity.* Biomacromolecules, 2005. **6**(5): p. 2833-42.
50. Jawad, H., et al., *Myocardial tissue engineering: a review.* J Tissue Eng Regen Med, 2007. **1**(5): p. 327-42.
51. Jawad, H., et al., *Myocardial tissue engineering.* Br Med Bull, 2008. **87**: p. 31-47.
52. Yuan, J., et al., *Chemical graft polymerization of sulfobetaine monomer on polyurethane surface for reduction in platelet adhesion.* Colloids Surf B Biointerfaces, 2004. **39**(1-2): p. 87-94.
53. Chollet, C., et al., *RGD peptides grafting onto poly(ethylene terephthalate) with well controlled densities.* Biomol Eng, 2007. **24**(5): p. 477-82.
54. Maheshwari, G., et al., *Cell adhesion and motility depend on nanoscale RGD clustering.* J Cell Sci, 2000. **113 (Pt 10)**: p. 1677-86.

CHAPTER 4
Cardiac stem cells on polyurethane films and scaffolds

Abstract

Endogenous progenitor cells are the best candidates for myocardial regeneration, both trough cell therapies and tissue engineering bioconstructs, since these cells are tissue-specific, pre-committed to a cardiac fate and expandable. In this part of the work, human endogenous Cardiosphere Derived Cells (CDCs) and cardiac Mesenchymal Stem Cells (MSCs), were extracted from human cardiac biopsies and both tested on KBC1250 dense and porous substrates for myocardial tissue applications. Cell quantification and cell health tests, respectively performed by Picogreen and AlamarBlue assays, showed encouraging results for the porous construct, that did not display toxic effects on cells and promote their proliferation.

4.1 Introduction

Researchers have believed for a long time that the heart is a non-regenerative organ composed of post-mitotic cardiomyocytes in which hypertrophy (cell enlargement) of surrounding viable myocardium compensates for cardiomyocyte loss in an infarcted heart. Nevertheless, during the last two decades, attempts in the scientific community have resulted in evidences that challenge this dogma, such as the identification of a reservoir of resident stem cells, defined as cardiac progenitor cells (CPCs) [1]. These endogenous progenitors may represent the best candidates for cardiovascular cell therapy, as they are tissue-specific, often pre-committed to a cardiac fate, expandable and display a greater propensity to differentiate towards cardiovascular lineages [2].
As a consequence, new cell-based therapeutic strategy are emerging, with an expectation of heart tissue regeneration. In addition to skeletal myocytes, blood or bone marrow-derived cells and embryonic stem (ES) cells, cardiac stem/progenitor cells from adult hearts have been explored as potential candidates for cardiovascular regenerative cell therapy and myocardial tissue engineering applications [1].

4.1.1 Cardiac progenitor cells (CPCs)

A progenitor cell in the heart is defined as an undifferentiated cell that is committed to the cardiac lineage and has the capacity to produce differentiated progenies, including cardiomyocytes, smooth muscle cells and/or endothelial cells. Resident cardiac progenitor cells (CPCs) represent a responsive stem cell reservoir within the adult myocardium. They may offer distinct advantages over other adult stem cell types, for cardiovascular therapy, being autologous, tissue-specific and pre-committed to the cardiovascular lineages [3]. CPCs are reported to exist in the heart of several species, including mouse [4, 5], rat [6, 7], dog [8], pig [9]

and human [4, 10, 11] as small clusters of progenitors characterized by the expression of stem cell antigens. Different pools of CPCs have been classified according to their properties and surface markers: side population, c-kit+, Sca-1+, Islet 1+, SSEA-1+, "cardiospheres" and/or "cardiosphere"-derived CPCs [2]. C-Kit+ cells in adult human heart were found in a specific microenvironment ("niche"), with a capacity for self-renewal and the ability to regenerate myocardium tissue in a rat model of acute MI [12]. Using Sca-1, a different CPC population was also isolated from the adult mouse heart. However, their differentiation into cardiomyocytes requires the presence of demethylating agents (e.g., 5-azacytidine and oxytocine) [13].
Due to their limited numbers, the study and therapeutic application of resident CPCs depends upon their expansion. This result has been achieved by two different approaches. The first one is based on their ex vivo isolation and expansion from cardiac biopsies, followed by transplantation into the damaged heart [7]; the second one focuses on stimulating and boosting CPC proliferation in situ, via administration of specific factors [14]. Although these cells hold an intriguing regenerative potential towards cardiovascular repair, several questions remain unanswered relating to CPC origin, what markers they express, the degree of overlap of the so-called distinct subpopulations and the precise mechanisms by which they benefit the injured tissue.

4.1.1.1 Cardiospheres and CDCs for myocardial regeneration

CPCs can be isolated from heart tissue biopsies into self-assembled clusters, referred to as "cardiospheres". These cells were shown to express surface stem and endothelial antigen markers (c-Kit, Sca-1, CD31, and CD34), suggesting a heterogeneous nature of progenitors at different stages, including differentiating progenitors, spontaneously differentiated cardiomyocytes and vascular cells [4]. Murine CS showed spontaneous beating soon after their generation, while human CS showed to beat only after co-culture with rat cardiomyocytes. CS could also be cultured as a monolayer of cardiosphere-derived cells (CDCs), upon mechanical dissociation, and expanded over many passages [4]. The in vivo cardiomyogenic potential of CS has been verified via transplantation studies into different MI models: when murine CS were injected into the ischemic heart of immunodeficient mice, they were shown to differentiate into vascular cells as well as myocytes with contractile activity and expression of sarcomeric proteins; porcine CDCs, delivered intracoronary in a preclinical model of postinfarct left ventricular dysfunction, resulted in the generation of new tissue, reduction of infarct size, and improvement of haemodynamics [9]. Although the in vivo cardiomyogenic potential in animal MI models was confirmed, further characterization before translation into a clinical setting is highly recommended, since the reproducibility and reliability of this protocol has been questioned [2].
Recently, studies about the application of cardiospheres or CDCs in myocardial tissue engineering have been carried out, although the combination of regenerative cells with functional scaffolds to create a vitro TE bioconstructs for ischemic heart remains a challenge. Chimenti et al. employed porous gelatin foams and collagen based scaffolds (RGD modified) as substrates for housing and enhancing the potency of CDCs for myocardial regeneration

[15]. They observed that both substrates showed a good cell retention and that the RGD-collagen scaffold offered an ideal structure for cell spreading, while the gelatin foam encouraged a 3D order. The most important result concerned CDCs cardiac commitment, that was maintained and promoted inside the constructs, as shown by the analysis of expression for the cardiac markers, especially in the collagen based scaffold. Similar results, that were achieved with mouse CDCs incorporated in hydrogels, confirmed the feasibility of TE approach on resident cardiac progenitor cells [16].

4.1.1.2 Side population (SP) and mesenchymal stem cells (MSCs) for myocardial regeneration

The SP cells have been found in several adult tissues, such as skeletal muscle and bone marrow [17]. The existence of a cardiac SP was first reported in the postnatal murine myocardium, where resident side population cells showing stem cell-like activity and cardiomyocyte differentiation potential, were detected [18]. In rodents, cardiac SP cells were described as Sca-1+, ckit+, CD34+, CD31−, and CD45− cells, expressing cardiac specific transcription factors, such as Gata4, MEF2C and Nkx2.5 upon isolation, and acquiring a cardiomyocyte phenotype [18, 19]. In myocardial regeneration studies, SP CPCs showed the ability to home to the injured heart and to differentiate in situ into cardiomyocytes, endothelial and smooth muscle cells, when intravenously infused into adult rats [20].
Cardiac SP cells may have heterogeneous nature, containing distinct subpopulations, identified by expression of VE-cadherin, CD31, CD34 and Sca1 and consisting of vascular endothelial cells, smooth muscle cells and mesenchymal progenitors, including cardiomyogenic precursors [21]. Proofs of mesenchymal stem cell existence in mice heart were shown in the work of Carlson et al., where a contribution from endogenous MSCs to the infarct fibroblast population has been demonstrated. Fibroblasts forming in the scar of an MI should arise from an endogenous pool of primitive CD44+ mesenchymal precursors that localize and proliferate in the wound within 36 h, as shown by the expression of the cell cycle marker Ki67. This population of CD44+ cells lack the haematopoietic marker CD45 as well as the inflammatory markers CD18 and CD73, indicating that they are not bone marrow-derived. In addition, a portion of these cells are multipotential stem cells that express the stem cell markers CD34, TERT, and Nanog and are capable of differentiating into multiple lineages in vitro as well as into CD44+ fibroblasts such as those seen in the infarct zone. In conclusion, the study of Carlson support the role of endogenous MSCs as important mediators of repair by generating and processing the extracellular matrix of the forming scar [22]

4.1.2 Cardiac progenitor cells in the present work

In this thesis work, cardiac Mesenchymal Stem Cells and Cardiosphere-Derived Cells were isolated from human heart tissue, expanded in vitro and seeded on KBC1250 dense and porous scaffolds, in order to test the capability of these substrates to provide a suitable microenvironment for the proliferation of these progenitor cells.

The PUR substrates were selected on the strength of previous biological results, obtained by viability test with cardiomyocytes and discussed in Chapter 2. Cell isolation, expansion and culture on polymeric substrates were performed at the Institute of Human Genetics of Newcastle University (Dr Annette Meeson's laboratory). MSCs used in this work were detected in the human heart, extracted and characterized for the first time by Dr Rachel Oldershaw and Dr Annette Meeson of Newcastle University (United Kingdom) (work under publication). In the next section, CDC isolation and culture and MSC culture will be described.

4.2 Materials and methods

4.2.1 CDC isolation and culture

Cardiosphere derived Cells were isolated though the Biopsy Specimen Process [4, 23]. A human cardiac biopsy (from female patient, 21 years old) was cut into fragments (1-2 mm^3 pieces) that were washed in phosphate-buffered solution (PBS, Sigma) and partially digested enzymatically for 5 minutes at 37°C with 0.05% trypsin (Gibco). The tissue fragments were cultured as "explants" on dishes coated with fibronectin (figure 4.1, step 1) for about 4 weeks in CEM (Iscove's Modified Dulbecco's Medium [IMDM, Gibco] supplemented with 10% fetal calf serum, 100 U/mL penicillin G, 100 g/mL streptomycin, 2 mmol/L L-glutamine, and 0.1 mmol/L 2-mercaptoethanol) at 37°C and 5% CO_2. After several days, a layer of cells arose from adherent explants. Once confluent, these cells surrounding the explants (cardiosphere-forming cells) were harvested by gentle enzymatic digestion (figure 4.1, step 2). These cells were seeded on poly-D-lysine- coated dishes in cardiosphere growth medium (CGM)(35% complete IMDM/65% DMEM–Ham F-12 mix containing 2% B27, 0.1 mmol/L 2-mercaptoethanol, 10 ng/mL epidermal growth factor [EGF], 20 ng/mL basic fibroblast growth factor [bFGF], 40 nmol/L cardiotrophin-1, 40 nmol/L thrombin, and L-Glu, as in CEM) (figure 4.1, step 3). Several days later, cells that remained adherent to the poly-D-lysine-coated dishes were discarded, whereas detached cardiospheres were plated on fibronectin coated flasks and expanded as monolayers (figure 4.1, step 4). CDCs were subsequently passaged by trypsinization and splitting at a 1:2 ratio up to obtain an adequate cell number for the subsequent culture on PUR substrates. Single cells were counted under phase microscopy with a hemocytometer during CDC passaging and before seeding on PUR samples.

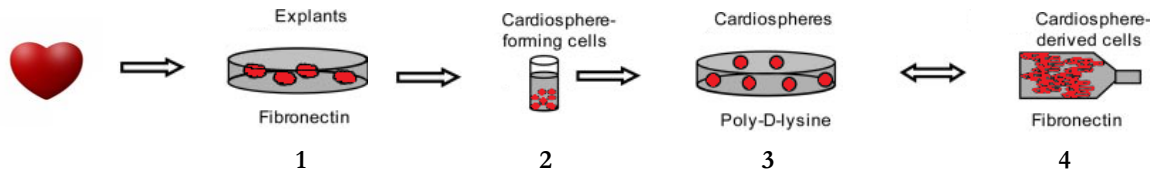

Fig. 4.1 Specimen processing for human cardiosphere growth and CDC expansion.

4.2.2 MSC culture

After cell isolation from a heart tissue biopsy (patient 28 years old), human cardiac MSCs were passaged by trypsinization and split 5 times at 1:3 ratio. Also in this case, cells were counted under phase microscopy with a hemocytometer before seeding on PUR samples.

4.2.3 CDC and MSC culture on PUR samples

KBC1250 films and scaffolds were cut in squared samples (1x1 cm^2), sterilized in ethanol/water (70/30 v/v) for 1 h and inserted into 96-well plates. Cells were detached using trypsin concentrated, resuspended in culture medium, and seeded upon KBC1250 substrates and tissue culture plastic (wells), as control (500,000 MSCs/sample and 170,000 CDCs/sample).
CDCs were seeded and cultured in Cardiomyocyte Cellutions Differentiation Medium (DV Biologics), while MSCs were seeded and cultured for 7 days in MSC medium (Gibco), that then was changed to Cardiomyocyte Cellutions Differentiation Medium for other 7 days. The seeded constructs were kept in cell incubator (Thermo Scientific Heracell150i for MSCs, Sanyo CO_2 Incubator for CDCs) and the medium was replaced every two days for both types of cells.

4.2.3.1 Cell viability and health tests

Cell viability was evaluated through Picogreen assay (Invitrogen), that employ a fluorescent nucleic acid stain (Picogreen) for quantitating double-stranded DNA (dsDNA), proportional to cell number. The amount of dsDNA was calculated adding a 200-fold diluted Picogreen solution in TE buffer (10 mM Tris-HCl, 1 mM EDTA, pH 7.5) to the samples (without culture medium and in triplicate) and by referring to a five-point standard curve from 0 to 1000 ng/ml in TE buffer. The absorbance of sample and standard solutions was recorded in the range 485-585 nm by a Fluoroscan Ascent (Thermo Lab System).
In the case of MSCs, cell health was also investigated through AlamarBlue assay (Invitrogen), that is based on detection of cell metabolic activity and incorporates a fluorometric/colorimetric indicator. Specifically, the system incorporates an oxidation-reduction indicator that fluoresces and changes color in response to chemical reduction of growth medium resulting from cell activity. AlamarBlue was added to the samples (triplicate), that were incubated for 4 h. The absorbance was read in the range 544-585 nm by a the same Fluoroscan Ascent that was used for Picogreen assay. Since the results obtained from the AlamarBlue assays depend from both the cell metabolic activity and the total number of cells, the absorbance values obtained were divided by the corresponding cell amount (DNA), in order to obtain values of health/cell, that indicate the averaged health of the single cells.
Data obtained from Picogreen and AlamarBlue assays were investigated for statistical significance using one-way analysis of variance (ANOVA). A *p*-value less than 0.05 was considered significant.

4.3 Results

4.3.1 CDC isolation and culture

In figure 4.2. a typical cardiosphere, that was created after cardiosphere-forming cells were seeded on poly-D-lysine- coated wells in cardiosphere growth medium, is shown. As already described, cardiospheres appear as clusters, characterized by a mixture of cardiac stem cells, differentiating progenitors and spontaneously differentiated cardiomyocytes. Vascular cells can also be present, depending on the size of the sphere and time in culture. Generally, differentiating/differentiated cells die or stop to divide, while stem cell continue to proliferate, creating secondary cardiospheres [4]. After transferring proliferated cardiospheres in a fibronectin- coated flasks, progenitor cell monolayers were obtained, as shown in figure 4.3. They were expanded as a common primary cell culture, achieving about one million of cells from a single biopsy after 2 passages (splits).

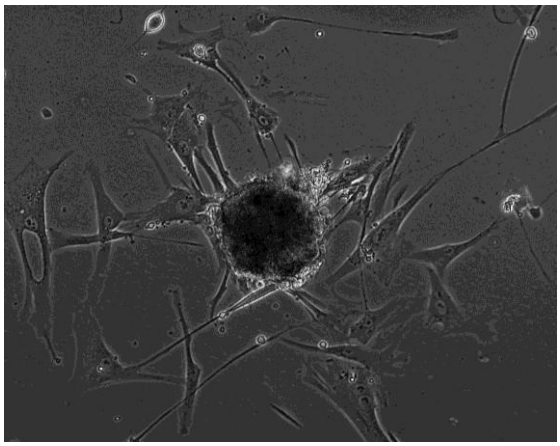

Fig. 4.2 A formed cardiosphere after seeding cardiosphere-forming cells on poly-D-lysine- coated wells.

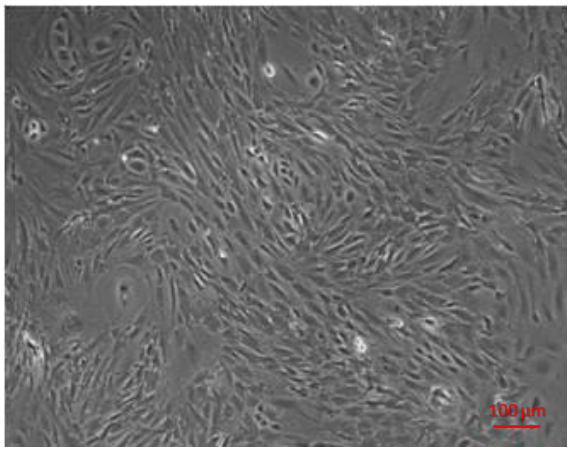

Fig. 4.3 CDC monolayer in fibronectin- coated flask.

4.3.2 CDC quantification on PUR substrates

Picogreen tests performed after 7 and 14 culture days on KBC1250 films and scaffolds, showed interesting results on CDC proliferation on porous scaffolds. In figure 4.4, a significant ($p<0.05$) higher cell number on the porous constructs with respect to films and control is observable. This evident difference in cell amount between scaffolds and the other two types of substrates could be due to the tridimensional porous structure of the scaffolds, that provides for a larger available space, allowing for a higher cell proliferation. This proliferation in the porous constructs demonstrated that they are appropriate matrices for CDC attachment and growth.
Between 7 and 14 days of culture, a clear decrease in cell number takes place for all the substrates, with a higher cell number ($p<0.05$) for the scaffolds with respect to films and control wells. Since after 7 days we observe a high cell amount on scaffolds, this drop is not caused by toxicity effects. This trend could be explained considering that, between days 7 and 14, there is no more available space where cell can further proliferate and expand.

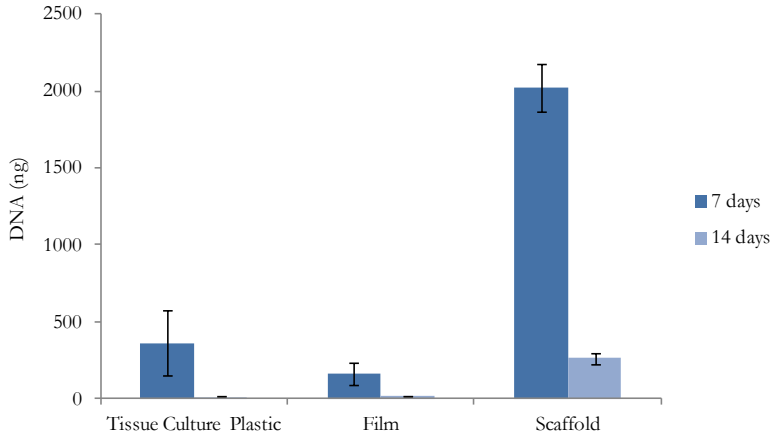

Fig. 4.4 Picogreen results for CDCs: DNA (cell) quantification on KBC1250 films and scaffolds and on tissue culture plastic, as control.

4.3.3 MSC quantification and health on PUR substrates

Results obtained by the Picogreen assay, performed after 1, 7 and 14 culture days, are shown in figure 4.5. It appears evident that there are significantly less cells at day 1 on the films and the scaffolds compared to the control ($p<0.05$ for both the constructs). This trend may reflect the available space for attachment and the initial "hydrophobic" effect of the porous surface. Nevertheless, a significant loss of cells on all the substrates is observable after 7 culture days, though the drop in number is lower for both the PUR based samples with respect to the control. This cell number decrease could be due to the high number of cell initially seeded.
Between day 7 and day 14, a significant increase in cell number is evident on scaffolds. This increase (not present on films and control wells) suggests that the cells have proliferated in the porous constructs and they have adapted to the environment, now suitable for their expansion.

Cell number decreased on control wells and did not significantly increase on films, probably because of the lack of a tridimensional structure and available space where cells can proliferate.

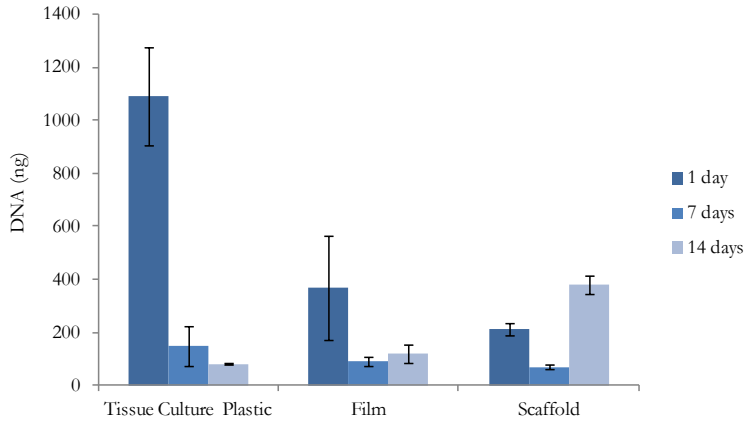

Fig. 4.5 Picogreen results for MSCs: DNA (cell) quantification on KBC1250 films and scaffolds and on tissue culture plastic, as control.

Data about MSC health, obtained from AlamarBlue assay, are reported in figure 4.6. On day 1 cells were significantly healthier on the scaffold compared to both the film and the control ($p<0.05$). In this case, there is no over seeding (Picogreen results in figure 4.3). and the increased surface area of the porous scaffold within the culture environment allowed the cells to move in and arrange themselves.

The health of the cells increased on both the films and the control wells throughout the experiment. On scaffolds, cell health increased up to the seventh day of culture, resulting twice as the value observed for films and control ($p<0.05$ for the scaffold with respect to the film and the control). This trend suggests that the cells became more adapted to their environment, probably because the loss of cells (decrease in cell amount) allowed the cells which survived to receive more nutrients and be exposed to more effective gaseous exchange. The superior health of the cells on the scaffolds at days 1 and 7 again suggests that the cells are in a very suitable environment.

After 14 culture days a significant decrease in cell health for the scaffold compared to both the film and the control ($p<0.05$) is observable. Since an increase in the number of cells was evident between days 7 and 14 (Picogreen results in figure 4.3), it is possible to state that there are no toxic effect caused by the scaffold. One technical issue that could affect this result may be that PUR scaffolds are initially hydrophobic but can absorb water solution with time. Consequently, the scaffolds could retain culture medium (they appeared swelled after 14 days compared to smaller time interval) which then diluted the Alamar Blue solution, reducing the value in cell health which is recorded. From a biological prospective, the increase in cell numbers, as noticed in the DNA graph, causes an increase in competition for resources (nutrients and oxygen) which reduces the metabolic activity of the cells. This aspect would be particularly relevant for cells inside the scaffold. The observed decrease in cell health may also be linked to an initial differentiation process, that generally requires activities such as the coordination of genomic programming and the energetic system maturation (from anaerobic glycolytic metabolism to the more efficient mitochondrial oxidative metabolism that secure

cardiac specification and excitation–contraction coupling) [24, 25]. These hypothesis will be assessed by histological studies, that have been planned as future work.
In conclusion, the scaffold appears to be the best substrate in supporting the cardiac MSCs within the first week. However, further optimization (particularly cell seeding density and assaying of cell health) will be necessary to demonstrate its positive effect over a longer period of time.

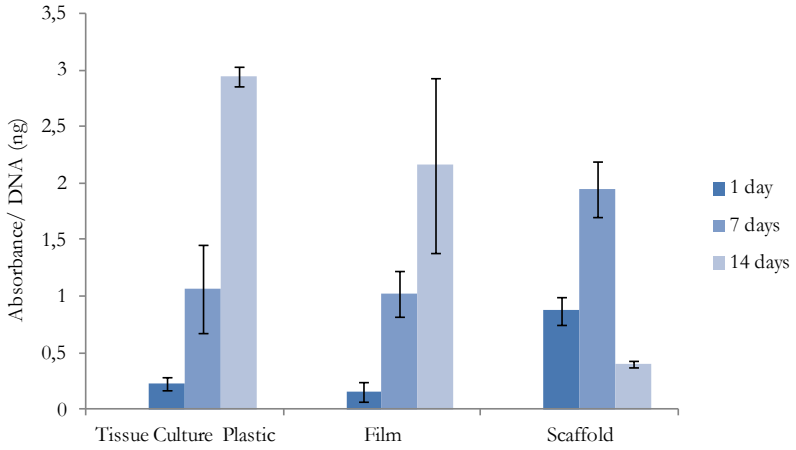

Fig. 4.6 AlamarBlue results for MSCs: cell health on KBC1250 films and scaffolds and on tissue culture plastic, as control.

4.4 Conclusions

Cardiac progenitor cells were successfully extracted and expanded as cardiosphere derived cells, through the formation of heterogeneous cell clusters, called "cardiospheres". These cells, that express progenitor cell markers, were seeded on KBC1250 dense and porous substrates, in order to test these constructs as suitable micro-environments for CDC attachment and proliferation. Picogreen tests showed that porous scaffold promote CDC growth after 7 culture days. After 2 weeks a decrease in cell number suggests that probably cells can not expand because of the total employment of the available space.
PUR based constructs were also tested with human mesenchymal stem cells, detected and characterized for the first time in human heart from Dr Rachel Oldershaw and Dr Annette Meeson from Newcastle University. Picogreen and AlamarBlue assays showed good results for the porous substrates both in terms of cell number (after 14 culture days) and cell health (after 1 and 7 days). The decrease in cell health after 14 days may be linked to technical problems during the tests and/or to the cell competition for nutrients. Another issue, that should be examined in depth, is the possibility of an initial differentiation in cardiomyocytes that causes a decrease in cell metabolic activity.
In conclusion, from preliminary tests on human cardiac progenitor cells, KBC1250 porous scaffolds resulted promising substrates for both CDCs and MSCs.

References

1. Ye, Z., et al., *Myocardial regeneration: Roles of stem cells and hydrogels.* Adv Drug Deliv Rev, 2011. **63**(8): p. 688-97.
2. Bollini, S., N. Smart, and P.R. Riley, *Resident cardiac progenitor cells: at the heart of regeneration.* J Mol Cell Cardiol, 2011. **50**(2): p. 296-303.
3. Gonzales, C. and T. Pedrazzini, *Progenitor cell therapy for heart disease.* Exp Cell Res, 2009. **315**(18): p. 3077-85.
4. Messina, E., et al., *Isolation and expansion of adult cardiac stem cells from human and murine heart.* Circ Res, 2004. **95**(9): p. 911-21.
5. Urbanek, K., et al., *Stem cell niches in the adult mouse heart.* Proc Natl Acad Sci U S A, 2006. **103**(24): p. 9226-31.
6. Beltrami, A.P., et al., *Adult cardiac stem cells are multipotent and support myocardial regeneration.* Cell, 2003. **114**(6): p. 763-76.
7. Dawn, B., et al., *Cardiac stem cells delivered intravascularly traverse the vessel barrier, regenerate infarcted myocardium, and improve cardiac function.* Proc Natl Acad Sci U S A, 2005. **102**(10): p. 3766-71.
8. Linke, A., et al., *Stem cells in the dog heart are self-renewing, clonogenic, and multipotent and regenerate infarcted myocardium, improving cardiac function.* Proc Natl Acad Sci U S A, 2005. **102**(25): p. 8966-71.
9. Johnston, P.V., et al., *Engraftment, differentiation, and functional benefits of autologous cardiosphere-derived cells in porcine ischemic cardiomyopathy.* Circulation, 2009. **120**(12): p. 1075-83, 7 p following 1083.
10. Urbanek, K., et al., *Myocardial regeneration by activation of multipotent cardiac stem cells in ischemic heart failure.* Proc Natl Acad Sci U S A, 2005. **102**(24): p. 8692-7.
11. Urbanek, K., et al., *Intense myocyte formation from cardiac stem cells in human cardiac hypertrophy.* Proc Natl Acad Sci U S A, 2003. **100**(18): p. 10440-5.
12. Bearzi, C., et al., *Human cardiac stem cells.* Proc Natl Acad Sci U S A, 2007. **104**(35): p. 14068-73.
13. Oh, H., et al., *Cardiac progenitor cells from adult myocardium: homing, differentiation, and fusion after infarction.* Proc Natl Acad Sci U S A, 2003. **100**(21): p. 12313-8.
14. Smart, N. and P.R. Riley, *The stem cell movement.* Circ Res, 2008. **102**(10): p. 1155-68.
15. Chimenti, I., et al., *Human cardiosphere-seeded gelatin and collagen scaffolds as cardiogenic engineered bioconstructs.* Biomaterials, 2011. **32**(35): p. 9271-81.
16. X., L.Z.G., *Differentation of cardiosphere-derived cells into a mature cardiac lineage using biodegradable poly(N-isopropylacrylamide) hydrogels.* Biomaterials, 2011. **32**: p. 3220-32.
17. Zhou, S., et al., *The ABC transporter Bcrp1/ABCG2 is expressed in a wide variety of stem cells and is a molecular determinant of the side-population phenotype.* Nat Med, 2001. **7**(9): p. 1028-34.
18. Hierlihy, A.M., et al., *The post-natal heart contains a myocardial stem cell population.* FEBS Lett, 2002. **530**(1-3): p. 239-43.
19. Martin, C.M., et al., *Persistent expression of the ATP-binding cassette transporter, Abcg2, identifies cardiac SP cells in the developing and adult heart.* Dev Biol, 2004. **265**(1): p. 262-75.
20. Oyama T., N.T., Wada H., Naito A.T., Matsuura K., Iwanaga K., et al. , *Cardiac side population cells have a potential to migrate and differentiate into cardiomyocytes in vitro and in vivo.* J Cell Biol, 2007. **176**: p. 329–41.
21. Yamahara, K., et al., *Heterogeneic nature of adult cardiac side population cells.* Biochem Biophys Res Commun, 2008. **371**(4): p. 615-20.
22. Carlson, S., et al., *Cardiac mesenchymal stem cells contribute to scar formation after myocardial infarction.* Cardiovasc Res, 2011. **91**(1): p. 99-107.
23. Smith, R.R., et al., *Regenerative potential of cardiosphere-derived cells expanded from percutaneous endomyocardial biopsy specimens.* Circulation, 2007. **115**(7): p. 896-908.
24. Chung, S., et al., *Developmental restructuring of the creatine kinase system integrates mitochondrial energetics with stem cell cardiogenesis.* Ann N Y Acad Sci, 2008. **1147**: p. 254-63.
25. Lopaschuk, G.D. and J.S. Jaswal, *Energy metabolic phenotype of the cardiomyocyte during development, differentiation, and postnatal maturation.* J Cardiovasc Pharmacol, 2010. **56**(2): p. 130-40.

CHAPTER 5
Final discussion and conclusions

5.1 General discussion

Myocardial infarction is one of the most common cardiovascular diseases, that are the number one cause of death in the world [1]. Since adult cardiomyocytes and the progenitor cells present in the adult heart have very poor capability to proliferate and differentiate, respectively, a myocardial infarction results in the formation of scar tissue with different contractile and mechanical properties from that of native tissue [2-4]. To this day, pharmacologic and surgical treatments did not reveal sufficiently adequate in completely restoring cardiac functions. As a consequence, new approaches of Regenerative Medicine and, in particular, of Tissue Engineering, have been considered.

One of the possible approaches of TE consists in employing a tridimensional construct (*scaffold* or *heart patch*, in the case of cardiac regeneration), that is generally prepared from natural or synthetic polymers. The most important challenge of myocardial TE researchers is to prepare adequate constructs combining the required morphological, mechanical, physical and biochemical properties, in order to create a suitable microenvironment for cardiac cells, both for *in vitro* and *in vivo* TE strategies.

Since one of the most fatal consequences of MI is LV remodeling, which consists in changes in size, shape, and function of the infarcted ventricle [5], a critical requirement for a heart patch is to mechanically support the infarcted ventricle. Consequently, a heart patch should show suitable strength and an elastomeric mechanical behavior, able to temporarily support the regeneration of the contractile tissue and restore the right shape and functionality of the ventricle. In addition, this scaffold should temporarily replace the injured tissue, providing a transitional support to cell colonization, migration and proliferation and degrading with times compatible with native tissue regeneration. In the case of *in vitro* TE approaches, the scaffold should avoid cell loss and control their distribution in the infarcted area. To fulfill these functions, myocardial scaffolds should mimic the chemical and biological characteristics of cardiac ECM, its structure, morphology and mechanical behavior [6].

Aim of this thesis work was to fabricate suitable biomimetic constructs, able to restore myocardial functions and promote cardiac tissue regeneration after a myocardial infarction. These constructs were prepared as dense (films) and porous (scaffolds) constructs from synthetic biodegradable polyurethanes. These polymeric materials were selected thanks to their versatility, since they can be prepared starting from a large number of building blocks (macrodiols, diisocyanates and chain extenders) and, consequently, their properties can be finely tuned. In addition, degradable PURs have been studied for a long time for cardiovascular applications, thanks to their biocompatibility and elastomeric behavior that allow them to withstand the cyclic stresses of the cardiac contractile tissue [7, 8].

In this work, biodegradable poly(ester urethanes) and poly(ether ester urethanes) based on PCL and PEG as macrodiols were proposed as starting materials for the fabrication of

myocardial patches. PEG was added in low amounts with the aim of tuning wettability, mechanical and biological properties of films and scaffolds. L-Lysine Ethyl Ester and Alanine-Alanine-Lysine (AAK) were selected as chain extenders due to their biocompatibility and because AAK peptide allows to modulate biodegradability properties, since the Alanine-Alanine sequence is a target for the elastase enzyme.

The chemical, thermal and mechanical analysis of the synthesized PURs showed the successful preparation of the polymeric materials with the desired physical-chemical properties for myocardial TE applications. Polymers revealed to be easily processable in dense films and porous scaffolds. Through the TIPS technique, a tridimensional construct with an anisotropic microstructure was obtained, starting from two different PUR formulations (KBC1250 and KBC1250-E1500-20). This structure was characterized in both cases by elongated and unidirectional pores, which showed a "structural biomimicry" of the streaked muscle tissue. In detail, the scaffold fabricated from KBC1250 showed interconnected porosity with pores of about 98 μm. These features seem to promote cell colonization, cell migration and nutrients supply [6, 9]. In addition, porous substrates showed melting temperatures well above the physiological one, avoiding a decrease in mechanical performance of the construct after implant, due to the softening of the material.

Mechanical tests revealed that the introduction of low amounts of PEG allowed a fine tuning of mechanical properties and that, although all the dense films were characterized by an elastomeric behavior and high toughness, the film obtained from the PUR containing 20% of PEG macrodiol (KBC1250-E1500-20) was characterized by the mechanical parameters closer to those required (elastic modulus of myocardial tissue: 20kPa-0.5MPa; strain at break in the range 22-90%; stress at break in the ranges 3-15 kPa [7, 8, 10, 11]). Porous devices, which were prepared by the formulation KBC1250-E1500-20 and that synthesized from 100% PCL macrodiol (KBC1250), showed mechanical properties lower than the corresponding films. However, if we consider that an ideal patch should be characterized by Young Moduli encompassing from tens of kPa to 1 MPa and by an elastomeric mechanical behaviour, the obtained scaffolds are appropriate for myocardial TE applications. They have elastic moduli very close to that of native tissue, maximum stress significantly higher than that of the myocardial tissue and an elastic mechanical behavior up to about 20% of deformation.

From what concerns biological properties, the porous structures, regardless of their PEG content, showed good results in terms of cardiomyocytes viability and adhesion. The best biological response was observed for the porous KBC1250, probably due to its stretched microstructure with morphological features (interconnected porosity and pores 98 μm diameter that seem to be ideal in promoting cell proliferation and colonization [6, 9, 12].

Hydrolytic and lipase degradation tests showed a faster weight loss for the scaffolds in the presence of the enzyme, probably because the enzymatic degradation mechanism takes place on the surface and porous constructs exhibit a larger exposed area. Elastase degradation tests, that were performed on KBC1250 and ABC1250 films, demonstrated the possibility to increase the degradation rate of PURs through a partial introduction of an enzyme-target peptide as chain extender. Nevertheless, a fine tuning of the degradation process was obtained, too. If we consider that Guan and co-workers [13] achieved 2-25% weight loss for similar polyurethane films introducing 100% AAK peptide in the polymer backbone and performing analogous enzymatic degradation tests, it is possible to state that, in this thesis work, the

replacement of 50% AAK peptide with L-Lysine resulted in a evident slowing down of the degradation process (0-5% weight loss) with respect to what obtained by Guan.
Based on the optimal biological and mechanical properties of dense and porous KBC1250 constructs, these substrates were selected to be surface modified with RGD peptides. This covalent modification aimed to obtain a "biochemical mimicry" of the natural ECM, and, as a consequence, to promote cell adhesion and proliferation. It was performed on films both homogeneously and through a silicone mask that allowed for the creation of a linear chemical micropattern. Data from literature have shown encouraging results on cardiomyocyte proliferation and stem cell differentiation into the cardiac lineage, in *in vitro* cultures on polymeric surfaces with fibronectin and laminin linear micropatterns [14, 15]. In detail, the adhesion on the modified strips seem to promote mesenchymal stem cell differentiation probably due the stretching of the cells, and cardiomyocyte spatial organization during novel tissue formation.
In this thesis work, surface modification with epitopes of fibronectin and laminin proteins was investigated, since the use of the entire proteins involves several disadvantages with respect to the use of peptides containing the active sequences. Proteins have to be isolated from other organisms and purified, increasing the risk of immune responses and infections. In addition, proteins have to be refreshed continuously, since they are object of proteolytic degradation, and only a part of the proteins reach the proper orientation for cell adhesion when adsorbed on or bound to surfaces[16-18].
Spectroscopic analysis, increase in surface wettability and colorimetric assays demonstrated the successful surface modification of both KBC1250 films and scaffolds, by the covalent attachment of RGD peptides. In addition, functionalized films were characterized by an optimal hydrophylicity (contact angle value of about 65°), very close to that reported in literature [19] and an appropriate peptide density (respectively 3.2 and 1.7 nmol/mm^2 for surfaces modified homogeneously and with the micropattern), able to promote cell adhesion [19, 20]. Amino group quantification and cell viability tests demonstrated indirectly the successful use of the siloxane stencil in covalently attaching the RGD peptides on the uncovered areas. The presence of peptides on film surfaces affected positively cardiomyocyte viability and adhesion, as showed from MTS tests and SEM micrographs, where a stretched cell shape and the presence of filaments are evident after 3 culture days. Although an increase in surface wettability and a good RGD density were obtained also for the porous constructs, the biological response on this type of substrates was not significantly higher after surface modification, with a slight increase in cell viability and adhesion measured only after 7 culture days. This behaviour may be explained considering that the porous surfaces achieved a contact angle value of about 90°, still far from the optimal values for promotion of cell attachment and proliferation and/or the possible presence of not covalently bound peptides inside the scaffold microstructure, that may induce cell detachment and apoptosis [21-23].
KBC1250 substrates were also selected to be tested with human cardiac Mesenchymal Stem Cells (MSCs) and Cardiosphere Derived Cells (CDCs) for potential *in vitro* and *in vivo* MTE applications. Cardiac progenitor cells are the best candidates for both cell injection and MTE applications, since they are autologous, tissue-specific and pre-committed to the cardiovascular lineages [24]. Human cardiac MSCs belong to the stem cell reservoir within the adult myocardium and were detected for the first time in a human heart by Dr Rachel

Oldershaw and Dr Annette Meeson at Newcastle University (work still unpublished). As a consequence, they were tested for the first time on TE substrates for myocardial repair in this thesis work. The second type of cells derive from heterogeneous cell clusters, that are characterized by a mixture of cardiac stem cells, differentiating progenitors and spontaneously differentiated cardiomyocytes ("cardiospheres") [25, 26]. Although CDCs have been already investigated for both cell therapies [27] and TE applications [28], they have been recently discovered and several aspects concerning their characteristics and their effects on myocardial regeneration have to investigated further [25]. In this thesis work CDCs were successfully extracted from human biopsies trough cardiosphere formation *in vitro* and expanded as a common primary cell culture. Subsequent culture of these CDCs and MSCs on KBC1250 films and scaffolds revealed interesting and encouraging results for the porous constructs for MTE applications. Viability cell test showed that scaffold promoted CDC growth after 7 culture days. Good results for the porous substrates both in terms of cell number (after 14 culture days) and cell health (after 1 and 7 days) were obtained for MSCs. Nevertheless, a decrease in cell health after 14 days was observed. This result may be due to the competition for nutrients and gases after an intense cell proliferation or to technical problems during the test, such as water uptake with time, that can alter the concentration of the dye (AlamarBlue) and affect the final result. Another cause of the observed decrease in cell health may be the possible differentiation of these stem cells into cardiomyocytes, since this process determines a decrease in cell metabolic activity. This issue should be examined in depth through the study of changes in cell morphology and protein expressions. However, from these preliminary tests on human cardiac progenitor cells, KBC1250 porous scaffolds resulted promising substrates for both CDCs and MSCs.

5.2 Conclusions and future developments

In conclusion, the discussed results suggest that the selected synthesised polyurethane (KBC1250) is non toxic and the scaffold prepared by TIPS has the requested thermal and mechanical properties for MTE applications. In addition, this construct provides a suitable environment for cardiac cells (cardiomyocytes and stem cells) and the surface modification with RGD peptides can improve and accelerate cell response, in terms of cell adhesion and proliferation.

Results obtained suggest work in order to further examine some aspects concerning degradability properties of the scaffolds, the biological effect of the RGD micropattern and clarify results related to progenitor cell proliferation and differentiation on the proposed substrates.

First of all, since elastase degradation tests (discussed in Chapter 2) showed the possibility to finely tune biodegradation rate of PUR films through a partial introduction of the AAK peptide as chain extender in the polymeric backbone, fabrication by TIPS of porous scaffolds based on the formulation ABC1250 has been planned as future work, in order to combine a controllable biodegradability with a suitable porous microstructure for cell attachment and proliferation. Subsequent enzymatic degradation tests on porous structures based on

KBC1250 and ABC1250 should be combined to a precise study of the optimal degradation times for a heart patch.

Further suggested activities may concern the surface modification with adhesion-peptides (see Chapter 3). The first aspect to be considered is the effectiveness of the linear micropattern in promoting cell adhesion and tissue organization, as suggested by data from literature on analogous micropatterns of laminin and fibronectin [14, 15]. This novel preliminary work on a linear RGD micropattern showed the successful use of the siloxane stencil during the peptide functionalization step in allowing the covalent attachment on the exposed areas of the polymeric surfaces. Nevertheless, cell tests that can visualize cell alignment along the modified strips will be necessary to understand the effect of chemical cues on cell spatial organization. The second aspect concerns the biological effect of the functionalization of the proposed scaffolds, since the results obtained show an almost unaltered cardiomyocyte response on the modified scaffolds with respect to the unmodified ones. As already discussed, this behavior could be ascribed to the hydrophobic effect of the surface micro-roughness or the presence of adsorbed, not covalently-linked, peptides. As a consequence, these aspects deserve further investigation in order to obtain on scaffolds results similar to those obtained on films. Increasing bound peptide density could be one possible approach to the decrease substrate hydrophobicity. Modified films and scaffolds could be tested also with CDCs and MSCs, in order to verify an acceleration and improving of the biological response also for what concerns progenitor cells. In particular, the effect of the micropatterned surfaces for progenitor cell differentiation into cardiomyocytes, as a consequence of cell stretch and alignment, is worth further study.

Finally, to assess the viable implementation of the proposed constructs (modified and not) as implantable devices, able to recruit cardiac cells and restore mechanical and biological functions of the infarcted ventricle, *in vivo* trials are required. These tests will allow to investigate also on the degradation times of the devices and to really assess the biocompatibility of their biodegradation products.

References

1. *Global Atlas on cardiovascular disease prevention and control*, P.P. S. Mendis, B. Norrving, Editor 2011, World Health Organization in collaboration with the World Heart Federation and the World Stroke Organization: Geneva.
2. Anversa, P., et al., *Myocyte growth and cardiac repair.* J Mol Cell Cardiol, 2002. **34**(2): p. 91-105.
3. Dimmeler, S., A.M. Zeiher, and M.D. Schneider, *Unchain my heart: the scientific foundations of cardiac repair.* J Clin Invest, 2005. **115**(3): p. 572-83.
4. Vunjak-Novakovic, G., et al., *Challenges in cardiac tissue engineering.* Tissue Eng Part B Rev, 2010. **16**(2): p. 169-87.
5. Sutton, M.G. and N. Sharpe, *Left ventricular remodeling after myocardial infarction: pathophysiology and therapy.* Circulation, 2000. **101**(25): p. 2981-8.
6. Causa, F., P.A. Netti, and L. Ambrosio, *A multi-functional scaffold for tissue regeneration: the need to engineer a tissue analogue.* Biomaterials, 2007. **28**(34): p. 5093-9.
7. Jawad, H., et al., *Myocardial tissue engineering: a review.* J Tissue Eng Regen Med, 2007. **1**(5): p. 327-42.
8. Jawad, H., et al., *Myocardial tissue engineering.* Br Med Bull, 2008. **87**: p. 31-47.

9. Cohen, S. and J. Leor, *Rebuilding broken hearts. Biologists and engineers working together in the fledgling field of tissue engineering are within reach of one of their greatest goals: constructing a living human heart patch.* Sci Am, 2004. **291**(5): p. 44-51.
10. Bouten, C.V., et al., *Substrates for cardiovascular tissue engineering.* Adv Drug Deliv Rev, 2011. **63**(4-5): p. 221-41.
11. Chen Q.Z., H.S.E., Ali N.N., Lyon A.R., Boccaccini A.R. , *Biomaterials in cardiac tissue engineering: Ten years of research survey.* Mater Sci Eng R, 2008. **59**: p. 1-37.
12. Guan, J., K.L. Fujimoto, and W.R. Wagner, *Elastase-sensitive elastomeric scaffolds with variable anisotropy for soft tissue engineering.* Pharmaceutical Research, 2008. **25**(10): p. 2400-2412.
13. Guan, J. and W.R. Wagner, *Synthesis, characterization and cytocompatibility of polyurethaneurea elastomers with designed elastase sensitivity.* Biomacromolecules, 2005. **6**(5): p. 2833-42.
14. McDevitt, T.C., et al., *Spatially organized layers of cardiomyocytes on biodegradable polyurethane films for myocardial repair.* J Biomed Mater Res A, 2003. **66**(3): p. 586-95.
15. Siepe, M., et al., *Construction of skeletal myoblast-based polyurethane scaffolds for myocardial repair.* Artif Organs, 2007. **31**(6): p. 425-33.
16. Hersel, U., C. Dahmen, and H. Kessler, *RGD modified polymers: biomaterials for stimulated cell adhesion and beyond.* Biomaterials, 2003. **24**(24): p. 4385-415.
17. Elbert, D.L. and J.A. Hubbell, *Conjugate addition reactions combined with free-radical cross-linking for the design of materials for tissue engineering.* Biomacromolecules, 2001. **2**(2): p. 430-41.
18. Lhoest, J.B., et al., *Fibronectin adsorption, conformation, and orientation on polystyrene substrates studied by radiolabeling, XPS, and ToF SIMS.* J Biomed Mater Res, 1998. **41**(1): p. 95-103.
19. Lee, J.H., et al., *Interaction of Different Types of Cells on Polymer Surfaces with Wettability Gradient.* J Colloid Interface Sci, 1998. **205**(2): p. 323-330.
20. Maheshwari, G., et al., *Cell adhesion and motility depend on nanoscale RGD clustering.* J Cell Sci, 2000. **113 (Pt 10)**: p. 1677-86.
21. Grano, M., et al., *Adhesion properties and integrin expression of cultured human osteoclast-like cells.* Exp Cell Res, 1994. **212**(2): p. 209-18.
22. Noiri, E., et al., *Cyclic RGD peptides ameliorate ischemic acute renal failure in rats.* Kidney Int, 1994. **46**(4): p. 1050-8.
23. Stromblad, S., et al., *Suppression of p53 activity and p21WAF1/CIP1 expression by vascular cell integrin alphaVbeta3 during angiogenesis.* J Clin Invest, 1996. **98**(2): p. 426-33.
24. Gonzales, C. and T. Pedrazzini, *Progenitor cell therapy for heart disease.* Exp Cell Res, 2009. **315**(18): p. 3077-85.
25. Messina, E., et al., *Isolation and expansion of adult cardiac stem cells from human and murine heart.* Circ Res, 2004. **95**(9): p. 911-21.
26. Smith, R.R., et al., *Regenerative potential of cardiosphere-derived cells expanded from percutaneous endomyocardial biopsy specimens.* Circulation, 2007. **115**(7): p. 896-908.
27. Johnston, P.V., et al., *Engraftment, differentiation, and functional benefits of autologous cardiosphere-derived cells in porcine ischemic cardiomyopathy.* Circulation, 2009. **120**(12): p. 1075-83, 7 p following 1083.
28. Chimenti, I., et al., *Human cardiosphere-seeded gelatin and collagen scaffolds as cardiogenic engineered bioconstructs.* Biomaterials, 2011. **32**(35): p. 9271-81.